

UC Berkeley

UC Berkeley Electronic Theses and Dissertations

Title

Changes in Mobile Source Emissions and Ambient Air Quality in California

Permalink

<https://escholarship.org/uc/item/45m6m2d8>

Author

Tao, Ling

Publication Date

2016

Peer reviewed|Thesis/dissertation

Changes in Mobile Source Emissions and Ambient Air Quality in California

by

Ling Tao

A dissertation submitted in partial satisfaction of the

requirements for the degree of

Doctor of Philosophy

in

Engineering – Civil and Environmental Engineering

in the

Graduate Division

of the

University of California, Berkeley

Committee in charge:

Professor Robert A. Harley, Chair

Professor Fotini Katopodes Chow

Professor John R. Balmes

Fall 2016

Abstract

Changes in Mobile Source Emissions and Ambient Air Quality in California

by

Ling Tao

Doctor of Philosophy in Engineering – Civil and Environmental Engineering

University of California, Berkeley

Professor Robert A. Harley, Chair

Air quality in California has undergone dramatic changes due to a variety of federal and state-wide regulatory efforts. The air pollutant monitoring network has evolved to achieve greater spatial and temporal coverage, incorporating novel measurement technologies such as the Beta Attenuation Method. Many key pollutants such as nitrogen oxides (NO_x), black carbon (BC) and particulate matter with diameter less than $2.5 \mu\text{m}$ ($\text{PM}_{2.5}$) have seen reductions in ambient concentrations. Controls on emissions from fuel combustion are a major contributor to these reductions, especially emission standards and reformulated fuel requirements for mobile sources. The goal of the research in this dissertation was to quantify changes in mobile source emissions and ambient pollutant concentrations as a result of emission regulations, using data from decades of air pollutant monitoring efforts.

Ocean-going vessels are an off-road source that contributes significantly to the emissions of sulfur dioxide (SO_2) and $\text{PM}_{2.5}$ in California, due to its long coastline and busy ports. In 2009, the state mandated that all ships operating within 24 nautical miles of the coastline burn fuels with lower sulfur contents, instead of heavy fuel oil. Ambient pollutant measurements near the Port of Oakland in the San Francisco Bay area were analyzed, before and after the lower-sulfur marine fuel mandate came into effect. Vanadium concentrations decreased by more than ten-fold, and 28 - 72% reductions in SO_2 concentrations were observed at nearby measurement sites, with the magnitudes of reduction approximately proportional to the distance from shipping lanes. It was estimated that the change in ship fuel reduced ambient $\text{PM}_{2.5}$ concentrations by about $3.1 \pm 0.6\%$, or $0.28 \pm 0.05 \mu\text{g}/\text{m}^3$. The site nearest to the port saw largest reductions in vanadium and SO_2 , whereas all sites experienced approximately the same magnitude of reduction in sulfate, a secondary $\text{PM}_{2.5}$ component.

On-road mobile sources emit carbon monoxide (CO), NO_x , and non-methane hydrocarbon (NMHC) from the burning of diesel fuel and gasoline in vehicle engines. These emissions can be estimated using the California On-Road Mobile Emission Model (EMFAC). Its predictions were evaluated using real-world emission measurements for on-road vehicles collected at

truck weigh stations, in highway tunnels, and at the roadside using emission spectrometers, also known as remote sensors. EMFAC tends to overestimate the population of newer engines and underestimate travels by older engines, but the overall emissions estimates from EMFAC agree in general with fuel-based estimates developed in the present research. Predictions of diesel engine age distribution also capture the accelerated diesel replacement program currently being implemented in California. In recent years, diesel engines contribute more to statewide NO_x emissions compared to gasoline engines, whereas gasoline engines are dominant for CO and NMHC emissions.

California has identified diesel particulate matter as toxic and has mandated that newer diesel trucks replace the existing older fleet by 2023. It is necessary to model the effects on air quality of changes in diesel emissions as well as in other sectors, such as gasoline burning and off-road sources, for the upcoming decade. Emission inventories for the South Coast Air Basin were modified to reflect changes in emission factors and population growth, and were used as input to the Community Multiscale Air Quality model (CMAQ). It was found that the accelerated diesel engine replacement program is effective in reducing ambient concentrations of BC, NO_x , and $\text{PM}_{2.5}$, but not of O_3 . Wintertime NO_x concentration was predicted to decrease by $71 \pm 5\%$ thanks to the universal use of newer selective catalytic reduction systems to reduce NO_x . CMAQ aerosol chemistry was unable to depict summer daytime secondary organic aerosol formation in Southern California.

The $\text{PM}_{2.5}$ ambient monitoring network in California has evolved to include the Beta Attenuation Monitoring (BAM), and the data from the network reflects the benefits of many on-road and off-road emission regulations. BAM is superior to the traditional filter methods because it minimizes evaporation of some components in $\text{PM}_{2.5}$ and human errors. BAM measures higher than traditional filter-based sampling methods by 3 - 6 $\mu\text{g}/\text{m}^3$ for annual averages. Since the 1990's, all the sites examined in this study have shown clear downward trends, with some showing reductions of more than 50%. The use of BAM produces hourly concentration measurements every day, in contrast to only 24-hour averages that were available only once every 3 or 6 days with the older method. $\text{PM}_{2.5}$ concentrations are higher in winter months in the San Francisco Bay area ($+80 \pm 25\%$) and the San Joaquin Valley ($+123 \pm 28\%$), but lower in the wintertime for inland sites in the South Coast Basin ($-46 \pm 12\%$). Night-time $\text{PM}_{2.5}$ concentrations reach maximum values due to the stagnant atmosphere and wood-burning. Weekend $\text{PM}_{2.5}$ concentrations decrease by $8.9 \pm 5.9\%$ for the San Francisco Bay area and $8.0 \pm 3.0\%$ for the San Joaquin Valley, relative to the midweek values. This study shows the significance of making continuous measurements a part of the monitoring network.

This dissertation analyzed trends in observed air pollution concentrations and used an Eulerian Air Quality model to assess the impacts of major pollution control regulations in California. These regulations are effective in controlling primary pollutants and some secondary pollutants. Recommendations for future research include updating on-road emission

inventories using real-world emission measurements, revising aerosol chemistry in CMAQ, and developing new methods to analyze hot spot pollution.

Contents

Contents	i
List of Figures	iii
List of Tables	viii
1 Introduction	1
1.1 Impact of air pollution	1
1.2 Air pollution in California	2
1.3 Regulated emission sources in California	3
1.4 Research objectives	5
2 Effects of Switching to Lower Sulfur Marine Fuel Oil on Air Quality in the San Francisco Bay Area	6
2.1 Introduction	6
2.2 Approach	8
2.3 Results and Discussion	12
3 A Fuel-Based Motor Vehicle Emission Inventory Evaluation	27
3.1 Introduction	27
3.2 Methods	28
3.3 Results	32
4 Effects on Air Quality of Controlling NO_x Emissions from Diesel Trucks	42
4.1 Introduction	42
4.2 Method	43
4.3 Results	50
4.4 Discussion	54
5 Changes in Fine Particulate Matter Measurement Methods and Ambient Concentrations in California	65
5.1 Introduction	65
5.2 Approach	67

5.3 Results and Discussion	68
6 Conclusions	89
6.1 Summary of Major Findings	89
6.2 Policy implications	91
6.3 Recommendations for Future Research	91
A Trends in ambient NO_x concentrations	93
References	102

List of Figures

1.1	Projected statewide NO_x emissions with and without the accelerated diesel engine replacement program mandated by the California Air Resources Board. Some adjustments to the implementation schedule were made after the regulation was adopted (not shown here).	4
2.1	Ambient air measurement sites in the San Francisco Bay area. Also shown are the Port of Oakland and the major oil refineries.	8
2.2	Time series plots of ambient sulfur dioxide concentrations at Bay area monitoring sites. The black dashed line marks the July 2009 effective date of the low-sulfur fuel regulation for main engines.	9
2.3	An example of exponential fitting to trace metal concentrations. The plot shows the distribution of vanadium concentrations at Point Reyes from July 2009 to June 2010 and its exponential fitting. The median obtained from fitting is $0.00035 \mu\text{g}/\text{m}^3$, marked in red.	11
2.4	Annual ship calls in the San Francisco Bay area by major port from 2007 to 2011.	13
2.5	Wind rose pattern near the West Oakland air monitoring site.	13
2.6	Time series plots of ambient vanadium concentrations at Bay area monitoring sites. The black dashed line marks the July 2009 effective date of the low-sulfur fuel regulation for main engines.	15
2.7	Box-and-whisker plots of ambient vanadium concentrations. Plots are based on measured data. Annual distributions are presented using data from July 1 through June 30 of the following year, to align pollutant data with the mid-year change in ship fuel in 2009 (shown as a dashed line). Each box represents the 25 th to 75 th percentile range for a given site and year. each pair of whiskers extend from the hinge to the highest and the lowest values that are within 1.5 times the inter-quartile range, respectively. The median and mean are marked using a horizontal line and a dot, respectively. The West Oakland box for 2008-09 is based on partial year data from 2009 only. The black dashed line marks the July 2009 effective date of the lower sulfur fuel regulation for main engines.	16
2.8	Time series plots of ambient nickel concentrations at Bay area monitoring sites. The black dashed line marks the July 2009 effective date of the low-sulfur fuel regulation for main engines.	17

2.9	Box-and-whisker plots of ambient nickel concentrations. Annual distributions are presented using data from July 1 through June 30 of the following year, to align pollutant data with the mid-year change in ship fuel in 2009 (shown as a dashed line). Each box represents the 25 th to 75 th percentile range for a given site and year, with the median and mean marked using a horizontal line and a dot, respectively. The West Oakland box for 2008-09 is based on partial year data from 2009 only	18
2.10	Box-and-whisker plots of ambient non-sea-salt sulfate concentrations. Other details are the same as in Figure 2.7.	19
2.11	Time series of ambient PM _{2.5} sulfate at Bay area monitoring sites.	20
2.12	SO ₂ emission from the five Bay area refineries from 2007 to 2011.	21
2.13	Wilcoxon test results for vanadium concentrations for each site, comparing every two consecutive periods for the seven periods: 2005 July through 2006 June, 2006 July through 2007 June, 2007 July to 2008 June, to 2011 July through 2012 March. The grey boxes represent invalid Wilcoxon test results. The white boxes mean a change in concentration is likely to have taken place, and show the corresponding 95% CI and the mean for the change, with positive numbers meaning a decrease in time, and vice versa.	23
2.14	Wilcoxon test results for non-sea-salt sulfate concentrations for each site for the same periods as in fig. 2.13.	24
3.1	Selected diesel vehicle age distributions from EMFAC county-level (yellow) and California statewide (blue) data, and on-road measurements (red).	32
3.2	Selected gasoline vehicle age distributions. Color scheme is the same as in Figure 3.1	33
3.3	Future model age distribution of diesel engines governed by the California accelerated engine turnover program. Distributions are shown for years 2017 (red), 2019 (orange), 2021 (yellow), and 2023 (green). Each Vertical dotted line marks the peak population age for the given year.	34
3.4	Trends in fuel-based emission factors for heavy-duty (HD) diesel vehicles measured in California on-road studies, as a function of calendar year. The solid lines represent linear fits to the emission factor trends over time (note the linear scaling of the vertical axis in this plot).	35
3.5	Trends in fuel-based emission factors for light-duty (LD) vehicles measured in California on-road studies, as a function of calendar year. The solid lines represent logarithmic fits to the emission factor trends over time (note the logarithmic scaling of the vertical axis in this plot). Differences in emission factors measured in the same calendar year at different locations (there are three or more study results plotted for each of 1999, 2001, and 2008; see Table 1 for details) may be due to differences in vehicle fleet/age distribution, driving conditions, and study design/measurement methods.	36

3.6	On-road vehicle NO_x emission inventories by calendar year: California state totals and results for selected air basins and counties, for annual average weekday conditions. Units are US tons per day (tpd); NO_x mass is reported on an NO_2 equivalent basis, although most of the emissions are in the form of NO . The shaded color bands denote 95% confidence intervals associated with the fuel-based inventory (solid lines). EMFAC model data shown as dashed lines. Separate results for gasoline (green) and diesel (blue) engines are shown together on each plot.	39
3.7	On-road vehicle CO emission inventories by calendar year. Color schemes are the same as Figure 3.6	40
3.8	On-road vehicle NMHC emission inventories by calendar year. Color schemes are the same as Figure 3.6	41
4.1	On-road heavy-duty truck exhaust emission standards by engine model year. Emissions limits are expressed per unit of useful work (hp-hr) output by the engine.	43
4.2	Model domain with measurement sites in 2005 with the following annotations: O_3 - yellow dots; CO - green diamonds; NO_x - blue asterisk; Speciated $\text{PM}_{2.5}$ - red dots with labels.	44
4.3	An example of normal fitting to the logarithm of gasoline NH_3/NO_x ratios.	46
4.4	Ratio of NH_3/NO_x by model age, fitting using two separate lines.	47
4.5	Contribution to total weekday emissions of BC, NO_x , $\text{PM}_{2.5}$ and NH_3 from five sectors. DSL and GAS represent on-road diesel and gasoline, respectively. Absolute emission in short tons/day is written above each pie chart.	51
4.6	Measured and predicted winter NO_x concentrations from 2005 to 2023 for selected sites. Site are ordered from west to east. Purple dotted lines represent the means of the measured concentrations, and purple bands represent the 25% and 75% quartiles. Green boxes represent the predicted values in 2005, 2016 and 2023, with black dots as means, black lines in the boxes as medians, lower and upper edges of the boxes as 25 and 75 percentiles, and whiskers extending to 95% confidence intervals. Note the time axis is discontinuous after 2016.	56
4.7	Measured and predicted summer O_3 concentrations. Plot specifications are the same as in Figure 4.6.	57
4.8	Diurnal variations in weekday NO_x concentrations in summer (red/orange) and winter (blue/cyan) at four selected sites. Sites are located from west to east. Dotted lines indicate 2015 measured concentrations and solid lines indicate 2016 model predictions. Color bands indicate 95% confidence intervals. Hours with less than 75% measured data available were not plotted (3 and 4AM).	58
4.9	Diurnal variations in weekday O_3 concentrations. Plot specifications are the same as in Figure 4.8.	59
4.10	Diurnal variations in weekday $\text{PM}_{2.5}$ concentrations. Plot specifications are the same as in Figure 4.8.	60

4.11	PM _{2.5} speciation pie charts from the 2005, 2016 and 2023 model simulations and 2005 and 2012 MATES measurements in summer (top) and winter (bottom). Both weekdays and weekends are included. Average PM _{2.5} mass concentration is written above each pie in $\mu\text{g}/\text{m}^3$. BC, NO ₃ ⁻ , SO ₄ ²⁻ , OC are represented in grey, red, blue, and green, respectively. All other components are lumped into 'Other', in white. The four sites are Burbank, Los Angeles, West Long Beach and Compton in the western half of the air basin.	61
4.12	PM _{2.5} speciation pie charts from the 2005, 2016 and 2023 model simulations and 2005 and 2012 MATES measurements. Plot specifications are the same as in Figure 4.11 except that the sites are North Long Beach, Pico Rivera, Anaheim and Riverside, in the Eastern (inland) half of the air basin.	62
4.13	Maps of predicted concentrations in ppb for (a) Summer NO ₂ and (b) Winter O ₃ in 2005 (top), 2016 (middle), and 2023 (bottom). Daily average (24-hour) values are shown for NO ₂ and only 10AM-6PM averages are used for O ₃ . Color scales are kept the same across all three emission scenarios.	63
4.14	Maps of predicted winter concentrations in $\mu\text{g}/\text{m}^3$ for (a) PM _{2.5} and (b) NO ₃ ⁻ . All hourly values are used for both pollutants. Other plot specifications are the same as in Figure 4.13.	64
5.1	Fine particle measurement sites in the San Francisco Bay area, with colors indicating annual averages.	70
5.2	Fine particle measurement sites in the San Joaquin Valley	71
5.3	Fine particle measurement sites in the South Coast Air Basin	72
5.4	Correlation between BAM and filter-based PM _{2.5} concentrations using data from 2009-2011. The solid lines represent linear regressions, the dashed lines represent the 1:1 relation, and the crosses show where solid and dashed lines intersect (see text).	74
5.5	Boxplots of daily average PM _{2.5} concentrations.	75
5.6	Distributions of hourly and daily-average PM _{2.5} measured at Riverside.	76
5.7	Diurnal variations in PM _{2.5} by season at selected sites, averaged over three-year periods. Summer season (red) is from June through August; winter season (blue) is from December through February. Dots represent means and the color bands represent 95% confidence intervals for hourly average PM _{2.5} concentrations. The exact years differ slightly from site to site depending on BAM data availability, but all profiles are for recent years between 2009 and 2013. Percentages following site names indicate the average changes in PM _{2.5} in winter relative to summer values.	79
5.8	Diurnal variations in PM _{2.5} for mid-week and weekend days at selected sites, averaged over three-year periods. Mid-week (yellow) is Tuesday-Thursday; weekend (green) is Saturday and Sunday. Percentages following site names indicate average changes on weekends relative to mid-week values.	80
5.9	Diurnal variations by season in PM _{2.5} in the San Francisco Bay area.	81

5.10	Diurnal variations by season in $PM_{2.5}$ in the San Joaquin Valley.	82
5.11	Diurnal variations by season in $PM_{2.5}$ in the South Coast Air Basin.	83
5.12	Diurnal variations by season in $PM_{2.5}$ in the San Francisco Bay area in periods 2004-2006 and 2011-2013.	84
5.13	Diurnal variations in $PM_{2.5}$ for mid-week (Tues-Thurs) and weekend (Sat-Sun) days in the San Francisco Bay area.	85
5.14	Diurnal variations in $PM_{2.5}$ for mid-week (Tues-Thurs) and weekend (Sat-Sun) days in the San Joaquin Valley.	86
5.15	Diurnal variations in $PM_{2.5}$ for mid-week (Tues-Thurs) and weekend (Sat-Sun) days in the South Coast Air Basin.	87
5.16	Diurnal variations by season in $PM_{2.5}$ in the San Francisco Bay area in periods 2004-2006 and 2011-2013.	88
A.1	NO_2 (blue) and NO_x (red) concentration boxplots from 1980 to 2014 for five sites: San Jose, Fresno, Bakersfield, Long Beach and Riverside. Blue horizontal lines indicate the current 100 ppb 98th percentile 1-hour daily maximum standard, and the 53 ppb annual mean standard, both for NO_2	95
A.2	NO_2 and NO_x concentration boxplot for two near-road sites in California, indicat- ing weekday/weekend and seasonal variations. Weekdays are Tuesdays through Thursdays and weekends are Saturdays and Sundays. Red represents warmer months (April to September) and blue represents colder months (October to March). Horizontal lines are the same standards as in Figure A.1.	96
A.3	NO_2 and NO_x concentration boxplot for two near-road sites and four ambient sites. Graphic features are similar to those in Figure A.2.	96
A.4	Scatter plots for NO_2 and NO_x concentrations in 2000 and 2010 and the respective linear fits. Measurements were taken at the North Long Beach site. Color schemes are the same as those in Figure A.2	97
A.5	Slopes (lines) and y-intercepts (dots) of linear regression done on NO_2 versus NO_x for five selected sites in California for two seasons. The bands around the line represent 95% uncertainty. Note that the missing data for some years is due to gaps in measurements.	98
A.6	Maps of selected NO_x monitoring sites in three major air basins in California. Sites were only shown if there were more than four consecutive years of data available during 2000-2014. Red indicates sites with clear trends in increasing ambient NO_2/NO_x ratios, gray indicates fluctuating ratios, and green indicates decreasing ratios.	99
A.7	Boxplots of NO_2/NO_x ratios by hour of the day.	100

List of Tables

2.1	Changes in ambient V, NSS-SO ₄ and SO ₂ concentrations following change in ship fuel. *	22
2.2	Contributions to ambient PM _{2.5} mass reductions in the San Francisco Bay area resulting from use of cleaner fuels in main engines of ships.*	25
3.1	Onroad measurements done in California used to derive fleet-averaged emission factors	30
4.1	Scaling factors used to modify emission inventories for 2016 and 2023.	48
4.2	Scaling ratios for NH ₃ from area sources by county.	48
4.3	Percentage (%) differences of weekday concentrations for four comparison cases. Mean ± standard deviation is reported. Sample sizes are N=11 for speciated PM _{2.5} measurements (BC, NO ₃ ⁻), N=24 for O ₃ ; N=16 for NO _x ; and N=14 for hourly PM _{2.5} measured by BAM. O ₃ concentrations were based on the 8-hour 10AM-6PM period. All other calculations were done on the 24-hour basis.	52
5.1	Number of PM _{2.5} monitoring sites and fractions of days sampled in selected California air basins. ^a	69

Acknowledgments

I would like to thank Professor Robert Harley, my Ph.D. advisor, for guiding me through my research and giving me countless intellectual and personal inspirations. I would also like to thank my preliminary and qualifying exam committee members, Tina Chow, William Nazaroff, Thomas Kirchstetter, John Balmes, Mark Stacey and David Sedlak, for their insightful advice on my research.

The work in this dissertation was made possible by funding from the following organizations: the University of California Transportation Center, the Carl W. Johnson Foundation, the University of California Multi-campus Research Program in Sustainable Transportation, and the California Air Resources Board. I would also like to acknowledge the Li Kuo Wei and Rong Yong Fellowship for financial support during my master's degree.

The California Air Resources Board, the Bay Area Air Quality Management District, and the South Coast Air Quality Management District have kindly provided me with data needed for my research.

I would like to thank my great colleagues at Berkeley who have provided me with both research and career advice as well as moral support: Brian McDonald, Tim Dallmann, Lucas Bastien, Chelsea Preble, Matt Vannucci, Yilin Tian, Regan Patterson, Xiaochen Tang, Seema Bhangar, and Sharon Shearer. Each one of them has been exemplary in their field and has helped me grow as a researcher. I am also very grateful for the collaboration with David Fairley from the Bay Area Air Quality Management District and Michael Kleeman from the University of California, Davis.

Lastly, I would like to dedicate this dissertation to my family members: My loving parents, Tao Tao and Lizhen Yun, who have always given me wise words and raised me in the best way possible; and my amazing husband, Adrien Pierre, who has brought so much more joy into my life than he himself could ever fathom. I would not be here without you.

Chapter 1

Introduction

1.1 Impact of air pollution

Nitrogen dioxide (NO_2), particulate matter with diameter less $2.5 \mu\text{m}$ ($\text{PM}_{2.5}$), and ozone (O_3) are three of the pollutants for which national ambient air quality standards have been established in the United States. Their ambient concentrations have been controlled under the Clean Air Act [141] due to their adverse impacts on human health and the environment.

NO_2 is an indicator for nitrogen oxides (NO_x), a sum of nitric oxide (NO) and NO_2 . In fact, most of the NO_x is emitted as NO from combustion and converted to NO_2 through reactions in the atmosphere. Studies have shown that short-term exposure to NO_2 has been associated with exacerbations of asthma and short-term exposure to NO_x can lead to inflammatory cardiovascular responses [152]. A study in Norway links mortality from respiratory diseases, lung cancer, and ischemic heart diseases to elevated NO_x concentrations near home addresses of the male participants [117]. NO_x and sulfur dioxide (SO_2) both produce acid rain that can harm forest and aquatic ecosystems and stone buildings and monuments, in addition to causing skin irritation. In the atmosphere, NO_x undergoes complex changes and hence acts as a precursor to many other pollutants, such as peroxyacetyl nitrate, nitric acid, ammonium nitrate aerosol, and O_3 .

$\text{PM}_{2.5}$ is a complex mixture of primary and secondary aerosol, both inorganic and organic. It is persistent in the atmosphere and can penetrate deeply into the lungs when inhaled. Past studies have shown clear correlation between chronic exposure to elevated $\text{PM}_{2.5}$ levels in urban areas with mortality rate [56, 96]. It is estimated that $\text{PM}_{2.5}$ contributes to approximately 800,000 premature deaths per year worldwide [150]. The composition of inhaled PM and the duration of exposure are both hypothesized factors that lead to adverse biological responses. Jacobs *et al.* [82] found that blood pressure of hypertensive elderly persons is positively correlated with short-term (24-hour) exposure to $\text{PM}_{2.5}$ and also the amounts of trace metals such as vanadium and nickel in $\text{PM}_{2.5}$. Salvi *et al.* [129] demonstrate that 1-hour exposure to $300 \mu\text{g}/\text{m}^3$ of particulate matter from diesel exhaust produced marked

pulmonary inflammatory responses in healthy humans. Short-term exposure to both $\text{PM}_{2.5}$ and NO_x has been found to affect sensitive groups, specifically, children with asthma [100]. In addition, $\text{PM}_{2.5}$ also contributes to direct and indirect radiative forcing to the atmosphere, through scattering, absorption, and cloud formation [98].

O_3 is formed from atmospheric photochemical reactions. It has been shown that even short term exposure to O_3 on the timescale of one day would increase mortality rate by 0.27-0.77%, mostly due to cardiovascular and respiratory diseases [19]. Long term exposure to ozone has been associated with increased mortality rate caused by respiratory diseases, significant over every 10 ppb of increase in concentrations [84]. Sensitive groups include children and the elderly [18]. O_3 and photochemical smog levels are typically elevated on days when its precursors (volatile organic compounds (VOC) and NO_x) are present at high concentrations on sunny days with high temperatures.

Complex relationships exist between NO_x , $\text{PM}_{2.5}$ and O_3 , and controlling their ambient concentrations becomes especially challenging in areas with a range of emission sources. California is one such area that has received ongoing attention for air pollution mitigation.

1.2 Air pollution in California

The battle against air pollution in the State of California has always been interesting because the state has a large economy and population, a climate that is sometimes favorable to pollutant formation, a mix of biogenic and anthropogenic emission sources, and a long regulatory history. California had 12% of the population in the US in 2015, and produced 14% of the total national Gross Domestic Product (GDP). Among the top ten US cities with the highest populations, three are located in California. Although the industries contributing the most to GDP are not traditional high polluters, the transportation sector and oil and gas refining and exploration activities contribute greatly to regional air quality problems.

Despite the lack of coal fired power plants that are responsible for sulfur dioxide and particulate sulfate in the Northeastern US, California faces photochemical smog and large amounts of organic aerosol formation due to its sunlight levels in the summer, and elevated particulate nitrate and other pollutants in the winter due to cooler and more stagnant conditions. There are other sources emitted according to seasons, such as summer wildfires, winter residential wood-burning, and some agriculture practices. In addition, some cities are situated in valleys that encounter occasionally severe stagnation events which cause low dispersion rates of pollutants in the boundary layer.

As a result, California is not in attainment of all the federal air quality standards, as of 2016. For instance, 19 out of 58 counties were under serious to extreme non-attainment under the 1997 8-hour O_3 standard, and 20 under the 2008 standard; 12 out of 58 counties were in moderate to serious non-attainment for 1997 $\text{PM}_{2.5}$ standards, and 14 for the 2012 standard.

All other criteria pollutant standards were met as of 2016.

Due to the difficulty and long history of air pollution problems, California has adopted many regulations in addition to those required by the EPA. A waiver was granted in 1967 for California agencies to enforce the state's own (and more stringent) emission standards. California was the first state to adopt vehicle tailpipe NO_x standards (1971) and limit lead concentrations in gasoline (1976), implement a smog check program (1985), ban MTBE in clean-burning reformulated gasoline (1999), regulate statewide greenhouse gas emissions (2006), and mandate retrofit or replacement of drayage trucks accessing ports and rail yards (2010) [34]. Air pollution has been reduced thanks to the array of regulations, despite the fact that the population has doubled and vehicle registration grew by 250% due to increased urbanization in many regions.

Understanding the air quality impacts brought about by these regulations helps to validate the efforts by the agencies and stakeholders involved, and provides reference cases for other states and countries considering similar air pollution control policies. This is one of the main motivations for the present dissertation: to examine specific regulations and resulting changes in air quality.

1.3 Regulated emission sources in California

Most anthropogenic emission sources are regulated in California, and many have seen increasingly stringent standards over time. The focus of this dissertation is on two major source categories, on-road vehicles and ocean-going vessels, but encompasses effects of many other emission regulations as well.

Gasoline and diesel engines make up the majority of on-road vehicles in the US. Proximity to roadways has been found to be correlated with decreased lung functions in adults with asthma [14]. In terms of regulations, gasoline engines have been required to use reformulated fuel since 1992 to minimize emissions of volatile organic compounds (VOC) that are harmful to health, such as benzene, and to reduce ozone formation. It is estimated that the use of the new fuel formulation resulted in a 43% of reduction in VOC, 18% in NO_x [92], 8-13% in O_3 in the Los Angeles area, and 3-15% in O_3 in the San Francisco area [97]. In addition, all passenger vehicles registered within O_3 non-attainment areas are required to go through smog checks. This program aims to remove or repair the dirtiest vehicles from contributing a significant portion of emissions. California also requires a more stringent set of light duty vehicle emission standards than the federal rules, such as enforcing Low Emission Vehicle (LEV) standards from 1994 to 2003, LEV II from 2004-2014, and LEV III from 2015-2025. Post-combustion emission control was incorporated into gasoline engines earlier than diesel engines, for instance, the three-way catalytic converters which oxidizes carbon monoxide (CO) to carbon dioxide (CO_2) and reduces NO_x to nitrogen.

In the US, diesel engines are more often used in heavy-duty trucks for long-distance freight transport. The industry has a slower engine turnover rate compared to light-duty gasoline vehicles, resulting in grandfathering of older, high-emitting vehicles. For instance, a tunnel measurement done in Oakland, California finds that 20% of trucks account for 64% of black carbon emissions from the entire diesel truck fleet [53]. In 1998, California officially recognized diesel particulate matter as a toxic air contaminant. In contrast to gasoline engines, diesel trucks emit more particles and NO_x but less CO and VOC, due to incomplete air-fuel mixing and differences in combustion stoichiometry and temperature. There are federal standards on diesel emissions, similar to those for gasoline engines, but California has started to implement a program that phases out older diesel engines gradually over a decade, and accelerates the turnover rate for old engines. The program aims to remove, for instance, the pre-1994 engines by 2014, 1994-1995 engines by 2015, and finally, all pre-2010 models by the year 2023. Figure 1.1 shows projections of NO_x emissions in California with and without the accelerated diesel replacement program.

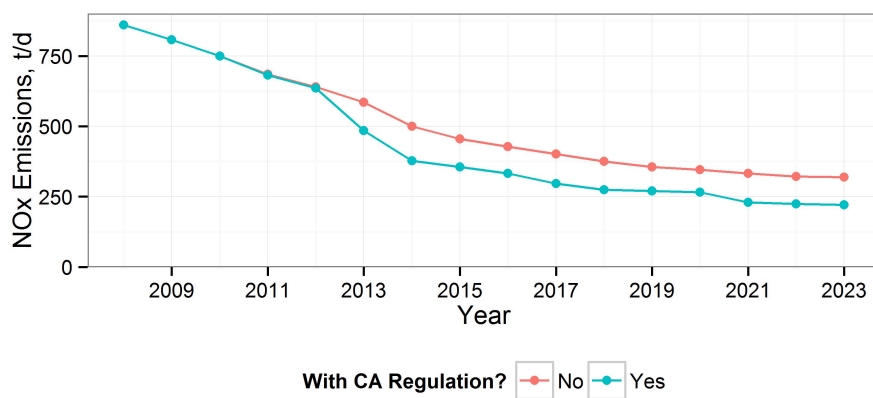


Figure 1.1: Projected statewide NO_x emissions with and without the accelerated diesel engine replacement program mandated by the California Air Resources Board. Some adjustments to the implementation schedule were made after the regulation was adopted (not shown here).

Ocean-going vessels make significant contributions to air pollution in California because the state has a long coastline as well as several major ports, including Los Angeles/Long Beach, which is the busiest port in the US. In 2009, California mandated that all vessels within 24 nautical miles of the coastline had to burn low-sulfur fuels, instead of the more traditional heavy fuel oil. In addition, there exists a voluntary speed reduction program for these vessels, encouraging shippers to slow to 12 knots near-shore by providing financial incentives. Both programs reduce the emission rates of heavy metals, $\text{PM}_{2.5}$, SO_2 , NO_x , as well as greenhouse gases.

Besides the three major mobile source categories mentioned above, there are other air quality regulations in California that are covered peripherally by this dissertation. Another major source of emissions in coexistence with ships is port operations, which includes: docking, drayage trucks at the port, and other off-road equipment such as harbor craft and cranes for cargo handling. These sources have also been included in emission reduction plans, for instance, increasing use of shore-power for vessels at berth, the drayage truck regulation similar to that of on-road diesel trucks but starting earlier, and various rules on low-sulfur fuel and engine idling for off-road diesel equipment.

Advances in measurement methods for air pollutants do not directly affect emissions, but help the assessment of pollution control immensely. Continuous measurements of $PM_{2.5}$ first became a federal equivalent method to the traditional filter depositing-weighing method in California. It provides much higher measurement frequency (hourly) in real-time, while reducing operation costs and enhancing spatial coverage. Air districts have also started to measure near-roadway NO_x concentrations. The near-roadway NO_x data provide more points of reference for community exposure as well as additional validation data for air quality models.

1.4 Research objectives

The research in this dissertation has been motivated by the need to assess the changes in emissions and ambient air quality due to a series of regulations in California, with the goal of providing objective analysis and examples for other jurisdictions aiming to reduce air pollution. More specifically, the research aims to:

1. quantify the historical changes in ambient $PM_{2.5}$ concentrations due to the switch from high-sulfur heavy fuel oil to cleaner fuels in 2009 (Chapter 2);
2. quantify the present and future changes in ambient $PM_{2.5}$, NO_x and O_3 concentrations due to the accelerated diesel engine replacement program along with other major projected changes, using deterministic air quality modeling (Chapter 4);
3. evaluate the California on-road motor vehicle emission inventory using an independent fuel-based emission inventory calculated using real-world measurements from roadway and tunnel studies (Chapter 3);
4. identify features and causes in time series of ambient $PM_{2.5}$ pollutant concentration measurements on diurnal, weekly, seasonal and decadal time scales (Chapter 5).

Chapter 2

Effects of Switching to Lower Sulfur Marine Fuel Oil on Air Quality in the San Francisco Bay Area

2.1 Introduction

Shipping is a significant source of air pollution both globally and for urban areas near sea ports [142, 60, 49, 13, 57]. It has been estimated that international shipping accounts for 14% of nitrogen oxides (NO_x) emissions and 5% of sulfur oxides (SO_x) emissions from all fossil fuel sources [71], and that about 60,000 deaths can be attributed to shipping-related particulate matter (PM) [50]. Regionally, near the Ports of Los Angeles and Long Beach, primary particle emissions from shipping are responsible for up to $\sim 9\%$ of total $\text{PM}_{2.5}$ concentrations [3]. Due to lax fuel quality standards in the past, commercial marine vessels typically burned heavy fuel oil (HFO), which has high sulfur content. Environmental concerns related to HFO combustion include emissions of pollutants such as SO_x , $\text{PM}_{2.5}$, and heavy metals. Therefore, quantifying vessel emissions in the urban context is relevant to public policy making in the transportation sector, due to the influence of ship traffic and emissions on populated areas, and the increasing volume of global sea trade.

Various methods have been employed to estimate the impacts of shipping on air quality. On-board *in situ* measurements of ship exhaust provide emission factors for representative fuel and vessel types under various load conditions [122, 149, 2], and examine the chemical characteristics of the exhaust [57, 113]. In particular, Williams *et al.* reported emission factors of nitrogen oxides (NO_x), sulfur dioxide (SO_2), carbon monoxide (CO) and formaldehyde (HCHO) for ~ 200 ships, both underway and stationary, in the Gulf of Mexico, and empha-

This chapter is a reproduction of the publication: Tao, L., Fairley, D., Kleeman, M. J., & Harley, R. A. (2013). Effects of switching to lower sulfur marine fuel oil on air quality in the San Francisco Bay area. *Environmental Science and Technology*, 47(18), 1017110178. <http://doi.org/10.1021/es401049x>

sized their variability which can lead to emissions modeling uncertainty [148]. To study aging effects on ship plumes, Murphy *et al.* used a research aircraft to measure emissions from a Post-Panamax class container ship and found that the mass ratio of particulate organic carbon (OC) to sulfate increases as the exhaust plume travels downwind, possibly due to condensation processes taking place in the exhaust [116]. Other experimental assessments of ship emissions include pollutant concentration measurements in ship plumes in the harbour of Göteborg, Sweden, showing the ship-related deposition of SO₂ to be significant for the city [81]; proposal of the vanadium-to-nickel ratio as a tracer for vessel activities [142]; and measurements near the ports of Los Angeles and Long Beach that suggested primary PM emissions from ships contribute as much as 8.8% of total PM_{2.5} at nearby receptors [3]. The available database of emission factors for marine vessels enables the construction of regional and global emission inventories [78, 60]. Several source apportionment studies have estimated the contribution of shipping activities to urban PM_{2.5} [102, 114, 90]. Vutukuru *et al.* employed an air quality model and concluded that 10% of ambient PM_{2.5} mass is due to ship emissions in the South Coast Air Basin [143]. Aircraft measurements of plumes from a container ship approaching the Port of Los Angeles have shown that use of cleaner fuel and vessel speed reduction together led to the significant decreases in emission factors: 91% for SO₂, 90% for PM, and 41% for black carbon (BC) [95].

The Port of Oakland in the San Francisco Bay area is the fourth busiest container port in the United States [125], recording around 2,000 ship arrivals per year [73]. Port-going heavy diesel trucks have been retrofit or replaced, with major reductions in emission factors of BC and NO_x [52]. A subsequent study of speciated fine particle concentrations at the Port of Oakland found that before and after the truck retrofit program, ships accounted for 12 and 29% of BC concentrations, respectively [94]. We are not aware of previous studies reporting on changes in emissions from ocean-going vessels at the Port of Oakland.

Beginning in July 2009, vessels operating within 24 nautical miles (44 km) of the California coast were required to switch from using high-sulfur HFO in their main engines to marine gas oil (MGO) or marine diesel oil (MDO) with lower sulfur contents [67]. Average fuel sulfur content is expected to drop from 2.4 to 1.5% or lower by 2009, 1.0% or lower by 2012, and eventually to < 0.1% by 2014 [131, 1]. In addition, ships operating within 200 nautical miles (370 km) of the coast are subject to a North American Emission Control Area that limits fuel sulfur content to 1%, beginning August 2012 [80]. The fuel change in 2009 may have had immediate and noticeable effects on ship emissions, and will augment emission reductions achieved by other measures, such as the use of lower sulfur fuels in auxiliary engines [66], and the California Shore Power Program [35], which is beginning to supply a fraction of ships berthed at the Port of Oakland with electric power.

In this study, we use vanadium as a tracer for HFO combustion since it is uniquely enriched in heavy fuel oil [90], and there are no other sources that saw significant changes during the time span of interest here. We examine the effects of the 2009 ship fuel regulation on

ambient air pollutant concentrations in the Bay Area from 2005 to 2011, both at the West Oakland monitoring site near the Port, and in the larger surrounding region.

2.2 Approach

Measurements

We acquired available data from ten urban ambient air measurement sites managed by the Bay Area Air Quality Management District (BAAQMD), and two rural sites, Pinnacles and Point Reyes from the Interagency Monitoring of Protected Visual Environments (IMPROVE) network [48]. The starting dates for the data record from each site vary from 2005 to 2009, with data continuing to the end of 2011 or beyond. The locations of the sites considered in the analysis are shown in Figure 2.1.

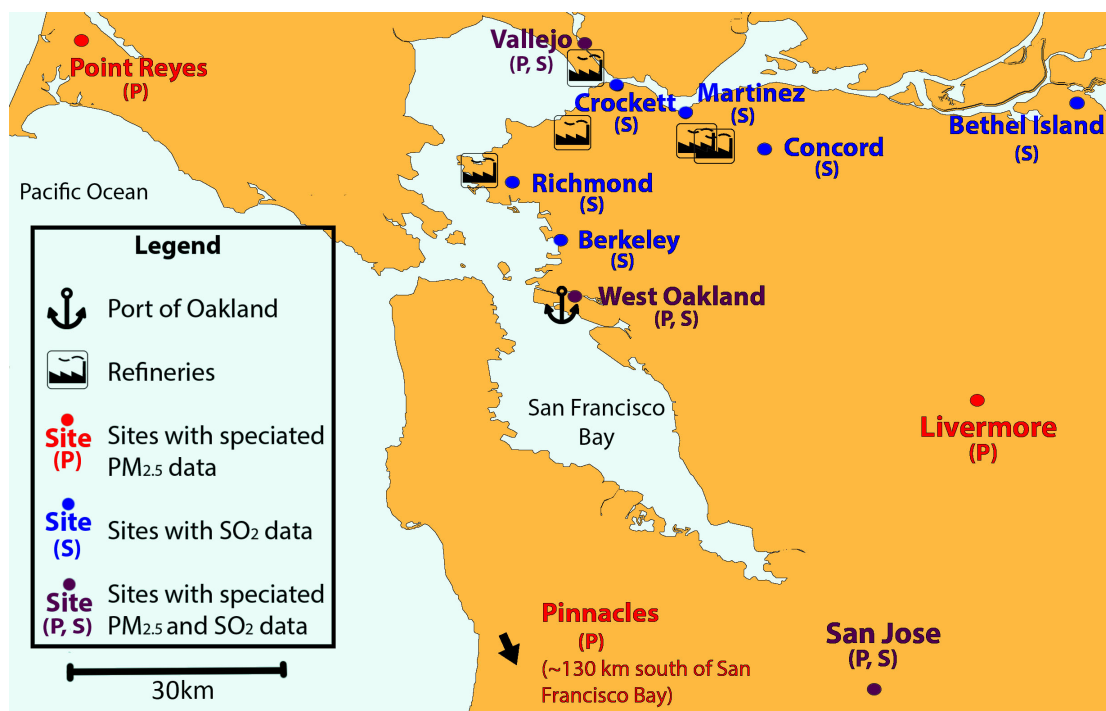


Figure 2.1: Ambient air measurement sites in the San Francisco Bay area. Also shown are the Port of Oakland and the major oil refineries.

BAAQMD measures SO₂ continuously using pulsed fluorescent analyzers, and reports measured values as hourly averages. We computed daily averages for sites and days on which at least 75% of the hourly data were present. Using this criterion, 98% of the days have data available at Concord, Richmond, Crockett, Bethel Island, Martinez and Vallejo; Berkeley

has 74% data availability; West Oakland, 69%; San Jose, 68%. Some sites show extended periods with an apparent 1 ppb offset in the SO_2 baseline; these time periods were excluded from further analysis. The 1 ppb SO_2 offset is possibly due to calibration problems. Periods with the offset are shown in Figure 2.2.

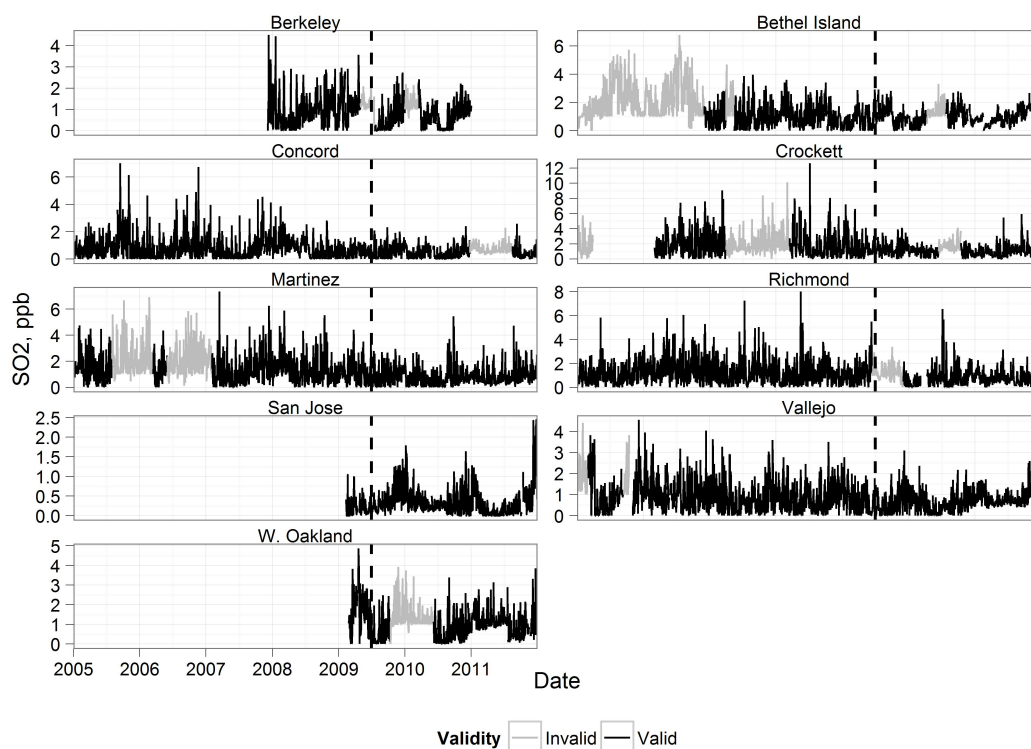


Figure 2.2: Time series plots of ambient sulfur dioxide concentrations at Bay area monitoring sites. The black dashed line marks the July 2009 effective date of the low-sulfur fuel regulation for main engines.

BAAQMD acquires detailed data on fine particle mass and chemical composition at four Bay area sites: West Oakland, Vallejo, Livermore and San Jose. Filter samples are collected on a once every sixth day schedule, and subsequently analyzed in the laboratory to quantify fine particle mass (gravimetric), water-soluble ions (by ion chromatography), and trace elements (by X-ray fluorescence). West Oakland, Vallejo and Livermore’s filter samples are analyzed at the Desert Research Institute (DRI), whereas filter samples from San Jose are analyzed by a different laboratory (RTI) [64]. Additional sites measuring only fine particle mass without speciation were not included in this analysis.

Fine particle mass concentrations and speciation were also measured at more remote and generally cleaner sites (Point Reyes and Pinnacles) from the IMPROVE network. There were various differences in sampling and analysis compared to the urban sites described

above. For example, IMPROVE filter samples were collected once every third day and a more sensitive analytical technique was used for trace elements (inductively coupled plasma-mass spectrometry, ICP-MS).

The most relevant data for this study are the results for fine particulate vanadium and sulfate. To remove the contribution of sea spray/marine aerosol to measured sulfate concentrations, we used sodium as a tracer for sea salt, and subtracted $0.25 \times$ measured sodium from sulfate concentrations to obtain non-sea salt (NSS) sulfate [107]. The ratio of 0.25 stays relatively constant ($\pm 1.5\%$) as salinity varies [16].

Characteristics of Fuels

Heavy fuel oil or HFO, also known as residual fuel or bunker oil, was used in 99% of main engines and 75% of auxiliary engines in ships prior to the regulation [136]. The average sulfur content of HFO for vessels berthing in California was 2.4% by weight in 2007 [131].

We select vanadium as an indicator for HFO combustion in this study. Source profiles for HFO combustion include sulfur compounds and some heavy metals such as barium and nickel, with vanadium as the most distinctive tracer [90, 2]. The vanadium-to-nickel ratio has been proposed in the past to identify shipping emissions, but the ratio varies according to port locations [142, 132]. Positive matrix factorization (PMF) and chemical mass balance (CMB) are also popular receptor-oriented models that can be used to derive contributions to $PM_{2.5}$ from different sectors. The use of PMF requires more input data than a once per six days sampling schedule provides. CMB requires detailed source profiles in addition to ambient concentration data, and cannot apportion source contribution to secondary pollutants such as sulfate [3, 102, 114, 90]. Regional pollutant dispersion models can be applied to take into account local topography and meteorology, but require even more information such as a gridded emission inventory [3, 143]. In California, shipping has been identified as a dominant source of vanadium emissions [134], and vanadium has proved to be a more robust marker than nickel [3]. Refineries in the Bay area could be a source of vanadium emissions. Since refinery throughputs have remained fairly stable in recent years, emissions of vanadium from refineries are not expected to have changed dramatically. Electricity generation using HFO is another source of vanadium emission. However, California generates electricity using mainly natural gas and nuclear power, and oil generation constitutes less than 3% of the total electricity output [38]. In the absence of major changes in the petroleum refining sector, it is practical to use changes in ambient vanadium concentrations to assess changes in emissions from the shipping sector.

Vanadium content in HFO varies depending on the source of crude oil and refining processes; a fuel weight fraction of 100 ± 47 ppm was reported in a prior study for California [3]. MGO and MDO are low-sulfur marine distillate fuels, required to be used in main engines of ships after July 2009. These fuels have sulfur contents lower than 1.5% and 0.5%, respectively

[67]. Vanadium content is less than 1 ppm in MGO and MDO [85].

We looked for changes in measured ambient concentrations of fine particulate vanadium and NSS-sulfate, associated with the change in ship fuel. Measured changes in vanadium were also used to infer related decreases in unburned heavy fuel oil (i.e., primary organic aerosol). We assumed EC emissions from ships are governed mainly by combustion conditions rather than fuel variables [95], and thus do not contribute significantly to changes in ambient $PM_{2.5}$ concentration. Also note that changes in ambient sulfate can result from both changes in primary sulfate emissions from ships, and due to reduced secondary formation of sulfate as a result of lower SO_2 emissions.

Statistical Analysis

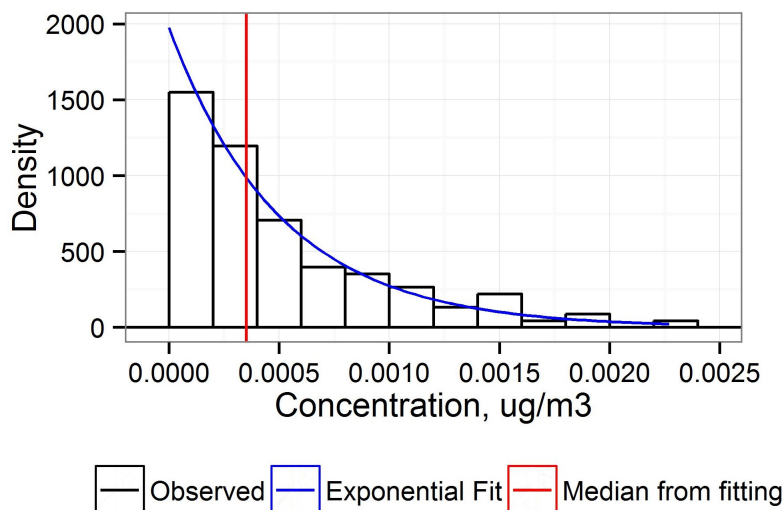


Figure 2.3: An example of exponential fitting to trace metal concentrations. The plot shows the distribution of vanadium concentrations at Point Reyes from July 2009 to June 2010 and its exponential fitting. The median obtained from fitting is $0.00035 \mu\text{g}/\text{m}^3$, marked in red.

Standard t-tests were used to compare means and Mann-Whitney tests were used to compare medians of concentrations of vanadium, sulfate and SO_2 , before and after July 2009. The Mann-Whitney test is a robust non-parametric method to compare the medians of two presumably statistically independent samples that does not assume a normal distribution [77]. For pairs of samples that differ significantly ($p < 0.05$) according to Mann-Whitney test, we used the Hodges-Lehmann estimator to quantify changes in the medians of the sulfate and SO_2 concentrations. For these pollutants, the relative changes were calculated by dividing the Hodges-Lehmann estimator by the mean of the concentrations before July 2009. Two-sample t-tests were also performed and were excluded from the report as their confidence intervals are consistent with those based on the Mann-Whitney test.

For trace metals such as vanadium, the means could change substantially if enough concentrations are below the limit of detection (LOD); when more than 50% of the observations are below the LOD, then medians become unsuitable for comparison as well. Therefore, we assumed the distributions of trace metals were exponential[74] and used maximum likelihood to estimate the medians. An example of exponential fitting for vanadium concentrations from July 2009 to June 2010 at Point Reyes is shown in Figure 2.3, and is representative of the goodness of fit for all other locations and periods. The reported absolute change in vanadium concentration is the difference of the medians from the two periods. Concentrations of trace metals reported as below LOD were treated as zeroes in the calculation of means.

All the graphics and statistical analysis were carried out using the open source programming language R [128, 146, 147].

2.3 Results and Discussion

Trends in key indicators of fuel change

Concentrations of vanadium decreased at Livermore, Point Reyes, Vallejo and West Oakland, around the effective date of the ship fuel regulation, as shown in Figure 2.6. This decrease is more evident in the box-and-whisker plots (Figure 2.7), where the sizes of the boxes (i.e., the inter-quartile range of concentrations) all shrink after the fuel change. West Oakland, Vallejo and Livermore show decreases in median vanadium concentrations that are of the same order of magnitude. At San Jose, decreases in vanadium concentrations were evident starting in 2008. San Jose is at the south end of San Francisco Bay and is more remote from shipping activities compared to West Oakland. At Pinnacles and Point Reyes, the absolute V concentrations are lower, also due to more remote locations away from port-related activities. Similar magnitudes of decrease in vanadium have been reported in Southern California comparing year 2005 and 2012 in preliminary results from the Multiple Air Toxics Exposure Study (MATES) [69]. Changes in vanadium concentrations shown in Figures 2.7 cannot be explained by fluctuations in ship traffic in the Bay area, since the latter varied less than 10% from year to year (Figure 2.4), and the number of ship calls has been stable or increasing since 2009, at the same time that vanadium concentrations are falling. Wind patterns were similar across years for all four urban sites. An example of wind rose diagrams is shown in Figure 2.5. Nickel has been purposed in literature to be another tracer of HFO. However, we find that neither the time series (Figure 2.8) nor the boxplots (Figure 2.9) show clear downward trends during the time period of interest, possibly due to the relatively large amount of nickel emitted from the nearby refineries.

Decreases in sulfate are not as large in relative terms as those observed for vanadium. However, box-and-whisker plots for NSS-sulfate (Figure 2.10) still indicate clear downward trends. The observed values span a lower range of concentrations after July 2009. At Pinnacles and

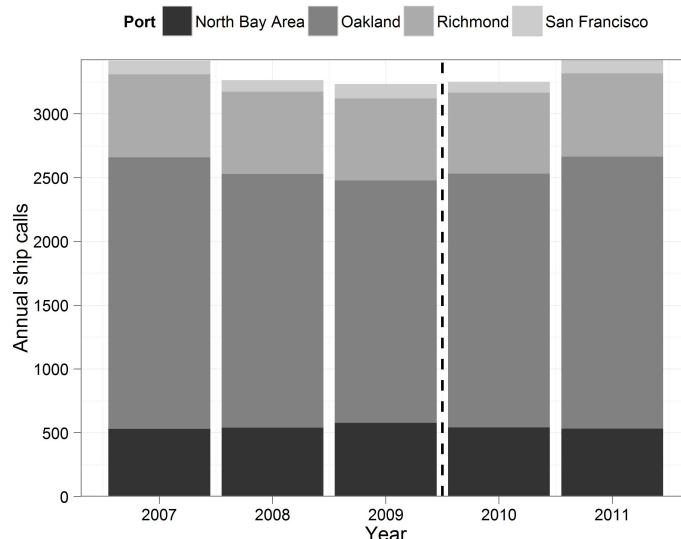


Figure 2.4: Annual ship calls in the San Francisco Bay area by major port from 2007 to 2011.

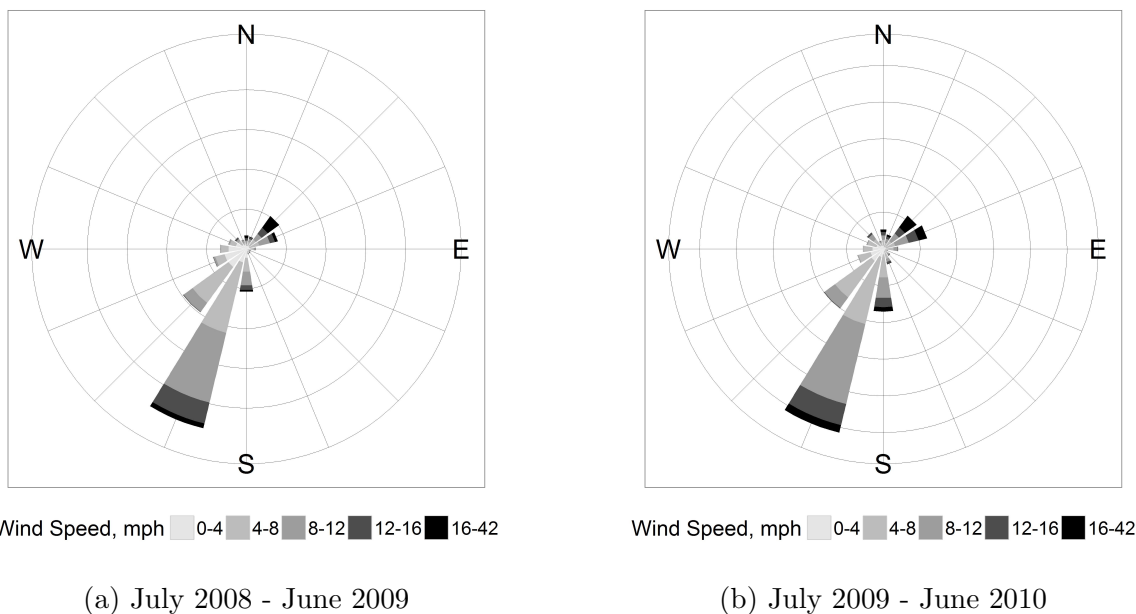


Figure 2.5: Wind rose pattern near the West Oakland air monitoring site.

Point Reyes, the decrease in sulfate is more pronounced than the decrease in vanadium. These two locations may experience a larger contribution from secondary sulfate as ship-emitted SO_2 has more opportunity for oxidation to sulfate in transit to these locations.

Sulfate concentrations have been separated into two categories: anthropogenic and sea-salt sulfate. Figure 2.11 shows that the anthropogenic contribution to overall sulfate concentrations is generally much larger than the natural source, except at Point Reyes. Day-to-day weather differences introduce large variations in Figure 2.11 in the contributions from sea-salt sulfate. It should also be noted that all sites show seasonal variability in total sulfate concentrations, with high values during summer and low values during winter. As will become clear in the next section, for the anthropogenic sulfate fraction, the change in primary sulfate after July 2009 due to the fuel change is small compared to the effects on secondary sulfate formation.

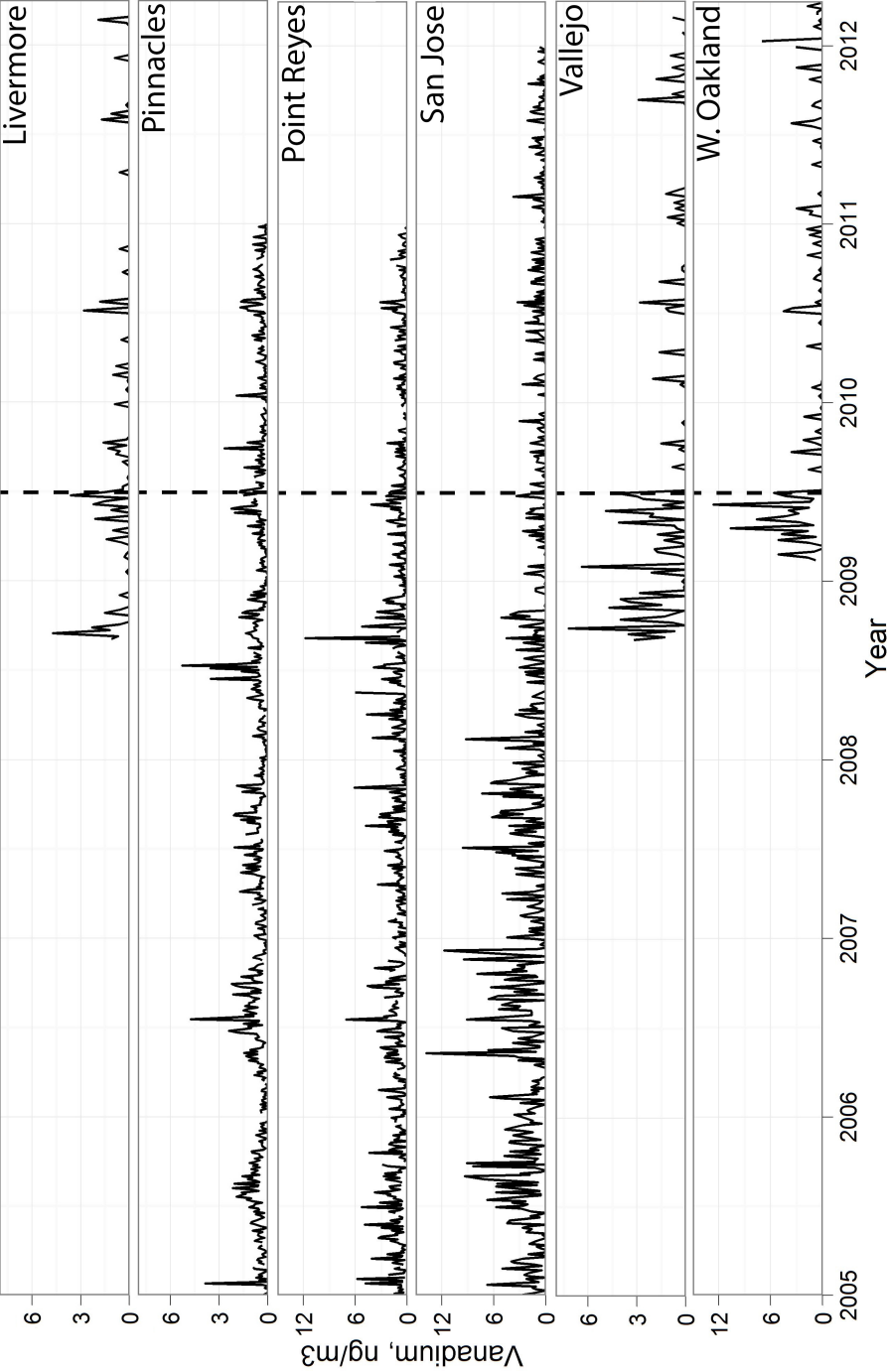


Figure 2.6: Time series plots of ambient vanadium concentrations at Bay area monitoring sites. The black dashed line marks the July 2009 effective date of the low-sulfur fuel regulation for main engines.

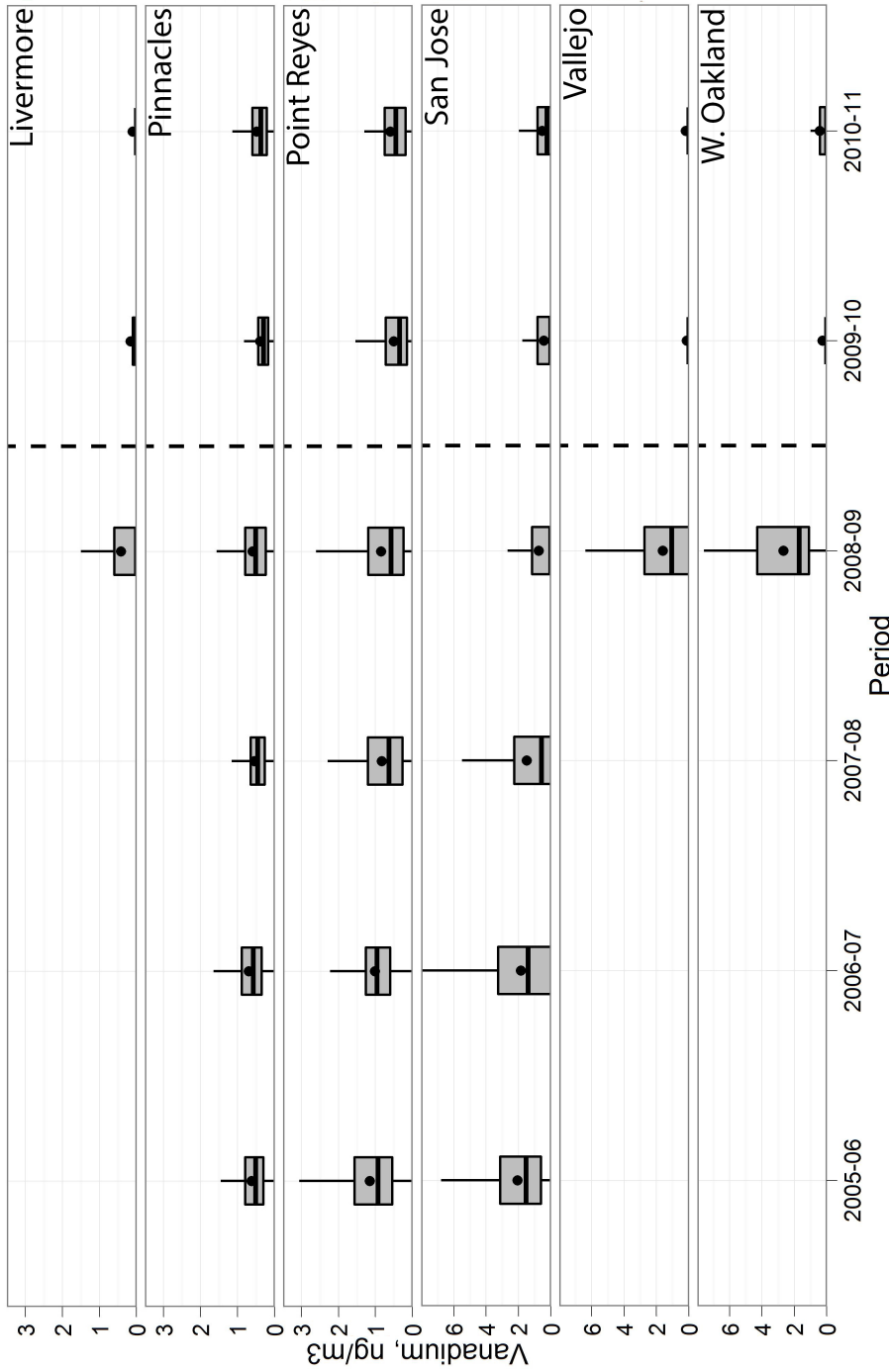


Figure 2.7: Box-and-whisker plots of ambient vanadium concentrations. Plots are based on measured data. Annual distributions are presented using data from July 1 through June 30 of the following year, to align pollutant data with the mid-year change in ship fuel in 2009 (shown as a dashed line). Each box represents the 25th to 75th percentile range for a given site and year. Each pair of whiskers extend from the hinge to the highest and the lowest values that are within 1.5 times the inter-quartile range, respectively. The median and mean are marked using a horizontal line and a dot, respectively. The West Oakland box for 2008-09 is based on partial year data from 2009 only. The black dashed line marks the July 2009 effective date of the lower sulfur fuel regulation for main engines.

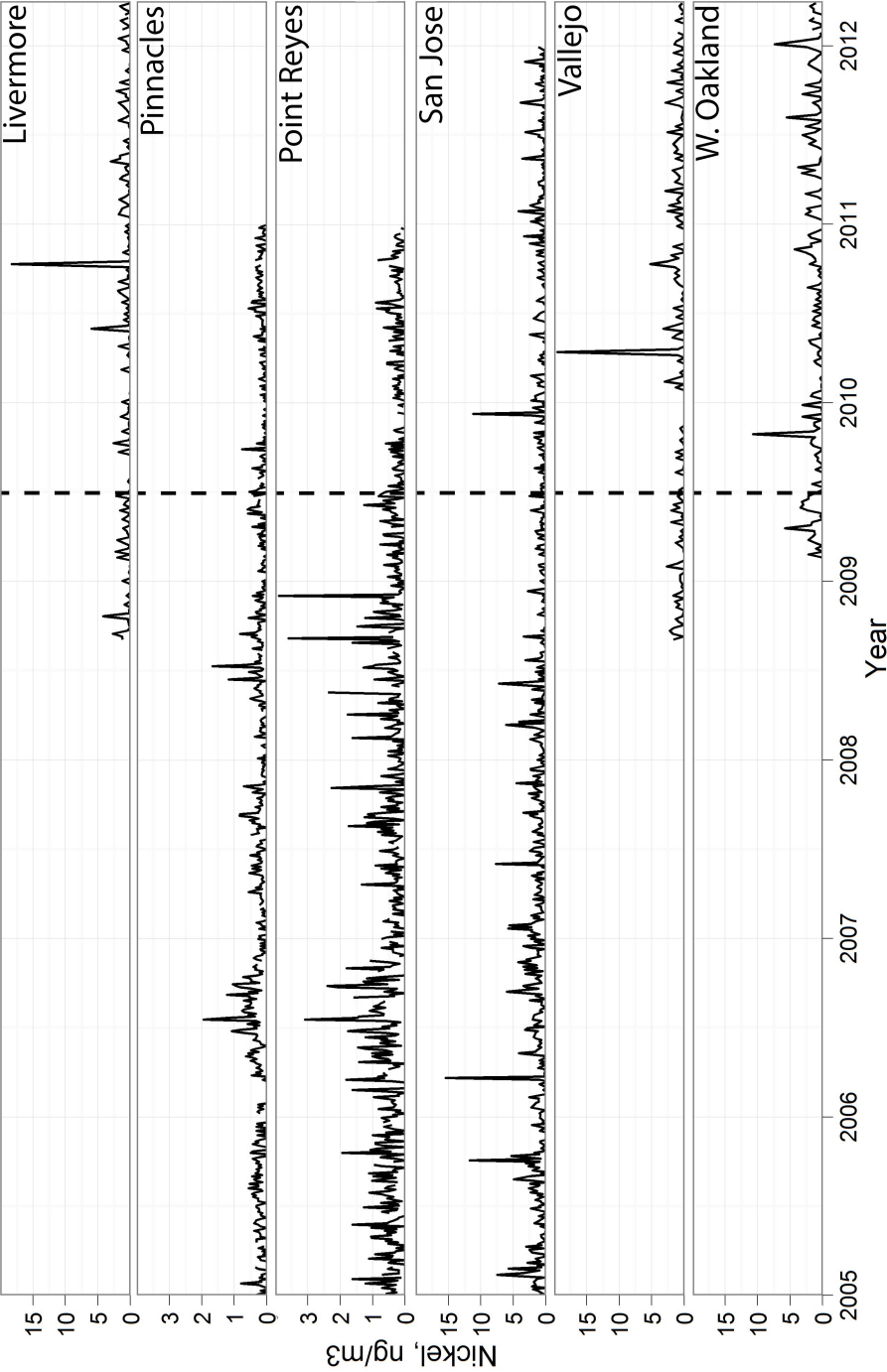


Figure 2.8: Time series plots of ambient nickel concentrations at Bay area monitoring sites. The black dashed line marks the July 2009 effective date of the low-sulfur fuel regulation for main engines.

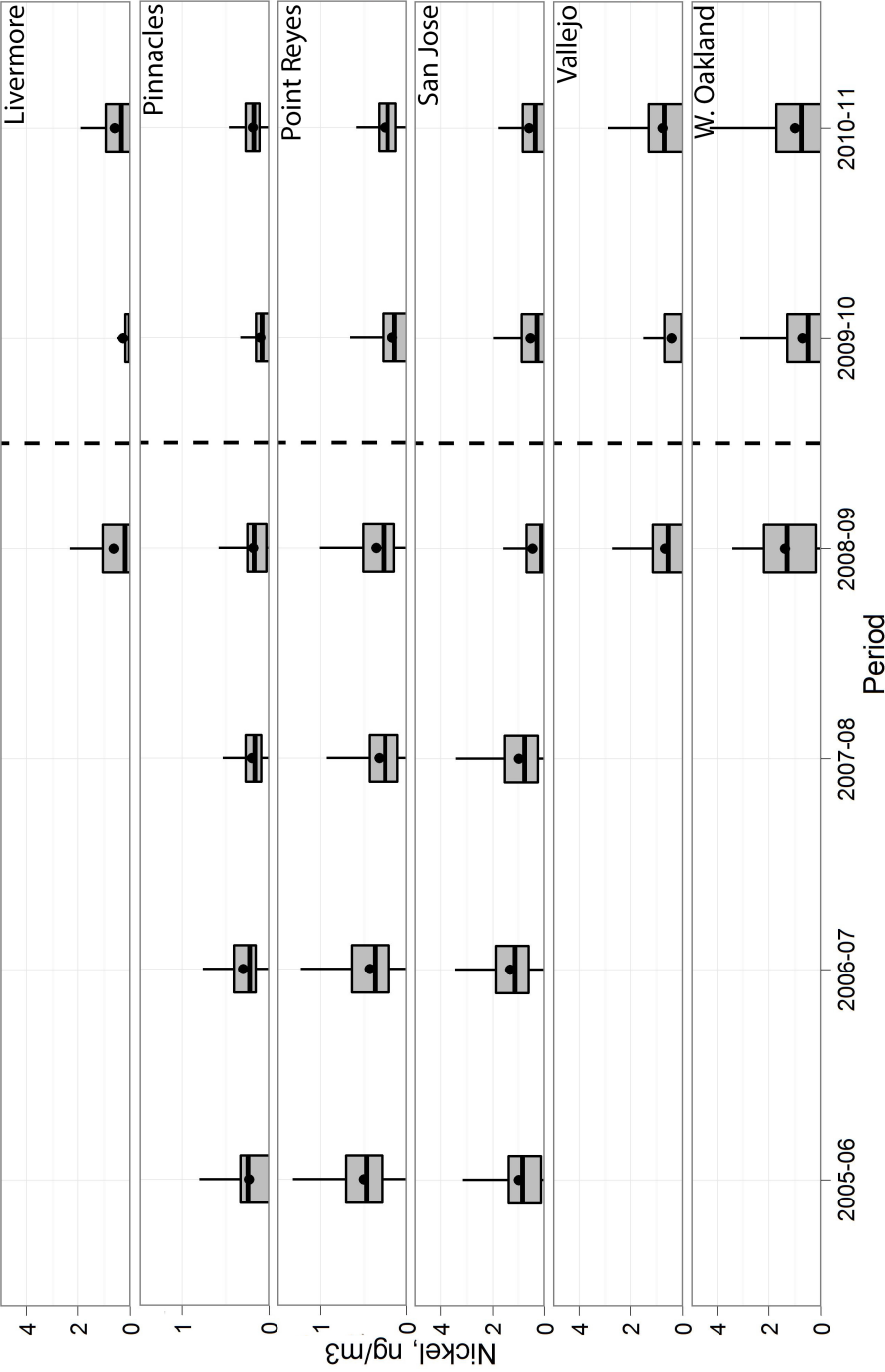


Figure 2.9: Box-and-whisker plots of ambient nickel concentrations. Annual distributions are presented using data from July 1 through June 30 of the following year, to align pollutant data with the mid-year change in ship fuel in 2009 (shown as a dashed line). Each box represents the 25th to 75th percentile range for a given site and year, with the median and mean marked using a horizontal line and a dot, respectively. The West Oakland box for 2008-09 is based on partial year data from 2009 only

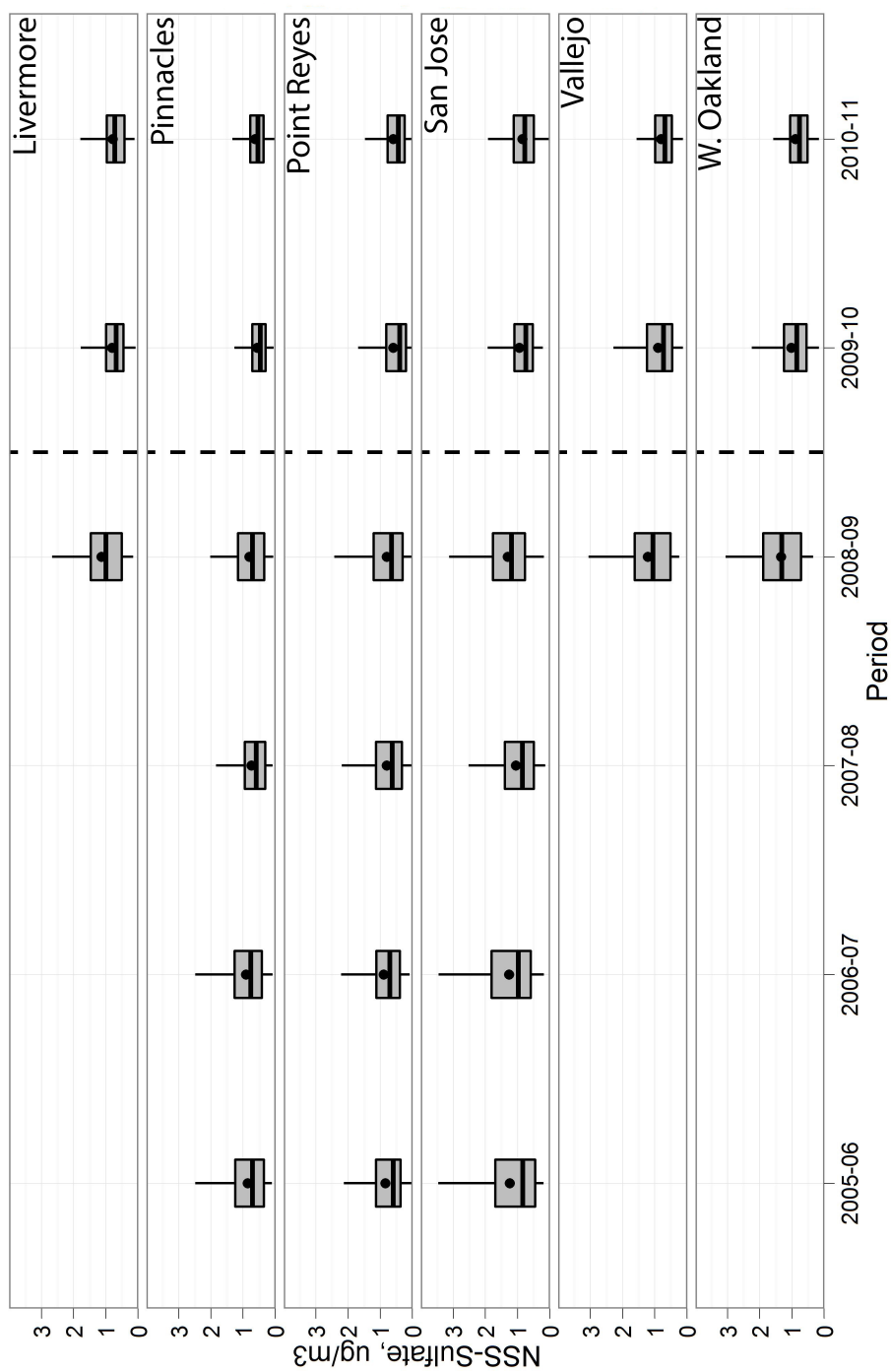


Figure 2.10: Box-and-whisker plots of ambient non-sea-salt sulfate concentrations. Other details are the same as in Figure 2.7.

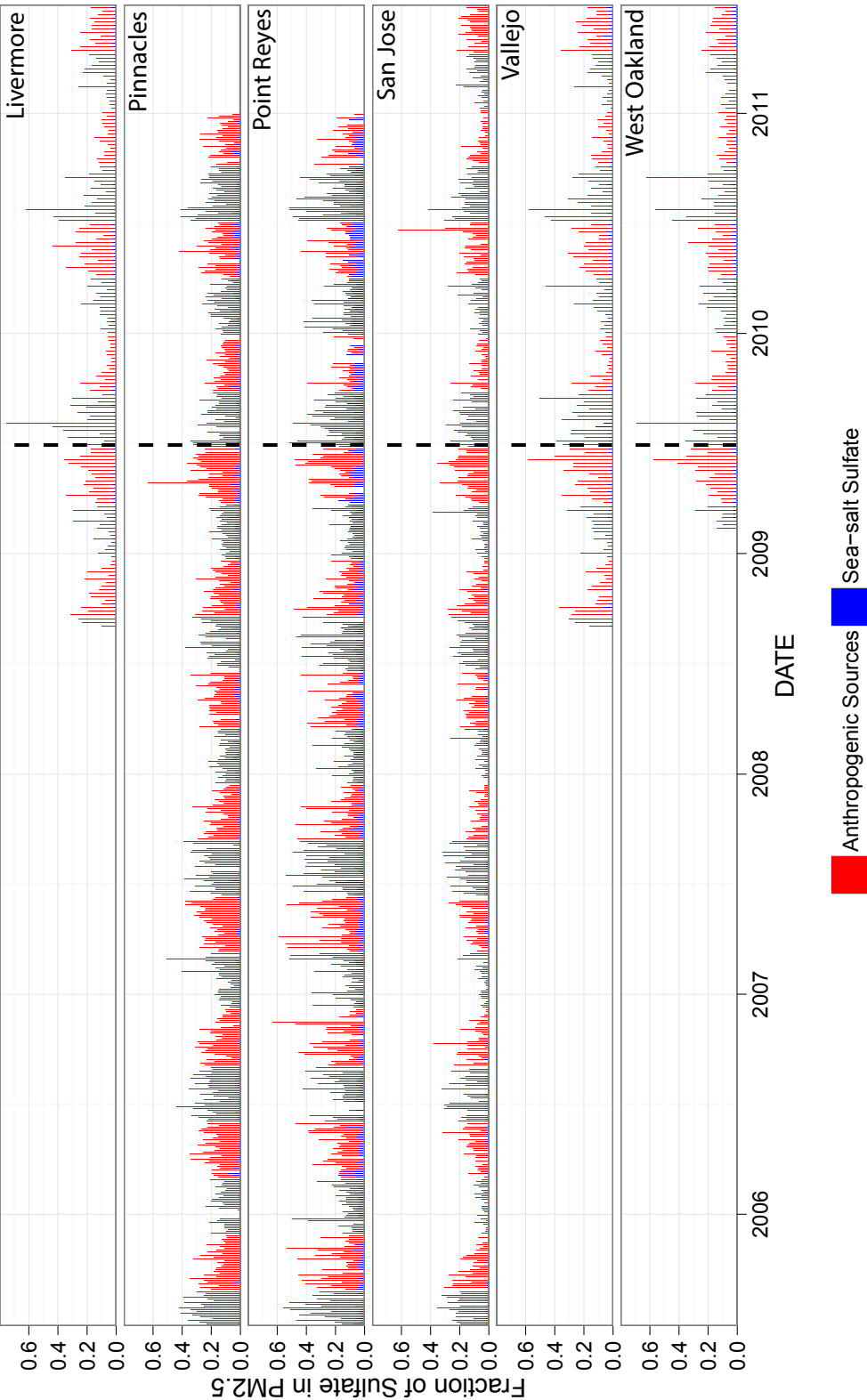


Figure 2.11: Time series of ambient PM_{2.5} sulfate at Bay area monitoring sites.

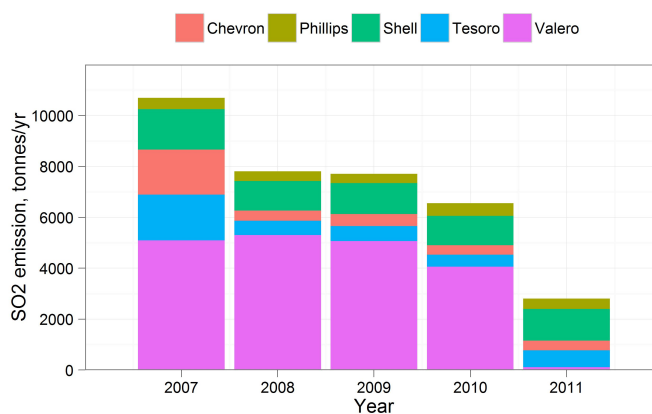


Figure 2.12: SO₂ emission from the five Bay area refineries from 2007 to 2011.

Quantifying changes in ambient concentrations

The Mann-Whitney test is robust in terms of showing the changes in concentrations which may not be obvious in time series and box-and-whisker plots. It indicates with 95% confidence that significant declines in concentrations after July 2009 were observed in the Bay area for V, SO₄ and SO₂ (Table 2.1). The changes in V are calculated by difference in the medians of exponential distribution fits. Changes in SO₄ and SO₂ are calculated by the Hodges-Lehmann estimator. The decreases in vanadium range from 64% at West Oakland and Vallejo to 28% at Pinnacles; for sulfate, the decreases range from 26% at San Jose to 17% at Vallejo.

The changes in ambient SO₂, although generally smaller in a relative sense compared to vanadium, range from 72% at West Oakland to 28% at Martinez. Aside from shipping, refineries are another important source of SO₂ emissions in the Bay area, and emissions from this source are also subject to changes over time. The five Bay area refineries all had stable SO₂ emissions during the period 2008-2010 that is the central focus of the present analysis (see Figure 2.12). Two refineries made significant changes that led to lower SO₂ emissions prior to 2008, and another made changes that had large effects in 2011. These SO₂ emission changes at refineries occurred outside of the time window then the transition to lower sulfur fuels in main engines of ships took place.

The decreases in vanadium are larger than the decreases in SO₂ because of other contributions to the Bay area SO₂ from sources such as petroleum refining. Table 2.1 shows that, in general, proximity of a monitoring site to shipping lanes dictates the magnitudes of decreases in V and SO₂. Among the sites, San Jose is an anomaly with inconclusive Mann-Whitney test results for V and SO₂, but significant decrease for sulfate.

Table 2.1: Changes in ambient V, NSS-SO₄ and SO₂ concentrations following change in ship fuel. *

Site	Distance to Port of Oakland (km)	$\Delta[V]$, %	$\Delta[\text{NSS-SO}_4]$, %	$\Delta[\text{SO}_2]$, %
West Oakland [⊕]	2	-64 [-78, -50]	-22 [-52, -1]	-72 [-82, -59]
Vallejo	34	-64 [-74, -54]	-17 [-39, -0.5]	-28 [-40, -18]
Livermore	45	-50 [-60, -40]	-23 [-45, -4]	
San Jose	61	-29 [†] [-37, -21]	-26 [-40, -12]	+25 [†] [+8, +24]
Point Reyes	66	-37 [-44, -30]	-25 [-45, -6]	
Pinnacles	177	-28 [-35, -21]	-24 [-38, -11]	
Berkeley	9			-50 [-63, -35]
Richmond	20 [•]			-35 [-44, -24]
Martinez	27 [•]			-28 [-37, -20]
Concord	27			0 [†] [-9, +9]
Crockett	29 [•]			-4 [†] [-12, +3]
Bethel Island	61			0 [†] [-10, +10]

* Tests were performed comparing July 2008 through June 2009 and July 2009 through June 2010. Percentage changes are based on annual averages from July 2008 through June 2009. Numbers in bracket represent 95% confidence intervals from exponential fittings for vanadium and the Mann-Whitney test for sulfate and SO₂.

[†] Pollutants with insignificant p-values from Mann-Whitney test results are in gray.

[⊕] West Oakland has partial year data starting from February 2009.

[•] Site located near additional shipping routes for oil tankers.

In addition to the two-period Mann-Whitney test conducted using 2008-2010 data, statistical tests were also performed for the Pinnacles and Point Reyes sites that have available data going back to 2005 (see Figure 2.13 and 2.14). The only other time that significant changes were detected was in July 2007, the effective date for cleaner fuel requirements on auxiliary

engines in ships. Those changes were smaller than observed in 2009 when fuel changes were required for main engines. For instance, at Pinnacles, a decrease of $15 \pm 8\%$ in vanadium concentrations was observed after July 2007, compared to a larger decrease of $28 \pm 7\%$ after July 2009.

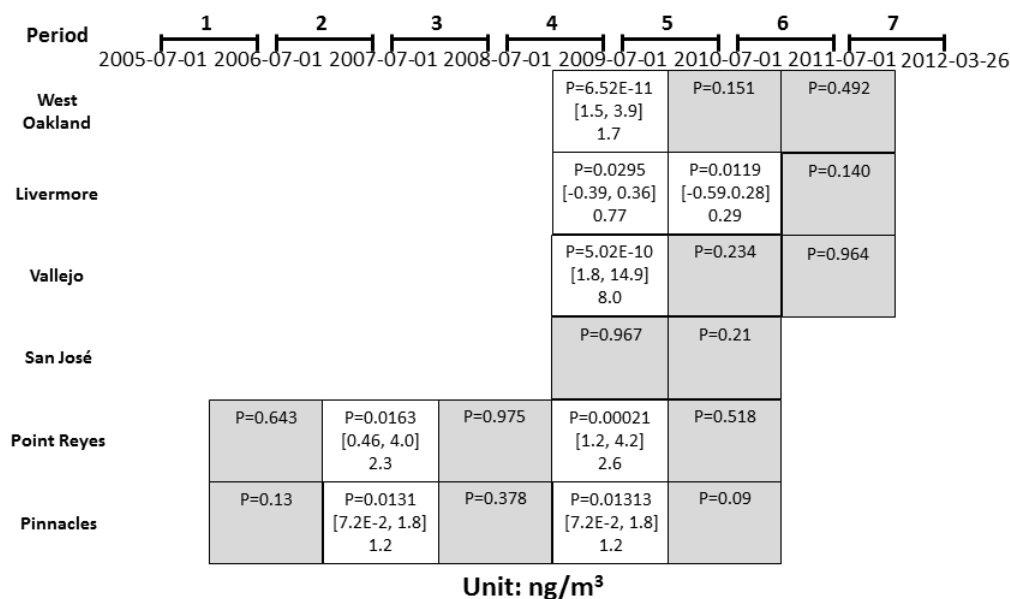


Figure 2.13: Wilcoxon test results for vanadium concentrations for each site, comparing every two consecutive periods for the seven periods: 2005 July through 2006 June, 2006 July through 2007 June, 2007 July to 2008 June, to 2011 July through 2012 March. The grey boxes represent invalid Wilcoxon test results. The white boxes mean a change in concentration is likely to have taken place, and show the corresponding 95% CI and the mean for the change, with positive numbers meaning a decrease in time, and vice versa.

Overall Reductions in PM_{2.5}

With the available data, we can estimate overall reductions in PM_{2.5} due to ship traffic in the larger context of ambient PM_{2.5} mass loadings. Since ships are not a dominant source of ambient PM_{2.5}, benefits from using cleaner fuels are not readily detected in PM_{2.5} mass concentration time series [64]. We calculate the sum of reductions in different chemically-resolved categories instead. We assume conservatively that the overall reduction in PM_{2.5} mass is the sum of reductions in trace metals (V₂O₅ + NiO), primary organic aerosol (POA) and NSS-SO₄, with other constituents of PM_{2.5} remaining constant. The emission ratio $\Delta V/\Delta POA = 0.27 \pm 0.22$, relating changes in V to changes in POA is obtained from Lack *et al* [95]. The changes in NSS-SO₄ are taken directly from the ambient data, and therefore reflect changes in both primary and secondary contributions.

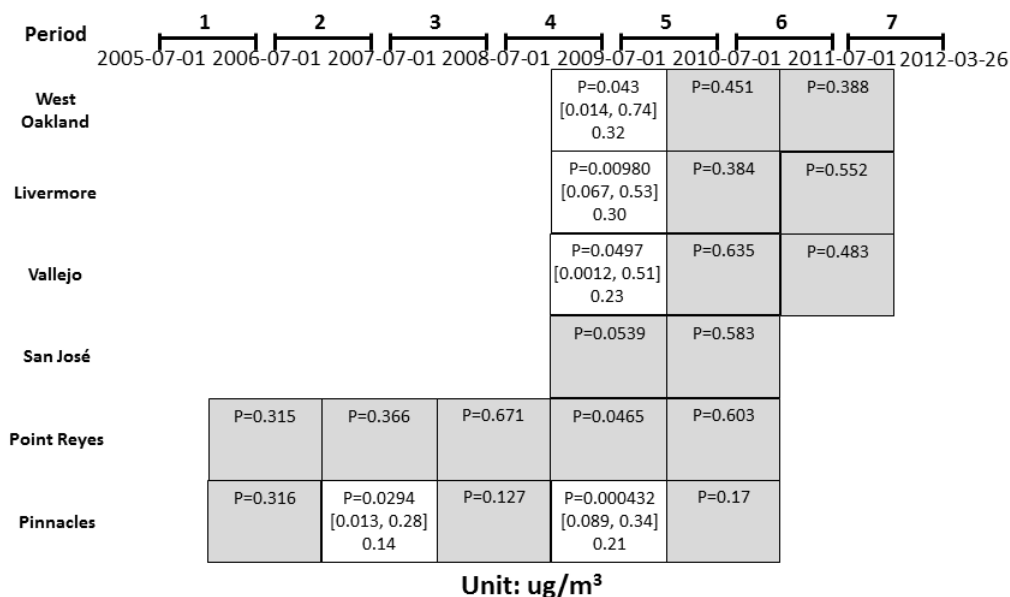


Figure 2.14: Wilcoxon test results for non-sea-salt sulfate concentrations for each site for the same periods as in fig. 2.13.

Table 2.2 shows estimates of total $\text{PM}_{2.5}$ reductions, and the breakdown of contributions by species at each site. West Oakland saw the highest relative reductions among the urban sites ($\sim 3.9\%$), because it is the closest to shipping lanes and receives high amounts of primary aerosol emitted by ships. Although Livermore did not see large reductions in trace metals, it still experienced a significant decrease in sulfate ($\sim 0.26 \mu\text{g}/\text{m}^3$), indicating that there may be a secondary sulfate effect as air parcels travel inland and SO_2 is converted to sulfate. Across the Bay area sites listed in Table 2.2, average reductions were $3.2 \pm 0.6\%$ or $0.25 \pm 0.05 \mu\text{g}/\text{m}^3$ in fine PM mass. Focusing on the urban sites (i.e., excluding Point Reyes and Pinnacles), the corresponding reductions were $3.1 \pm 0.6\%$ or $0.28 \pm 0.05 \mu\text{g}/\text{m}^3$. With coefficients of variation of 2-6% for the Federal Reference Method [121] and of $1 \mu\text{g}/\text{m}^3$ for the Beta Attenuation Method currently employed by BAAQMD to measure fine particles, such reductions would be difficult to detect directly using $\text{PM}_{2.5}$ mass measurements.

It is of interest to separate the reduction in sulfate into contributions due to direct emissions and secondary formation. Ault *et al.* suggested that vanadium can act as a catalyst for the oxidation of SO_2 to sulfate [9]. Therefore, fuel substitution may not only decrease the amount of sulfur available to form secondary sulfate aerosol, but also may act to slow the rate of sulfate formation. We infer that the majority of non-sea-salt sulfate reductions are due to regional changes in secondary formation resulting from lower SO_2 emissions, given that $< 5\%$ of ship-emitted sulfur is in the form of sulfate [122].

Ozone is also an air quality concern in the Bay area, and it is relevant to consider whether

emissions of NO_x are influenced by the change in ship fuels. However, a prior study suggests that NO_x emission factors are highly dependent on engine types, but only slightly dependent on fuel quality [78]. It is also difficult to control for functional relationships between NO_x emission and ship variables such as speed and load [148]. The nitrogen content on a mass-per-mass basis in residual oil is in the range of 0.1 to 0.5%, producing a fuel contribution to NO_x that is only $\sim 10\%$ of the total NO_x emission factor, with the rest being thermal NO_x formation [89]. Since the contribution from ocean-going vessels to NO_x in the San Francisco Bay area air basin was only $\sim 3\%$ in 2008 [33], this reduction represents a small change in a relatively small contributor to the overall inventory. Changes in vanadium and sulfur are much more significant and noticeable in terms of ambient air quality.

The methods used here are appropriate in settings such as California where electric power generation uses natural gas rather than fuel oil or coal, with very low resulting vanadium and sulfur emissions. Changes in ambient concentrations of these pollutants can therefore be linked more readily to changes in emissions from ships.

Ambient vanadium concentrations did not fall to zero after July 2009 (figure 2.7). Even

Table 2.2: Contributions to ambient $\text{PM}_{2.5}$ mass reductions in the San Francisco Bay area resulting from use of cleaner fuels in main engines of ships.*

Site	$\Delta[\text{V} + \text{Ni}]$, ng/m^3	$\Delta[\text{POA}]$, ng/m^3	$\Delta[\text{NSS-SO}_4]$, $\mu\text{g}/\text{m}^3$	Total reduction, $\mu\text{g}/\text{m}^3$	Mean [$\text{PM}_{2.5}$], $\mu\text{g}/\text{m}^3$	Total reduction, %
Livermore	0.73 [0.54, 0.92]	1.1 [0.46, 6.8]	0.26 [0.044, 0.52]	0.26 [0.044, 0.52]	8.8	3.0 [0.50, 5.9]
Pinnacles	0.40 [0.30, 0.51]	0.67 [0.27, 4.6]	0.20 [0.090, 0.32]	0.20 [0.10, 0.33]	5.1	4.0 [1.8, 6.5]
Point Reyes	0.55 [0.37, 0.73]	0.67 [0.21, 5.2]	0.18 [0.047, 0.33]	0.19 [0.048, 0.34]	5.9	3.2 [0.8, 5.8]
San Jose [†]	0.55 [0.37, 0.72]	0.78 [0.31, 5.4]	0.34 [0.16, 0.53]	0.34 [0.16, 0.53]	11	2.9 [1.4, 4.6]
Vallejo	1.9 [1.5, 2.3]	3.8 [1.8, 24]	0.22 [0.0063, 0.51]	0.23 [0.0096, 0.54]	9.4	2.4 [0.1, 5.7]
West Oakland	4.5 [3.4, 5.7]	8.1 [3.5, 54]	0.26 [0.0095, 0.70]	0.27 [0.016, 0.76]	7.1	3.9 [0.23, 11]

* Tests were performed comparing July 2008 through June 2009 and July 2009 through June 2010.

Column 1 is based on difference in medians of exponential distributions; Column 2 is calculated from Column 1 using the $\Delta\text{V}/\Delta\text{POA}$ ratio; Column 3 is based on Hodges-Lehman estimator; Column 4 is the sum of Columns 1, 2 and 3; Column 5 is the mean concentration from July 2008 through June 2009; Column 6 is from dividing Column 4 by Column 5.

[†] San Jose has some results with insignificant p-values from Mann-Whitney test, marked in gray.

though HFO burned by ocean-going vessels is thought to be the main source of vanadium in the San Francisco Bay area, other sources may still make small contributions such as catalyst emissions from refineries. Another factor may be the transport of vanadium-containing $PM_{2.5}$ from the area more than 24 nautical miles away from the California coast, since ships operating in outlying areas were not required to use lower sulfur fuels until 2012. It is also possible that compliance with fuel regulations may not be 100%, and that occasional peaks in observed vanadium concentrations at urban sites were caused by ships violating the fuel regulations. In order to monitor compliance, it may be desirable to install real-time SO_2 detectors near shipping channels within San Francisco Bay to monitor individual ship exhaust plumes, since a high SO_2 emission factor indicates possible usage of HFO, and SO_2 detection is affordable and fast.

Chapter 3

A Fuel-Based Motor Vehicle Emission Inventory Evaluation

3.1 Introduction

On-road vehicles emit significant amounts of nitrogen oxides (NO_x), carbon monoxide (CO), and non-methane hydrocarbons (NMHC). These pollutants contribute to short-term and long-term cardiovascular diseases and participate in the formation of secondary pollutants such as ozone (O_3) and secondary organic aerosol [29]. To support air quality planning, California developed its own emission model for on-road vehicles, EMFAC [59]. The model includes the latest data on car and truck activity and reflects the effects of new and ongoing vehicle emission control regulations, as well as changes in vehicle activity. EMFAC predictions are available online or as downloadable software. Emission data can be obtained from EMFAC on a specific or aggregated vehicle type, engine year, speed, fuel type, geographical area of user's choice. The purpose of this study is to evaluate the latest version of the EMFAC emission model against tunnel and remote sensing studies. ¹

On-road vehicles have a long regulatory history in the United States. Due to the Clean Air Act, the sulfur contents of gasoline and diesel fuel have been steadily decreasing nationwide since the 1990's. California has implemented its own reformulated gasoline program, eliminating lead, reducing vapor pressure and requiring addition of oxygenates to winter season fuel in Phase I (1992), lowering olefins, aromatics, sulfur, and benzene in Phase II (1996), and banning use of Methy-tertiary-butyl-ether (MTBE) in Phase III (2003). Three-way Catalytic Reduction has been employed in reducing NO_x concentrations in the exhaust from gasoline engines since 1980's [65]. Thanks to the stringent standards on engines and fuel, as well as improving fuel economy, the total emissions from gasoline-powered vehicles have been decreasing and are expected to continue to do so. Emission control for diesel engines, on the

¹The evaluation is done in collaboration with Robert A. Harley and Lucas Bastien, written as a technical report submitted to the California Air Resources Board [138], and based on the previous work done for EMFAC 2011 [103].

other hand, was set back in the early 1990's due to vehicle software on some model years that could cheat the standardized cycles in the emission tests. Since 1996, emissions from diesel engines have decreased, although slowly, due to the lower engine turnover rate typical of heavy diesel trucks. More recently, the 2010 engine standard requires post-combustion treatments such as diesel particle filter (DPF) and SCR, and California has implemented an accelerated engine replacement program that spans from 2010 to 2023, to phase out older engines at a faster rate [137]. This study summarizes the emission changes over the past two decades and puts the effects of these regulations in a long-term perspective.

The on-road measurements used in this study were done in California and tracked vehicle emissions at specific sites where the traffic was likely to represent the region-wide fleet. Sampling locations include tunnels, roadside sites and weigh stations. Due to different driving conditions that may influence exhaust constituents, fleet-averaged emission factors vary between locations, but combined together present a realistic picture of average driving speed, vehicle age distribution, and traffic patterns.

3.2 Methods

Direct comparisons are made between total emissions estimates by fuel category derived from the EMFAC 2014 database and from on-road measurements. Results are examined for six domains: Statewide, Sacramento County, San Francisco Bay area, San Joaquin Valley, South Coast, and San Diego County. Annual total emissions are calculated using a the fuel-based method (Eq.3.1). In this approach, vehicle activity is measured by the amount of fuel consumed, and emission factors are expressed per unit mass of fuel burned (*e.g.* grams of NO_x emitted per kilogram of gasoline or diesel fuel burned). In contrast, EMFAC measures vehicle activity based on total distance traveled, and emission factors are expressed in gram per mile units.

$$E_p = EF_{p,f} \times F_f \quad (3.1)$$

where E_p is annual emissions in tons per day for pollutant p for a given domain; $EF_{p,f}$ is emission factor of p for fuel category f ; and F_f is annual consumption of fuel f by the specified domain.

For EMFAC, all gasoline-powered vehicles are included in the comparison, as well as all diesel-powered vehicles except for fuel tax-exempt buses and motor homes.

Emission factors obtained from on-road measurements typically reflect on stabilized emissions from fully warmed-up vehicles. Emissions were measured when vehicles were either accelerating or going at a constant speed on uphill slopes (*i.e.* with load on the engines). Therefore, they do not include excess emissions associated with cold engine starting, which vary with ambient temperature because the catalytic converter only operates effectively when engines are warmed up. Since these starting emissions are not captured in the on-road

measurements, estimates were obtained from EMFAC and added to the fuel-based running emissions for a fair comparison. For NMHC, emissions of reactive organic gases (ROG) include both exhaust and evaporative emissions. EMFAC fuel-use and emissions have no associated uncertainty; only point estimates are provided. Methane emissions were excluded in all cases in this study, as the vehicular source of this pollutant does not contribute significantly to urban and regional-scale photochemical air pollution in California.

For emissions from on-road studies, calculation of $EF_{p,f}$ is elaborated in the following sections.

Emission factors of NO_x and CO

NO_x and CO emission factors were derived from data collected in remote sensing and tunnel studies, for a period of about 20 years [22, 21, 24, 26, 23, 53, 54, 87, 86]. A list of relevant studies used is provided in Table 3.1. Fuel Efficiency Automotive Test (FEAT) data were obtained from the website of the University of Denver [72]. FEAT measures individual vehicle emissions at the roadside using a dual-beam infrared/ultraviolet spectrometer. Some FEAT data were omitted from the emission factor derivation in this study, because the sites did not represent the general roadway conditions, such as a high-altitude site in Golden, CO. On-road Heavy-duty Vehicle Emission Monitoring System (OHMS) was implemented at a truck weighing station near Redding, CA. OHMS consists of a plume-containment tent that trucks drive through one at a time, vehicle property tracking (velocity, license plate, etc), and a suite of gaseous and particle analyzers. Tunnel measurements capture plumes of vehicles passing through a tunnel in Oakland as well as license plate information. The studies used to derive emission factors have been limited to those done in California to make the analysis more relevant to comparison with EMFAC. For diesel engines, NO_x and CO emission factors were directly reported in g/kg fuel; for gasoline engines, concentrations of species emitted were reported as percentages of total exhaust, so the following formula was used to calculate the fuel-based emission factors:

$$EF_p = \frac{MW_p \times Q_p}{0.014(1 + Q_{CO} + Q_{HC})} \quad (3.2)$$

where MW_p is the molecular weight of pollutant p in g/mol ; Q_p is molar ratio of p over CO_2 in the exhaust; and 0.014 is the weight of fuel per mole of carbon in the fuel, in kg/mol .

NO_x emitted from engines contains mainly NO. In some studies, only NO was reported, and was converted to NO_x using molecular weight of 46 g/mol ; Both NO and NO_2 were used to calculate EF_{NO_x} when available.

Linear regression analysis was performed from year 1996 to 2014 with a total of 10 data points for diesel engines and 21 for gasoline engines. A linear scale was used for diesel engines and a logarithmic scale was for gasoline engines. The emission factor for each on-road study was

fleet average. The uncertainty in the fitted emission factors was taken to be two times the standard error of the estimate, $2\sigma_{EF}$, to denote the 95% confidence interval:

$$\sigma_{EF} = \sqrt{\frac{\sum (EF_{measured} - EF)^2}{N}} \quad (3.3)$$

where N is the number of data points used in the fitting. For CO emissions, as the light duty gasoline vehicle fleet becomes cleaner over the year, the relative uncertainty grows, even though the absolute uncertainty remains approximately the same, so the lower bounds of confidence intervals that are negative were treated as zero in the calculation.

Location	Method	Type	Year(s) available
Caldecott Tunnel, Oakland, CA	Tunnel	Heavy Diesel Trucks	1996, 1997, 2006, 2010, 2014
Peralta, CA	FEAT	Heavy Diesel Trucks	1997, 2008-2010, 2012
Cottonwood, CA	OHMS	Heavy Diesel Trucks	2013
Caldecott Tunnel, Oakland, CA	Tunnel	Light Duty Gasoline	1997, 1999, 2001, 2006, 2010
West Los Angeles, CA	FEAT	Light Duty Gasoline	2001, 2003, 2005, 2008, 2013
Riverside, CA	FEAT	Light Duty Gasoline	1999-2001
San Jose, CA	FEAT	Light Duty Gasoline	1999, 2008
Los Angeles I-710, CA	FEAT	Light Duty Gasoline	1999
Sacramento, CA	FEAT	Light Duty Gasoline	1999
Fresno, CA	FEAT	Light Duty Gasoline	2008
Van Nuys, CA	FEAT	Light Duty Gasoline	2010

Table 3.1: Onroad measurements done in California used to derive fleet-averaged emission factors

Emissions of NMHC

NMHC emissions were inferred based on CO levels, using ratios derived from ambient air measurement studies. The mass ratio between NMHC and CO was elaborated in the previous studies [145, 105, 103]:

$$\frac{HC}{CO_{Diesel}} = \frac{2,083 + 0.000423(CY - 1990)}{19.25 - 0.47(CY - 1990)} \quad (3.4a)$$

$$\frac{HC}{CO_{Gasoline}} = 0.12 \quad (3.4b)$$

where CY is the calendar year. The 95% confidence interval for $\frac{HC}{CO}$ is 0.02 for both diesel and gasoline sources. These ratios include tailpipe exhaust as well as evaporative emissions from gasoline engines.

Vehicle age distribution

For EMFAC, vehicle miles traveled as a function of vehicle age are taken into account when calculating the vehicle age distribution. For a given calendar year and domain:

$$p_i = \frac{\sum_j VMT_{i,j}}{\sum_{i,j} VMT_{i,j}} \quad (3.5)$$

where p_i is the probability of any vehicle of age i driving a unit distance within the domain, $VMT_{i,j}$ is the EMFAC output of vehicle miles travelled by all vehicles in category j aged i . Age i is calculated by subtracting the engine model year from the calendar year.

For on-road studies, since measurements were done at specific geographical points, vehicle age distribution is based on the frequency of vehicles of age i driving past the the measuring location;

$$p_i = \frac{N_i}{\sum_i N_i} \quad (3.6)$$

where N_i is the number of times any vehicle of age i passing by was measured. To accurately describe the age distribution, only on-road studies that included >2000 vehicles were included in the comparison.

3.3 Results

Model Age Distribution

The vehicle age distribution is crucial to making fleet-averaged estimates of emission factors. Shown in Figure 3.1 is the age distribution of diesel engines from EMFAC and on-road measurements. EMFAC estimates vehicle populations based on vehicle type data from the Department of Motor Vehicles and travel data from regional governments and planning agencies. It takes into account economic factors such as recession-related decreases in vehicle travel and sales of non-taxable diesel fuel as well. However, the comparison in Figure 3.1 still reflects some discrepancies between EMFAC and on-road observations.

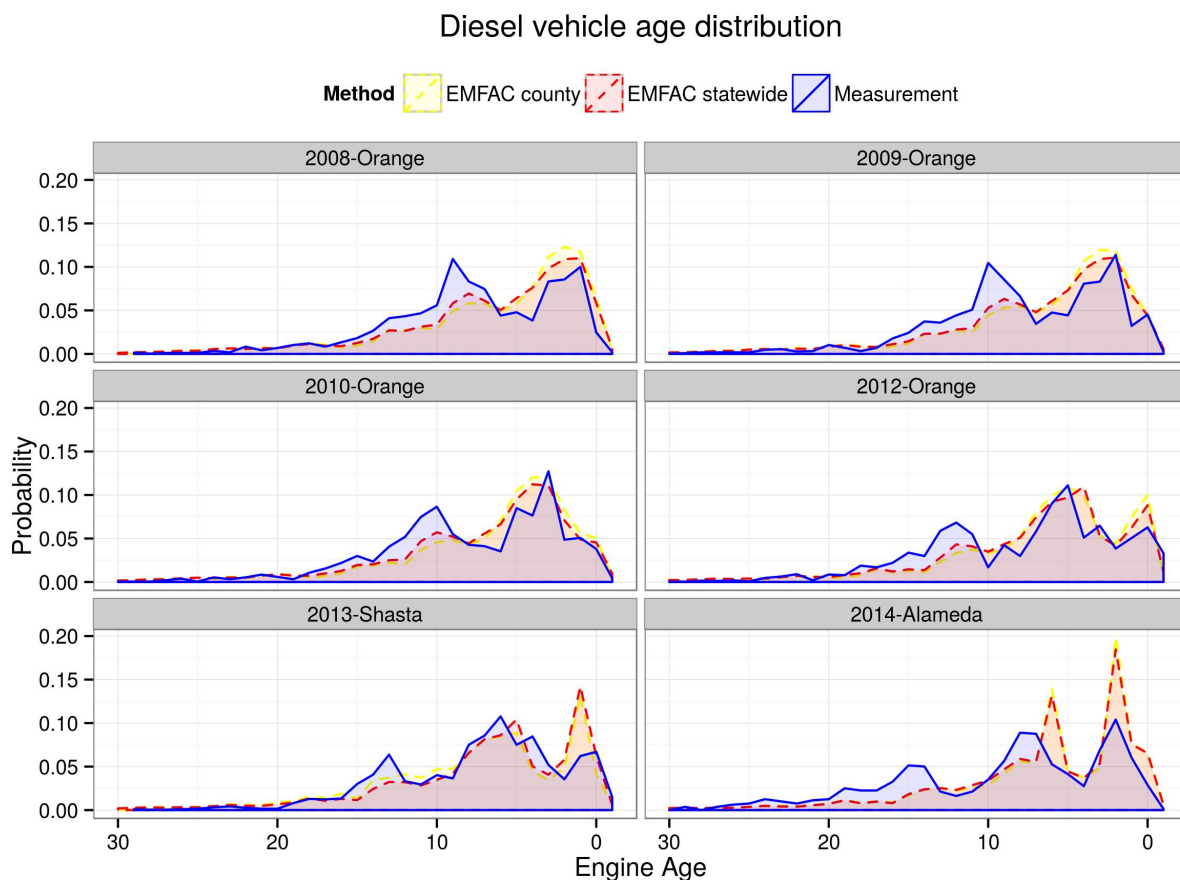


Figure 3.1: Selected diesel vehicle age distributions from EMFAC county-level (yellow) and California statewide (blue) data, and on-road measurements (red).

Overall, EMFAC captures the approximate age distribution of diesel engines, with the correct peak ages. On the other hand, the magnitudes of these peaks do not match that seen in on-

road measurements. EMFAC tends to overestimate the population of newer engines within the age range of 0-5 years, especially for 2012-2014. On the other hand, it underestimates the number of engines older than 8-10 years old. The mismatch is especially pronounced for engine age 12-20 years. The difference in median engine age between EMFAC and on-road measurements can be as large as three years. Granted that modeling the age distribution is difficult after accelerated diesel truck engine replacement program came into effective since 2010, the discrepancy is still large enough to merit further study of the prevalence of older models.

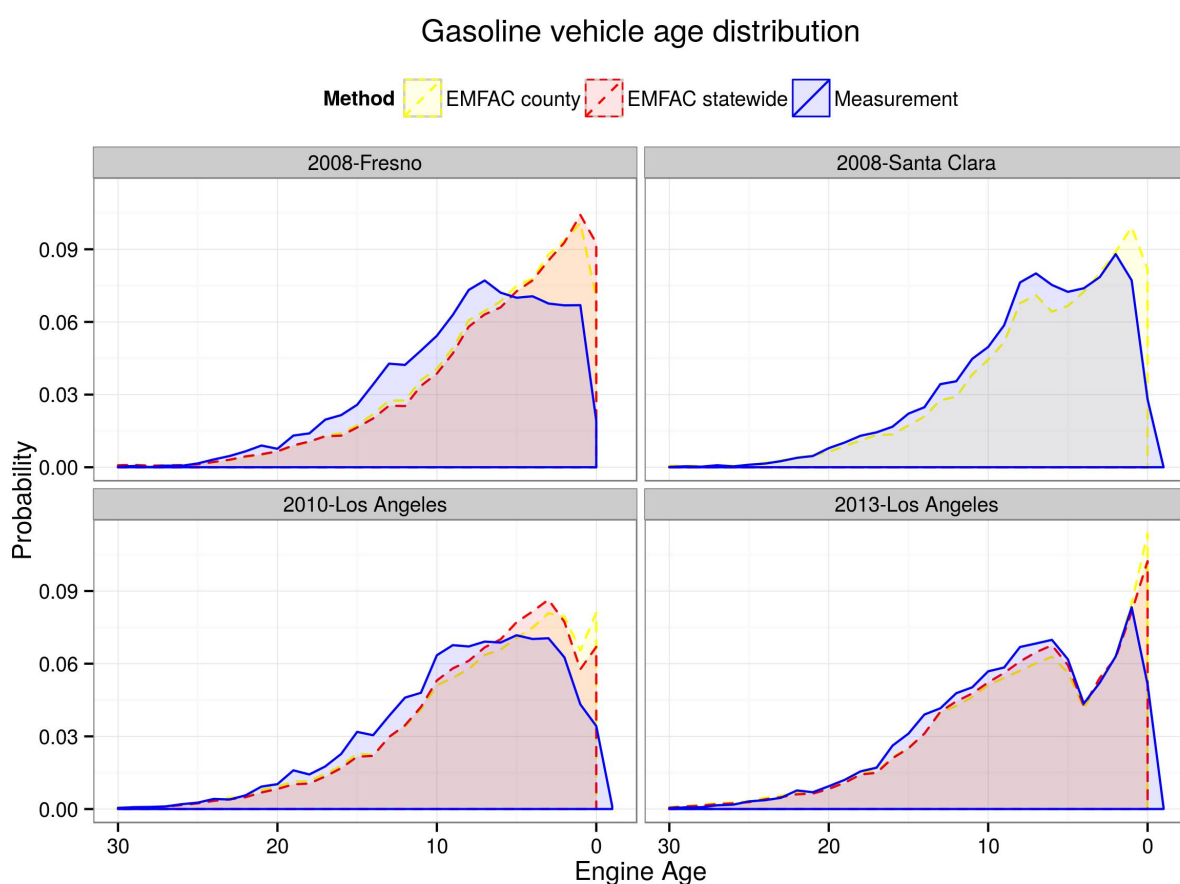


Figure 3.2: Selected gasoline vehicle age distributions. Color scheme is the same as in Figure 3.1

Similarly, EMFAC overestimates the fraction of travel by the population of newer gasoline engines, shown in Figure 3.2. The differences between EMFAC and on-road observations are especially pronounced for the 2008 Fresno and 2010 Los Angeles cases, where gasoline engines under 5 years old are overestimated by EMFAC as much as 50% more of the on-road

observations. However, EMFAC seems to agree better for the 2013 Los Angeles case. More comparison for light duty gasoline vehicles is needed for recent years (2013-2016) to further evaluate the accuracy of EMFAC model in the most recent years.

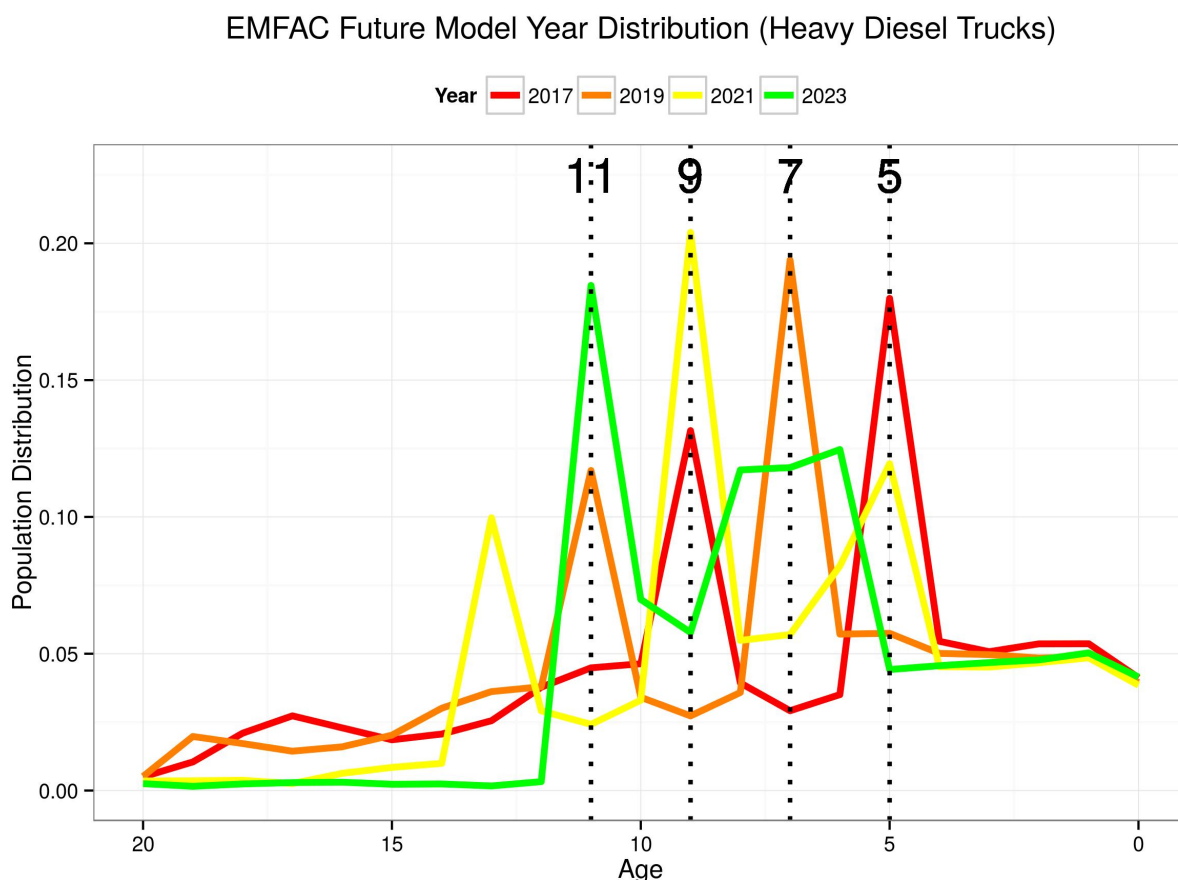


Figure 3.3: Future model age distribution of diesel engines governed by the California accelerated engine turnover program. Distributions are shown for years 2017 (red), 2019 (orange), 2021 (yellow), and 2023 (green). Each Vertical dotted line marks the peak population age for the given year.

Unlike light-duty gasoline vehicles, whose turnover rate is mainly governed by the market, diesel engines are under the accelerated replacement program in California [137]. Figure 3.3 shows the future model age distributions from EMFAC of such engines up to the year 2023, when all the heavy diesel trucks will be using post-2010 engines. The distribution gradually shifts the peak population age from 5 to 11 years over this time span. According to EMFAC, there will also be many more engines of the age 5-9 years old in 2023, possibly because many fleet owners are buying much newer engines to substitute the pre-2010 ones. Overall, the

prediction for the future age distribution in Figure 3.3 is reasonable and accurately takes into account the regulations in California.

Trends in NO_x and CO emission factors

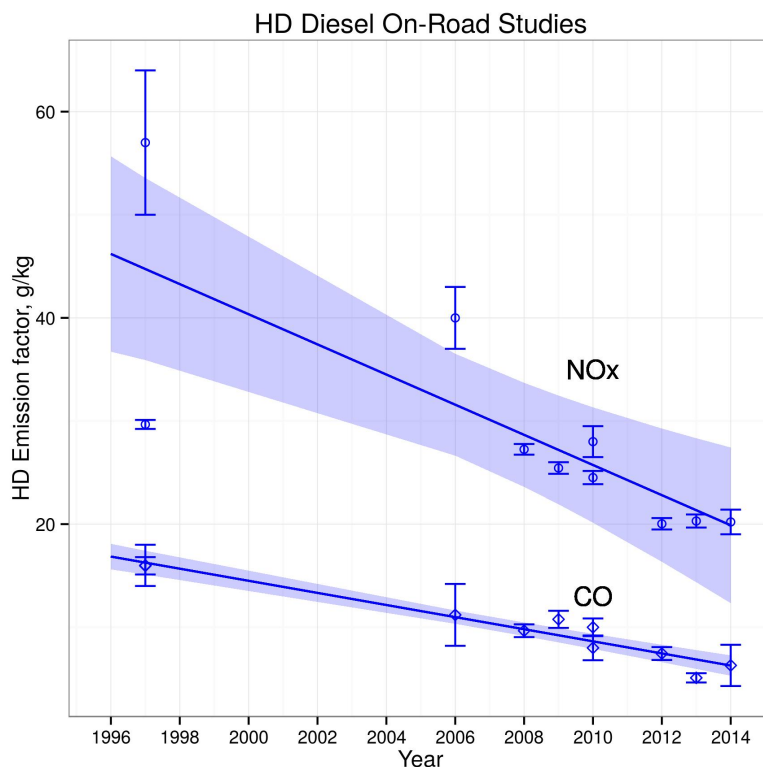


Figure 3.4: Trends in fuel-based emission factors for heavy-duty (HD) diesel vehicles measured in California on-road studies, as a function of calendar year. The solid lines represent linear fits to the emission factor trends over time (note the linear scaling of the vertical axis in this plot).

Both NO_x and CO emission factors have decreased significantly over the past two decades, for all on-road vehicles, as shown in Figures 3.4 and 3.5. For diesel engines, NO_x is emitted at higher rates due to the higher operating temperatures and less advanced emission control systems in legacy fleets compared to gasoline engines. In contrast, CO is emitted at a lower rate due to the more complete oxidation of diesel fuel. In Figure 3.5, linear fits to the data gave unrealistically low values for LD emission factors for the most recent years. The emission factors start to level off as they approach zero, so a linear fit is not appropriate.

NO_x emission factors for diesel engines were about three times higher than that of gasoline engines in 1996, and has become nine times higher as of 2014, thanks to the universal

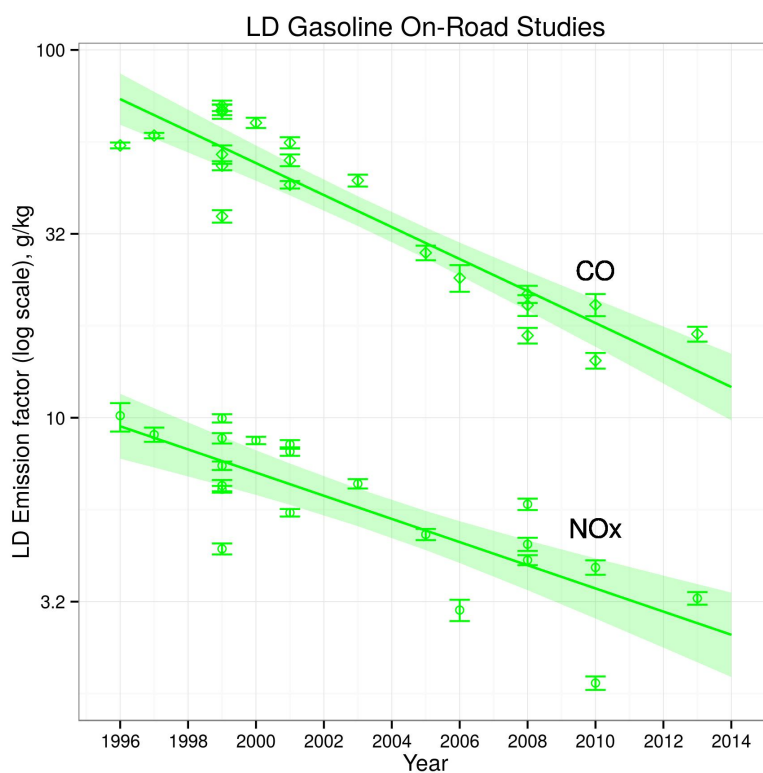


Figure 3.5: Trends in fuel-based emission factors for light-duty (LD) vehicles measured in California on-road studies, as a function of calendar year. The solid lines represent logarithmic fits to the emission factor trends over time (note the logarithmic scaling of the vertical axis in this plot). Differences in emission factors measured in the same calendar year at different locations (there are three or more study results plotted for each of 1999, 2001, and 2008; see Table 1 for details) may be due to differences in vehicle fleet/age distribution, driving conditions, and study design/measurement methods.

deployment of catalytic converters on gasoline engines starting in the mid-1970's. Selective catalytic reduction has been applied to newer diesel engines since 2010. Diesel engines also show a slower rate of decrease in NO_x emission factors than gasoline engines (roughly 55% for diesel compared to 80% for gasoline from 1996 to 2014). Taking into consideration the fleet turnover rate, the diesel NO_x emission factor is expected to decrease further up to the year 2023.

Fleet-averaged CO emission factors have decreased significantly for gasoline engines for the last two decades. Due to incomplete combustion, gasoline engines used to have more than three times the CO emission factor of diesel engines in 1996. As of 2014, it is only about 1.5 times, because of improved performance of catalytic converters that manage to control both CO and NO_x , as well as a newer mix of engines in the fleet. All of California is currently in

attainment with regards to ambient CO [36].

Trends in emissions

Total on-road vehicle emissions for six domains in California are shown in Figures 3.6, 3.7, and 3.8, for both EMFAC and onroad fuel-based estimates. Overall, the degree of agreement between the two methods is decent for the downward trends, but the discrepancy in absolute values can be large depending on the time period.

For NO_x (Figure 3.6), the total emissions from diesel and gasoline vehicles are comparable in magnitude, except in San Joaquin Valley, where diesel still dominates the emissions, and Sacramento County, where diesel sources still emit twice as much as gasoline sources, as of 2014. In contrast, the urban areas where light-duty gasoline vehicles make up the majority of the fleet no longer have diesel engines as the larger source of NO_x . Among the five local domains, South Coast Air Basin sees the greatest amount of emissions from both diesel and gasoline engines. EMFAC and the fuel-based method compare relatively well for diesel sources. For gasoline sources, EMFAC underpredicts the contribution for all six domains since 2003, and the discrepancy between EMFAC and the fuel-based method seems to be consistent over time.

As seen in Figure 3.7, gasoline engines are the dominant source of CO by far, and the contribution of diesel engines is negligibly small. There is consistent and steep reduction across all six domains. Similar to NO_x , South Coast Air Basin also ranks the first by far compared to the other four domains. The reduction in CO is about 75% since 2000. EMFAC and the fuel-based method compare relatively well since 2005 for all domains except for Sacramento County, where EMFAC overpredicts about 10-15%, but still within the uncertainty range.

NMHC emissions in Figure 3.8 follow the same trend as Figure 3.7, since the ratios of NMHC/CO remain approximately constant across the years. EMFAC and the fuel-based methods estimate combined tailpipe and evaporative NMHC emissions similarly for gasoline sources. For diesel engines, most of the years and domains have fair comparisons, except for in the more recent period 2011-2014, the discrepancy seems to have increased between the two methods. NMHC is a difficult pollutant to obtain an accurate estimate, since it is a combination of many organic gases, some of which are difficult to measure. Evaporative emissions are also independent process from exhaust, and require completely separate models.

Uncertainties in total emissions are large because for NO_x and CO, ΔEF is 15%-25%, and ΔF is 10%-15%. Combined orthogonally by the rule of multiplication, the resulting uncertainty can be up to 30%. This uncertainty is inherent in the linear regression applied to on-road measurements from different locations and plume-capture methods.

Total emissions agree relatively better compared to the vehicle model year distributions in Figures 3.1 and 3.2. The fuel consumption in EMFAC and the method based on fuel sale data also agree [138]. Therefore, this raises the question of whether EMFAC has inaccurate distribution for age-specific emission factors. EMFAC presents a younger fleet than that of the on-road measurements, and assigns higher emission factors to older engines. This results in good fleet-average emissions, but may indicate compensating effects in the EMFAC model that merit further consolidation.

This is the first study to evaluate both emissions and model year distributions in the EMFAC 2014 model. The conclusion is that EMFAC provides credible estimates for model year distributions and total emissions for both historical and future years. This is important because the model is widely used by air districts, consulting companies and academia. Chapter 4 in this dissertation uses EMFAC output extensively to compile gridded emission inventories for the years 2005, 2016 and 2023 as input into an air quality model. The relatively small gaps between EMFAC and the fuel-based method in this chapter justify the further use of EMFAC for emission calculation.

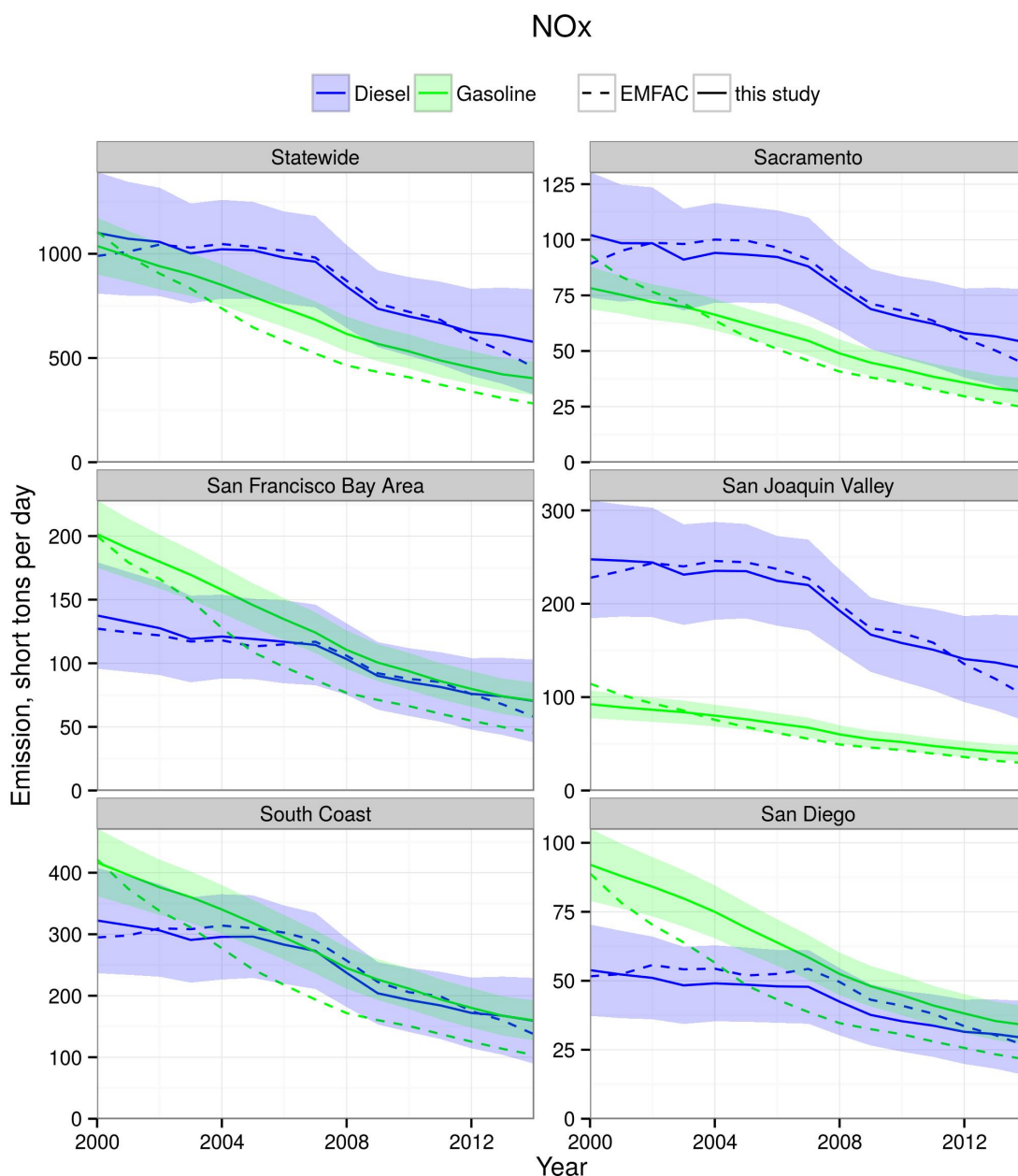


Figure 3.6: On-road vehicle NO_x emission inventories by calendar year: California state totals and results for selected air basins and counties, for annual average weekday conditions. Units are US tons per day (tpd); NO_x mass is reported on an NO₂ equivalent basis, although most of the emissions are in the form of NO. The shaded color bands denote 95% confidence intervals associated with the fuel-based inventory (solid lines). EMFAC model data shown as dashed lines. Separate results for gasoline (green) and diesel (blue) engines are shown together on each plot.

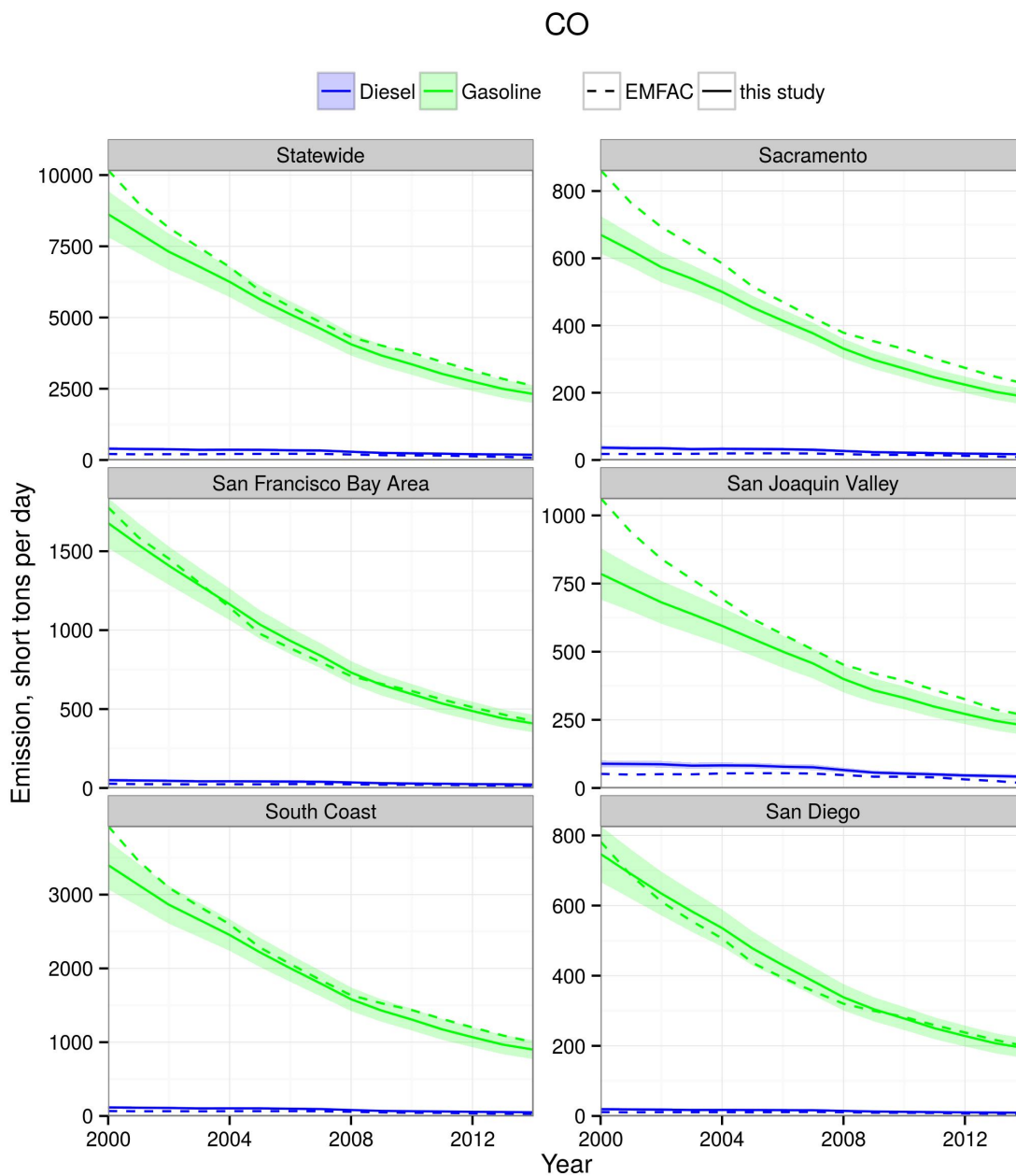


Figure 3.7: On-road vehicle CO emission inventories by calendar year. Color schemes are the same as Figure 3.6

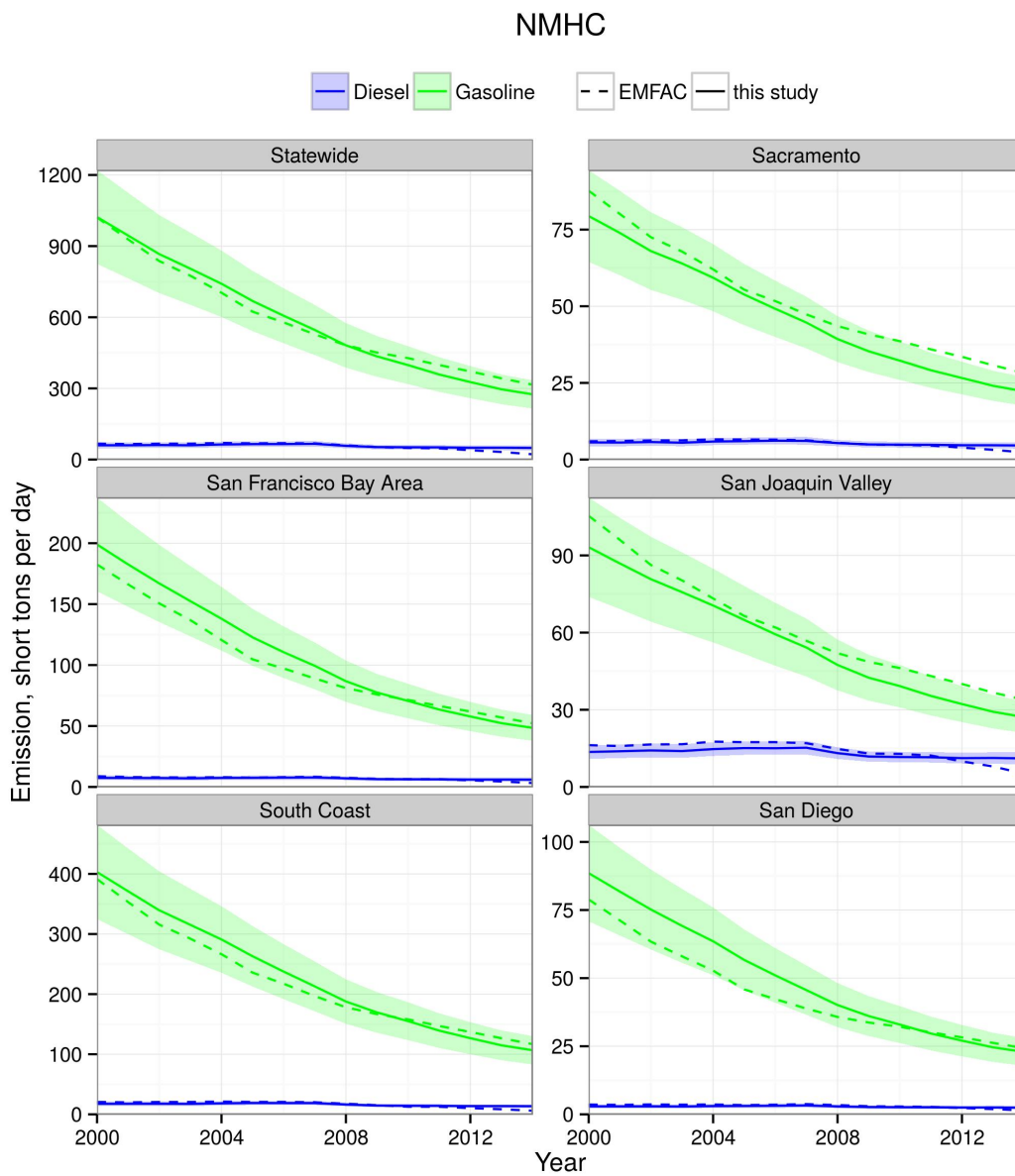


Figure 3.8: On-road vehicle NMHC emission inventories by calendar year. Color schemes are the same as Figure 3.6

Chapter 4

Effects on Air Quality of Controlling NO_x Emissions from Diesel Trucks

4.1 Introduction

Nitrogen oxides are primary pollutants and participate in the atmospheric chemistry of ozone (O_3) and fine particulate matter ($\text{PM}_{2.5}$) [51]. The primary pollutants are mainly nitric oxide and dioxide (NO and NO_2); secondary species include nitric acid (HNO_3), dinitrogen pentoxide (N_2O_5), and peroxyacetyl nitrate (PAN). Exposure to these species could lead to inflammation in respiratory tracts and increased cancer risks [55]. The United States Environmental Protection Agency (EPA) determines NO_2 to be a criteria pollutant, and sets the standards to be 100 ppb for one-hour peaks and 53 ppb for annual means [141].

Anthropogenic NO_x is mainly released from fuel and biomass combustion in the form of NO . In California, mobile sources contribute to 83% of the anthropogenic NO_x emissions as of 2012 [33]. The US has a long history of controlling NO_x from on-road vehicles. Gasoline engines in light duty passenger vehicles have had three-way catalytic converters installed since model year 1975. Fraud software installed in diesel engines produced in 1990's could cheat on driving cycles specified by the standardized emission testing, and prevented effective NO_x reductions for on-road heavy diesel trucks. Hence, the pace of NO_x control on diesel engines has not picked up until the 2000's. Since 2000, the fuel-based emission factors have decreased by about 70% for gasoline engines, and 55% for diesel engines [138]. Changes in emissions from the on-road sector, as well as industrial sources and off-road equipment, result in clear reduction trends in ambient NO_x concentrations, as shown in the next section.

Regulations on heavy diesel trucks in California

Heavy-duty engine emission standards are set by model year, as shown in Figure 4.1, and became much more stringent between 1990 and 2010. PM emissions have to be below 0.01 g/hp-hr since 2007 and NO_x emissions below 0.2 g/hp-hr since 2010. However, the on-road

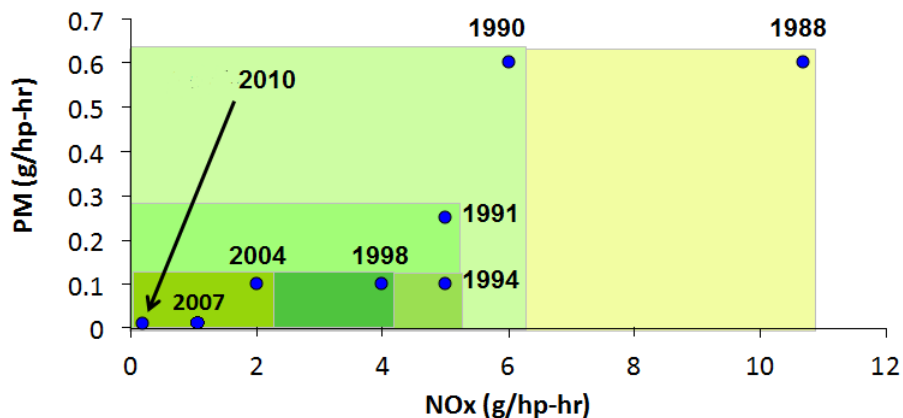


Figure 4.1: On-road heavy-duty truck exhaust emission standards by engine model year. Emissions limits are expressed per unit of useful work (hp-hr) output by the engine.

fleet emissions decrease more slowly than the requirements on new engines, because diesel trucks tend to have slower turnover rates than passenger vehicles, and engines tend to remain in use for several decades.

California has implemented an accelerated diesel engine replacement program for heavy-duty trucks. The regulation requires that all on-road trucks have a diesel particle filter (DPF) installed by about 2018 [110], and mandates post-combustion control technologies for NO_x such as selective catalytic reduction (SCR) by 2023 [68]. The SCR uses urea to react with tailpipe NO to produce nitrogen, water, and carbon dioxide in the exhaust. Past studies have shown that SCR is successful in reducing in-use NO emissions by almost 70% [126], but does not function optimally when the engine is operating with exhaust temperature below 200-500°C, for example, during driving modes such as accelerating after complete stop [21].

In this study, resulting air quality for three emission scenarios before, during, and after the accelerated diesel engine replacement regulation was analyzed, focusing on the South Coast Air Basin in California where NO_x, PM_{2.5} and O₃ have historically exceeded standards. The gridded atmospheric transport and chemical model simulates both primary and secondary pollutants, which were then compared against past ground measurements, and used to analyze the impacts on the regional air quality from the on-road diesel truck emission regulation.

4.2 Method

CMAQ setup

The air quality model used in this study is CMAQ version 5.0.2 [32], with the gas-phase chemical mechanism SAPRC07 [39] and aerosol module AE5 [11]. SAPRC07 is an improved

version of SAPRC99 that describes atmospheric reactions of almost 780 types of volatile organic compounds, with updated peroxy reactions, aromatics mechanisms and chlorine chemistry. AE5 was the newest at the time of the study, and has incorporated updated coarse-mode treatment and inorganic species. Meteorological input was developed using the Mesoscale Meteorological model (MM5) version 3.6.1. More details on meteorology and boundary conditions were described in the previous studies [108, 110].

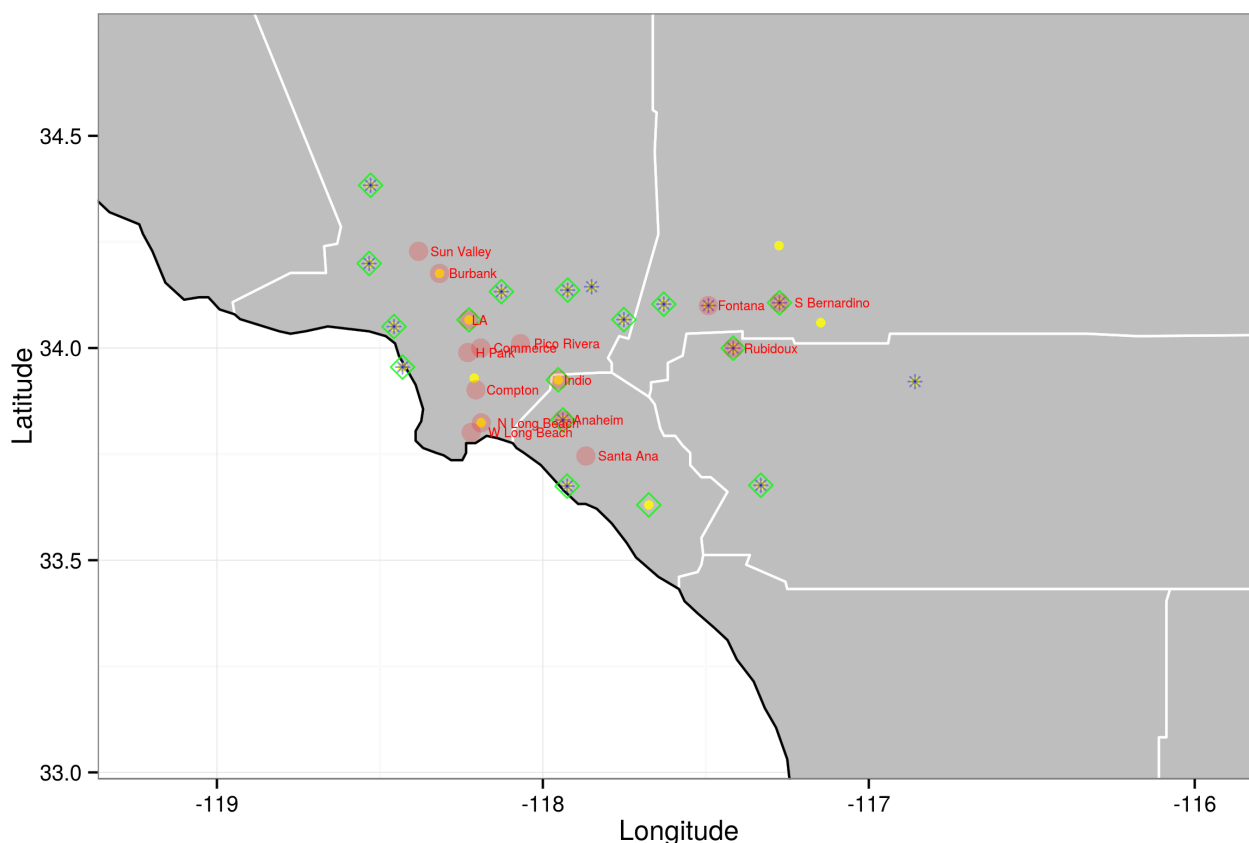


Figure 4.2: Model domain with measurement sites in 2005 with the following annotations: O_3 - yellow dots; CO - green diamonds; NO_x - blue asterisk; Speciated $\text{PM}_{2.5}$ - red dots with labels.

Figure 4.2 shows the modeling domain as well as the sites with available pollutant measurements in 2005. The domain is gridded into 65×40 cells with 5 km resolution. The model was run on this domain for two periods: summer (July 6 - August 30), and winter (October 30 - December 7) of year 2005. These periods span changes in seasonal meteorology in Southern California, with high O_3 conditions in the summer. A 72-hour model spin-up period was

excluded from the analysis of the model outputs to reduce any influence from uncertainties in initial conditions.

Emission Scenarios

Base case (2005)

Gridded emission inventory files were prepared by the South Coast Air Quality Management District and the California Air Resources Board [4]. Biogenic emissions were estimated using the BEIGIS model [133].

Emissions from off-road diesel construction equipment have been scaled as well as shifted in space to better reflect actual location of construction activity, following Millstein and Harley [111].

For the on-road sector, emissions were estimated using a fuel-based method that could achieve high spatial (1 km) and temporal (1 hour) resolution for diesel and gasoline engines separately, developed McDonald *et al.* [104]. Emissions were obtained by combining fuel sales, traffic counts and time-resolved weigh-in-motion traffic count data. The mobile fuel consumption was originally provided in 1-km annual average format. ArcGIS was used to re-grid the data to match the 5-km domain used for the model. Temporal resolution was achieved by scaling the annual-average values according to urban/rural-specific traffic patterns. Lastly, fuel-based emission factors were derived from the EMFAC model [59] and multiplied by grid-specific fuel consumptions to obtain on-road diesel and gasoline engine emissions.

The NO₂ fraction in NO_x has been changed from 10% to 1% for on-road gasoline engines [15], and from 10% to 3.4% for diesel [126]. Both fractions were from highway tunnel measurements and reflect loaded driving on a leveled road either accelerating or cruising. The fraction for diesel engines was from heavy diesel trucks without any DPF or SCR. Diesel particle composition was modified to have 64% BC, 32% OC, 0% nitrate, 0% sulfate, and 4% other materials such as metals.

NH₃ emissions for the on-road sectors are developed separately from other pollutants (VOC, NO_x, CO, SO_x, PM_{2.5}) for 2005. Diesel engines have negligible NH₃ output [31], and gasoline engine NH₃ emissions are proportional to the amount of NO_x emitted, as a function of engine model year.

On-road remote sensing campaigns in west Los Angeles in 2008 and 2013 were used to explore the NH₃/NO_x relationship, because the measurements described the fleet in the South Coast relatively well. We found that given the engine age, the NH₃/NO_x ratios exhibit a log-normal distribution, shown in Figure 4.3. The results from fitting for every engine age

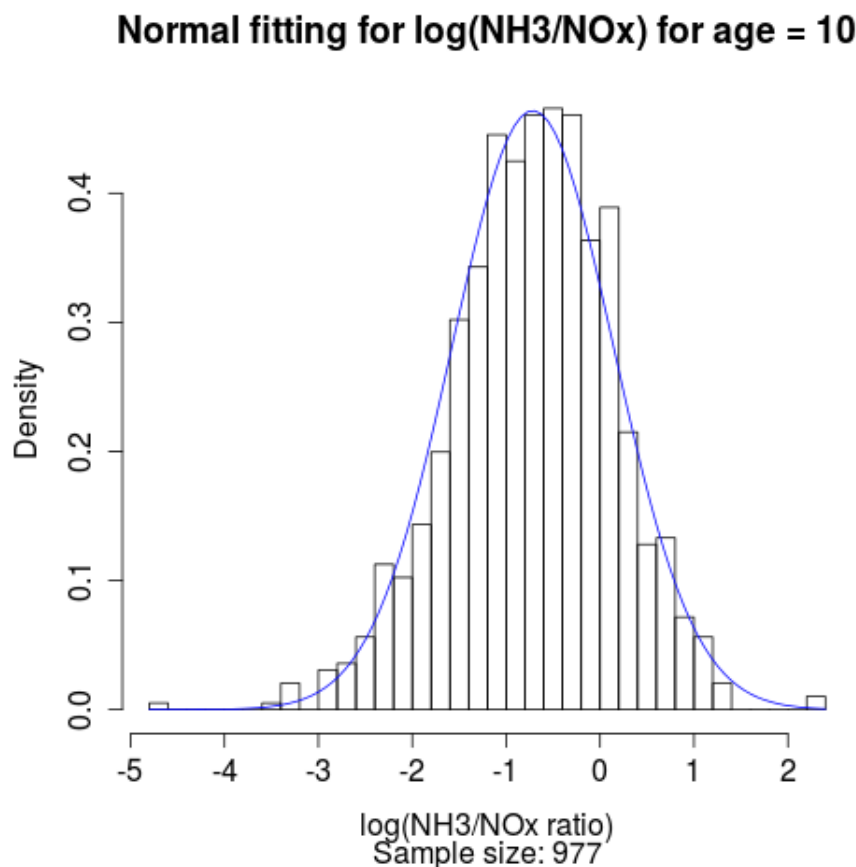


Figure 4.3: An example of normal fitting to the logarithm of gasoline NH_3/NO_x ratios.

are presented in Figure 4.4, well-described by two separate fitting lines for engines younger (red) and older (blue) than 9 years. The fitted ratios for all the engine ages were applied to the model year probability distribution of gasoline engines in 2005, obtained from EMFAC. A fleet-average NH_3/NO_x was obtained to derive NH_3 emissions in every grid-cell based on NO_x . The fleet-average NH_3/NO_x was 0.14 by mass calculated this way.

Present year (2016)

Biogenic emissions were left unchanged for both the present and the future year cases. All the anthropogenic emissions have been scaled to reflect population growth and other changes, such as advances in emission control policies and technologies.

Point, area and off-road sources were scaled uniformly across the domain for each major pollutant category except for NH_3 . Scaling factors were calculated using published emission estimates and tables compiled by the SCAQMD [4] and CARB [33]. The ratios are summarized in Table 4.1.

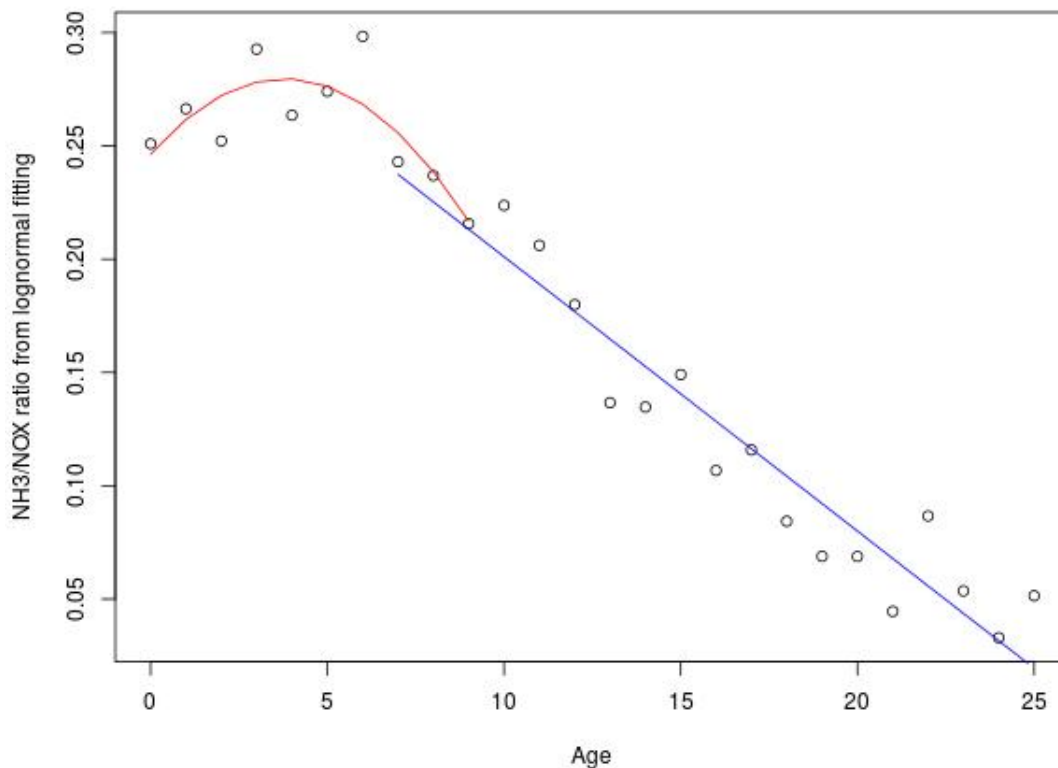


Figure 4.4: Ratio of NH_3/NO_x by model age, fitting using two separate lines.

For the on-road sector, fuel use was scaled uniformly from the 2005 base case based on the EMFAC model fuel estimates. Diesel consumption increased by 8% whereas gasoline use decreased by 4% between 2005 and 2016. Gasoline consumption decreased because of improved fuel economy in passenger vehicles. Fuel-based emission factors for major pollutant categories were also derived from EMFAC. Composition of organic gases and particulate matter were assumed to be the same as 2005. Diesel NO_2/NO_x ratio in 2016 was increased to 18% to account for nearly all the trucks having DPF installed [126].

NH_3 emissions were scaled uniformly using the same method as for the five major pollutant categories except the NH_3 emissions for area sources and gasoline on-road vehicles.

For area sources of NH_3 , it is expected that the changes from 2005 to 2016 would not be geographically homogeneous, because a major source of NH_3 is from farming and the dairy industry, and these agricultural activities are likely to shift from the coastal region eastward or to San Joaquin Valley due to the urbanization in the South Coast [119]. Therefore, scal-

		Point	Area	Off-road
$r_{\frac{2016}{2005}}$	VOC	0.95	0.95	0.62
	NO _x	0.67	0.67	0.61
	CO	0.98	0.98	0.81
	SO _x	0.19	0.19	0.10
	PM _{2.5}	0.96	0.96	0.46
$r_{\frac{2023}{2005}}$	VOC	1.3	1.3	0.54
	NO _x	0.87	0.53	0.50
	CO	0.89	0.89	0.95
	SO _x	0.34	0.91	0.039
	PM _{2.5}	0.97	1.1	0.38

Table 4.1: Scaling factors used to modify emission inventories for 2016 and 2023.

ing factors for each county in the domain were obtained from the farm production indices in the California County-Level Economic Forecast [37]. The ratios are summarized in Table 4.2.

County	% change from 2005 to 2016	% change from 2005 to 2023
Imperial	+35	+28
Los Angeles	-40	-47
Orange	-72	-72
Riverside	-3.0	-7.0
San Bernardino	-50	-31
San Diego	+2.3	-4
Ventura	+46	+39

Table 4.2: Scaling ratios for NH₃ from area sources by county.

For on-road gasoline sources of NH₃, the same analysis for fleet-average NH₃/NO_x ratio was performed as in 2005. For 2016, NH₃/NO_x is 0.23 (versus 0.15 in 2005), taking into account a different model year distribution. NH₃ emission inventory of the on-road sector was then obtained by applying the new ratio to the 2016 gasoline NO_x emissions.

Future case (2023)

The modifications on 2005 base case to make the 2023 emission inventory were similar to the ones for 2016. The scaling ratios were different, listed in Table 4.1 and 4.2.

In 2023, since all the heavy diesel trucks will have SCR controls installed, the NO₂/NO_x ratio for on-road diesel sector is set to be 0.22 [126]. Electric vehicles may substitute part of the light-duty passenger fleet and natural gas trucks may make up a significant fraction

of long-haul truck transportation. However, according to EMFAC predictions for 2023, the fraction of vehicle miles traveled is only 3.7% of that traveled by gasoline vehicles. Therefore, we conclude that the contribution of the electric vehicle is negligible.

The NH₃/NO_x ratio applied to gasoline emissions for 2023 was 0.23.

For natural gas trucks, the NH₃ emitted per vehicle would not be negligible compared to diesel trucks. To create the emissions from natural gas trucks, NH₃ emitted by the region for the whole year of 2023 (m_{NH_3}) was calculated, then assigned emission pattern identical to that of diesel trucks. To calculate m_{NH_3} , Equation 4.1 was used:

$$m_{NH_3} = EF_{NH_3} \times m_{CNG} \quad (4.1)$$

where EF_{NH_3} is the NH₃ emission factor of natural gas trucks in g/kg fuel, m_{CNG} is the total mass of compressed natural gas (CNG) consumed by natural gas trucks in 2023. A previous study done at weigh stations has shown that EF_{CNG} is about 3.5 g/kg [25], averaging between Port of Los Angeles and Peralta in the South Coast. To calculate m_{CNG} for 2023, sales of CNG from 2006 to 2014 were obtained from the California Board of Equalization, assuming all the CNG was burned in heavy-duty trucks [139]. The following linear fit was derived to describe the projection in sales:

$$\text{Sales} = 6.24 \times 10^8 \times \text{Year} - 1.247 \times 10^{12} \quad (4.2)$$

where sales of CNG is in cubic foot. Converting the result to mass using the density of methane, California would have 2.5×10^8 kg of CNG in 2023 in trucks. According to EMFAC, the South Coast Basin burns approximate 39% of the diesel consumed in the state. Therefore, scaling the domain down to the South Coast, the resulting NH₃ emissions is 3.4×10^8 g for 2023. This number was then divided to emissions per grid cell per hour according to the patterns of diesel emission.

Model validation

Two sources of ground measurements were used to evaluate the base case (2005) model results and the changes in 2016.

The first source was the year-round hourly gaseous and PM_{2.5} monitoring network maintained by the local air district. Since at the time of this research, the 2016 data was not available yet, data from one year earlier, 2015, were used as proxy to compare with the 2016 model scenario. All gaseous measurements were available in 2005 and 2015; the PM_{2.5} concentrations measured hourly by the Beta Attenuation Method (BAM) were only available in 2015, since BAM was not yet in use in 2005 [6].

The second data source was the Multiple Air Toxics Exposure Studies (MATES) III and IV conducted by the local air district. MATES III and IV were carried out in 2005 and

2012, respectively, each lasting about a year [135]. This research uses the PM_{2.5} speciation measurements from MATES, focusing on BC, nitrate (NO₃), sulfate (SO₄), and organic carbon (OC). The speciation was done once every three days (MATES III) or every six days (MATES IV). Days when there was mass closure discrepancy ($[\text{PM}_{2.5}] < [\text{OC}] + [\text{BC}] + [\text{NH}_4^+] + [\text{NO}_3^-] + [\text{SO}_4^{2-}]$) were excluded from the comparison with the model.

4.3 Results

On-road diesel emissions of pollutants such as BC, NO_x, and PM_{2.5} have decreased dramatically in terms of contribution to total emissions (Figure 4.5). In particular, diesel contribution to BC and PM_{2.5} reduced significantly from 2005 to 2016. The contribution to PM_{2.5} changes from 11% to 4% over this decade. The DPF retrofit and fleet modernization program was mostly complete by 2016 according to the regulation, explaining why the changes in particulate species happen in the first decade of the time period examined. For NO_x, on-road diesel contributed 38% in 2005, 34% in 2016, and 20% in 2023. Since not all the heavy diesel trucks are required to install SCR until 2023, the reduction in emissions in NO_x was more gradual.

The contributions from on-road gasoline vehicles to BC and PM_{2.5} remain approximately the same by percentage from 2005 to 2023, changing from 4.9% to 3.5% and from 7.4% to 7.5%, respectively. Gasoline emission control has been effective since the 1980's and the sector is not a major source of emissions for particulate species. The contribution to NO_x from gasoline engines is roughly half of that from on-road diesel for all three emission scenarios.

Area and point sources dominate emissions for all four species in Figure 4.5, including NH₃. The focus of this research is not on these two sources and more in-depth emission projections are needed to accurately depict the changes in these two sectors. CARB has an extensive program controlling off-road diesel equipments. Therefore, the contributions in the future (2023) may be less than what Figure 4.5 represent.

Table 4.3 presents statistical comparison between available surface measurements and modeled results. Note that not every particulate and gaseous specie measurement was available for all four cases. In particular, PM_{2.5} measured hourly by BAM was not available in the South Coast until around 2008. At the time of study, measurements for 2016 were not yet available. Therefore, the 2015 measurements were compared against the 2016 model simulation as a proxy.

The base case (2005) simulation results in lower concentrations compared to the surface measurements. The discrepancies in winter season are more pronounced than summer. The relatively large magnitudes in standard deviations also indicate that site-to-site variability is significant. In some cases, the standard deviations from the comparison between mea-

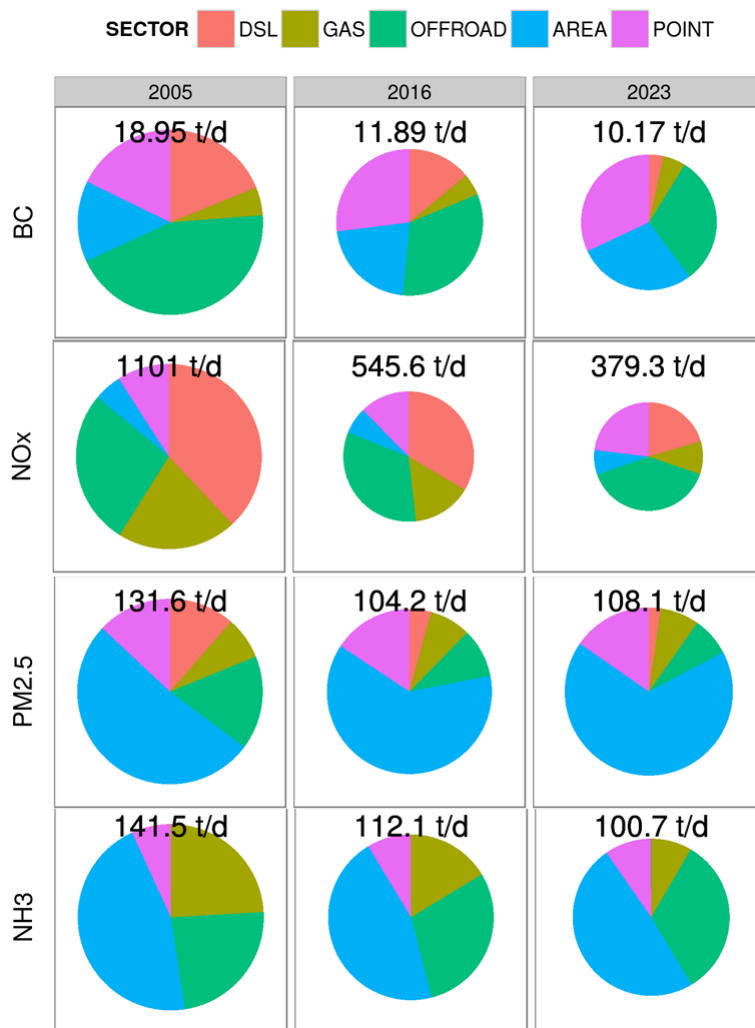


Figure 4.5: Contribution to total weekday emissions of BC, NO_x , $\text{PM}_{2.5}$ and NH_3 from five sectors. DSL and GAS represent on-road diesel and gasoline, respectively. Absolute emission in short tons/day is written above each pie chart.

measurements and simulations can be more than 50%. Taking into account the uncertainties, predicted values for the summer cases are acceptable. For the winter cases, the simulated concentrations of NO_3^- , NO_x and O_3 seem to be problematic for 2005, indicating that total emissions of reactive nitrogen species may be biased, or that undiagnosed model biases remain.

For the comparison of the three scenarios, almost all pollutants examined are reduced in 2016 and even more so in 2023, except for O_3 concentrations. NO_x concentrations in 2016 and 2023 will be less than 50% of those in 2005. However, only NO_3^- simulations in summertime see approximately the same reductions as NO_x . NO_3^- in wintertime continues to

	BC	NO ₃ ⁻	O ₃	NO _x	PM _{2.5} (BAM)
2005 predicted vs. observed values					
summer	0±31	-4±10	-10±15	-6.7±19	
winter	-13±54	-45±16	-25±17	-46±17	
2016 predicted vs. 2015 observed values					
summer			-8.7±17	27±40	-12±35
winter			-45±14	-12±29	-43±65
2016 predicted vs. 2005 predicted values					
summer	-33±5.6	-46±14	21±19	-52±3.3	-33±5.8
winter	-36±5.1	0±20	55±27	-54±2.2	-13±7.0
2023 predicted vs. 2005 predicted values					
summer	-42±7.6	-63±16	32±25	-66±7.8	-34±7.4
winter	-45±7.3	-13±26	95±41	-71±4.9	-14±6.3

Table 4.3: Percentage (%) differences of weekday concentrations for four comparison cases. Mean ± standard deviation is reported. Sample sizes are N=11 for speciated PM_{2.5} measurements (BC, NO₃⁻), N=24 for O₃; N=16 for NO_x; and N=14 for hourly PM_{2.5} measured by BAM. O₃ concentrations were based on the 8-hour 10AM-6PM period. All other calculations were done on the 24-hour basis.

show little change in 2016 and 2023, possibly because the formation of NO₃⁻ in California is largely driven by meteorology rather than emissions, or NH₃, a driver of NO₃⁻ formation in Southern California, may have been underestimated by the emission inventory [88]. Despite the uncertain changes in wintertime NO₃⁻, a major component of PM_{2.5}, the overall PM_{2.5} concentrations show significant decreases in winters of 2016 and 2023 (13±7% and 14±6%, respectively).

In contrast, O₃ concentrations continue to increase in 2016 and 2023 according to the simulations, for example, by 21±19% in winter of 2016 and 32±25% in 2023. This may be due to the VOC-sensitive O₃ formation mechanism in some parts of California [101]. O₃ could increase for a VOC-limited region if the rate of decrease in NO_x overtime is much larger than that of VOC.

Figure 4.6 and 4.7 show measured concentrations of NO_x and O₃ as trend lines with predicted values as overlaying boxplots. From Figure 4.6, it is clear that ambient NO_x concentrations have decreased steadily since 2005 for all the sites examined, and the simulation results confirm the trend. The reductions seem to be steeper from 2005 to around 2012, and slow down from 2012 to 2023. In general, model simulations result in lower average values (except for Los Angeles-Westchester Parkway), and less variations in concentrations, as the boxes are not as wide as the purple bands. There seems to be better predictions by the model near Los Angeles (top two panels) than for the more inland sites.

For O₃ in Figure 4.7, measured concentrations show no apparent changes, and models show slight increases across the sites, especially at downtown Los Angeles (North Main Street), Pasadena, and Anaheim from 2016 to 2023. In contrast, West Los Angeles, Riverside and San Bernardino see increases from 2005 to 2016, but the concentrations stay approximately the same level from 2016 to 2023. This could be due to the fact that although over all NO_x emissions reduce from 2016 to 2023, there is more primary NO in the mix nearby Los Angeles/Long Beach from traffic than the inland sites. Figure 4.7 confirms the relative 20-30% increase from 2005 levels in 2016 and 2023.

Hourly measurements of NO_x, O₃ and PM_{2.5} (by BAM) were used to compare against the predicted values in Figures 4.8 through 4.10. In Figure 4.8, model simulations roughly capture the peaks in NO_x concentrations during morning traffic hours and late night. However, there are 1-2 hours of delay in the modeled peak concentrations in Los Angeles, Anaheim and Riverside. The model's capability to estimate concentrations seems to vary by site and time, for instance, it over-predicts summer concentrations of NO_x at Riverside, but underestimates winter concentrations from 0-9AM at the same site.

In Figure 4.9, the model accurately determines the diurnal trends in O₃ concentration. Predicting O₃ is relatively easy because it is a secondary pollutant and its variations mainly depend on photochemistry. Concentrations usually peak in early afternoon and this has been consistently observed at all the sites. The highest concentrations occur at Riverside in the summertime. The simulations underestimate concentrations most of the time, except at Long Beach in the summer. The underestimation is especially prominent in winter.

The simulations were poor at capturing the diurnal trends in PM_{2.5} concentrations, shown in Figure 4.10. First of all, the model over-predicts winter concentrations at all sites, despite approximately capturing the peak hours, which are during late morning and late night. Secondly, during the summer season, the model consistently over-predicts PM_{2.5} concentrations at night (10PM-6PM) and under-predicts during daytime. The underestimation at night might be due to meteorology, possibly lower atmospheric boundary layers and/or mixing rates in the model. The overestimation in the day points to inaccuracy in the secondary aerosol formation mechanism.

PM_{2.5} speciation changes significantly over the period of study, shown in Figure 4.11 and 4.12. The MATES 2005 and 2012 data show that nitrate and sulfate decreased across all the sites. Nitrate was reduced because of the continuous reduction in on-road emissions, and sulfate was reduced because of the cleaner ship fuels used after 2010 and the low-sulfur diesel fuel requirement for both on-road and off-road engines after 2006. Percentage contribution from BC has not changed significantly, but the absolute BC concentrations have decreased from 2005 to 2012.

The simulations capture approximately the right magnitudes of contribution from BC for

all the sites, and nitrate for most of the sites in 2005. However, the major problem is that the simulations do not show much contribution from OC at all. Again, this points to the inadequacy of the aerosol chemistry in CMAQ.

Rates of reduction in PM_{2.5} are faster from 2005 to 2016, and slower from then on. Some of the reasons may be that DPF installation was largely completed by 2016, and growth from 2016 up to 2023 in population and almost all sectors is likely to offset the reductions in emission factors.

Figures 4.13 and 4.14 focus on the model concentrations in the three scenarios and compare the spatial variations in NO_x, O₃, PM_{2.5} and NO₃⁻ due to emission changes. In Figure 4.13a, it is clear that the hot spots in Los Angeles and Long Beach have reduced NO_x by 50% from 2005 to 2016, and by about 30% from 2016 to 2023. Assuming no significant changes in traffic patterns from 2005 to 2023, the universal installation of NO_x control in heavy diesel trucks should result in major reductions in NO_x as predicted.

In Figure 4.13b, concentrations of O₃ increase by about 10-20 ppb from 2005 to 2016. Concentrations in some areas are likely to exceed the national ambient air quality standard of 70 ppb. The areas affected are San Bernardino and Riverside in 2016, and San Bernardino, Pasadena, and Burbank in 2023. Unfortunately, the implementation of NO_x controls, combined with changes in other emission sectors, does not seem sufficient to resolve the persistent problem of high summer O₃ in the South Coast.

Reductions in PM_{2.5} look more gradual than NO_x in Figure 4.14a. The area with PM_{2.5} concentrations above 10 μg/m³ remain in the proximity of Long Beach and Los Angeles, extending into San Bernardino and Riverside, although the affected areas have shrunk slightly. The hot spots at Long Beach have seen reductions of PM_{2.5} on the order of 10 μg/m³ from 2005 to 2016, and increased very slightly from 2016 to 2023. Overall, PM_{2.5} predictions show better reductions and suggest a future with lesser problems of air quality standard exceedance compared to O₃ in Figure 4.13b.

Figure 4.14b shows that the region with the highest NO₃⁻ concentrations is in south and central Los Angeles and some parts of San Bernardino and Riverside counties. Hot spots remain with high concentrations, although the areas with higher than 0.5 μg/m³ of nitrate have shrunk in size slightly from 2005 to 2023.

4.4 Discussion

The model simulations incorporate changes in all emission sectors while focusing on the benefits of universal NO_x controls on heavy diesel trucks. The model reflects changes in some primary pollutants fairly well, such as BC and summertime NO_x and PM_{2.5}, and shows discrepancies compared to measurements in some other cases, including O₃ and secondary

organic aerosol.

Comparison between the simulations and ground measurements may not be reliable because the spatial resolution of the model is 5 km, whereas ground measurements could be easily influenced by nearby local roadways and residential sources. In general, models with coarse spatial resolution tend to underestimate when compared to ground measurements. Such is the case in this modeling study.

The emission scenarios also predict that O₃ may increase slightly in 2016 and 2023. This prediction remains to be tested because modifying VOC emissions is not the focus of this study, and therefore emission uncertainties limit confidence in this conclusion. However, the model supports the evidence that the South Coast is VOC-limited and may continue to be so in the next decade, and that large O₃ reductions are unlikely.

In conclusion, this study shows the impacts on air quality in Southern California from the universal use of advanced emission control technologies required on heavy diesel trucks. The regulation, combined with changes in other emission sectors, has positive effects on BC, NO_x, and PM_{2.5}, but may have little or even slightly adverse effects on O₃.

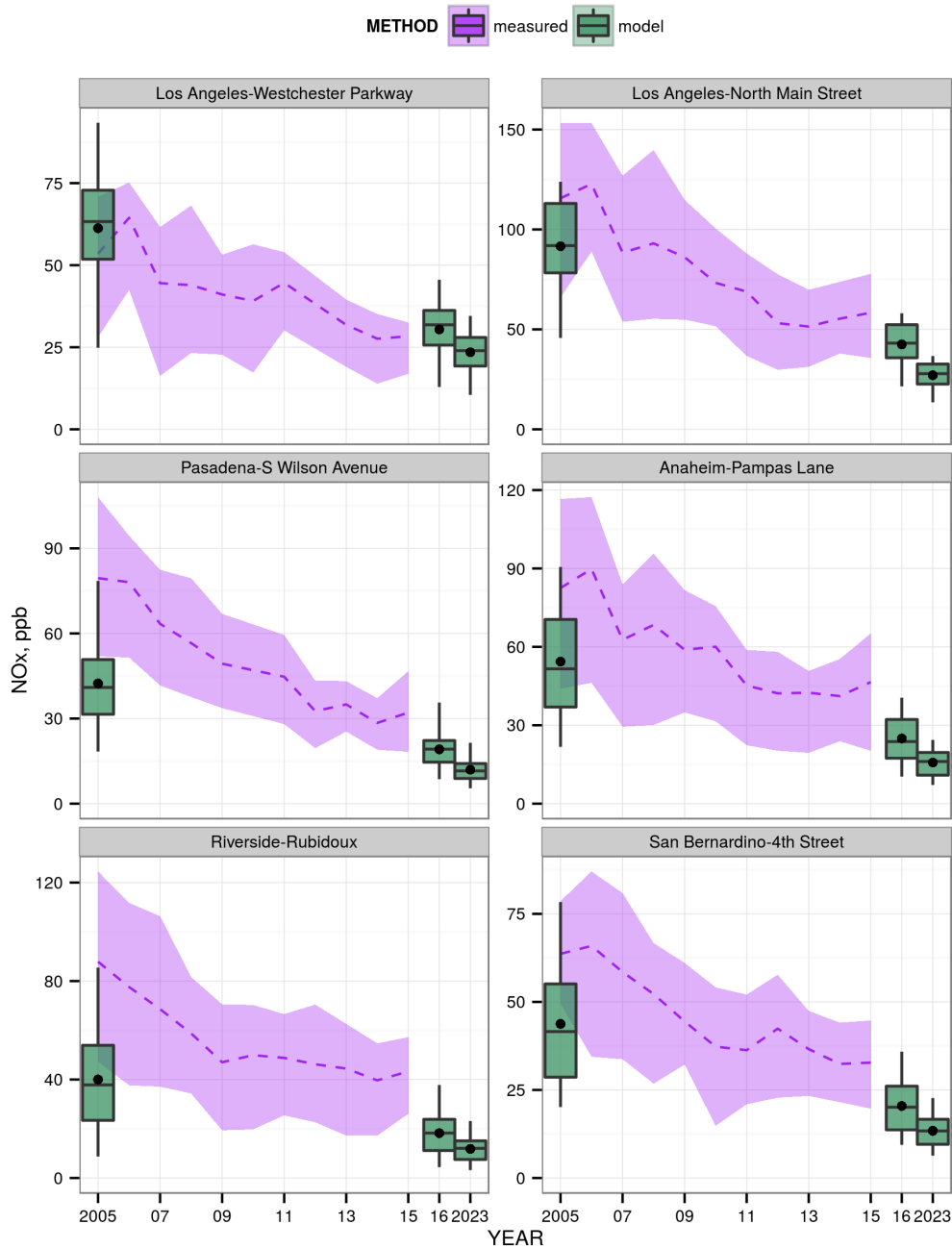


Figure 4.6: Measured and predicted winter NO_x concentrations from 2005 to 2023 for selected sites. Site are ordered from west to east. Purple dotted lines represent the means of the measured concentrations, and purple bands represent the 25% and 75% quartiles. Green boxes represent the predicted values in 2005, 2016 and 2023, with black dots as means, black lines in the boxes as medians, lower and upper edges of the boxes as 25 and 75 percentiles, and whiskers extending to 95% confidence intervals. Note the time axis is discontinuous after 2016.

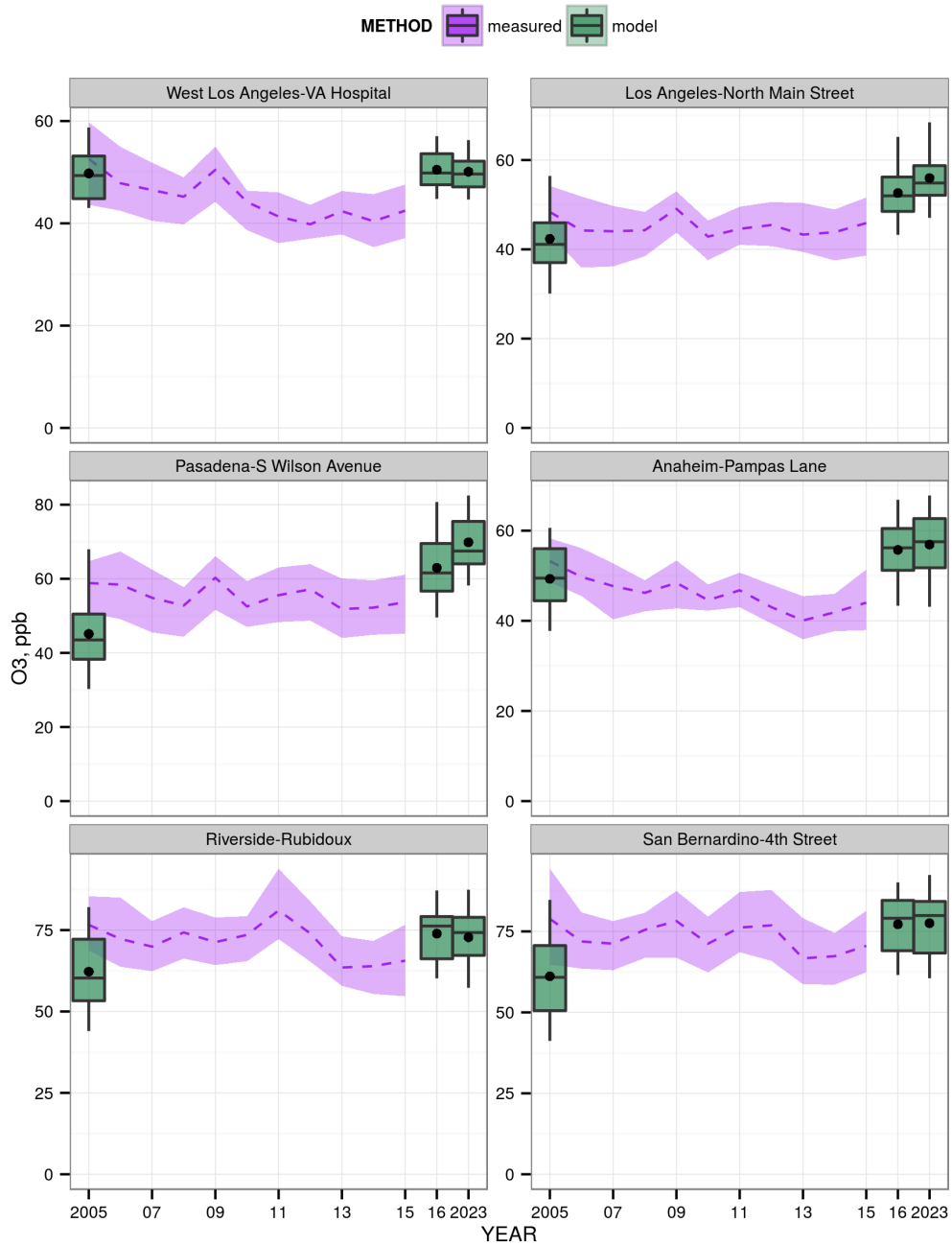


Figure 4.7: Measured and predicted summer O₃ concentrations. Plot specifications are the same as in Figure 4.6.

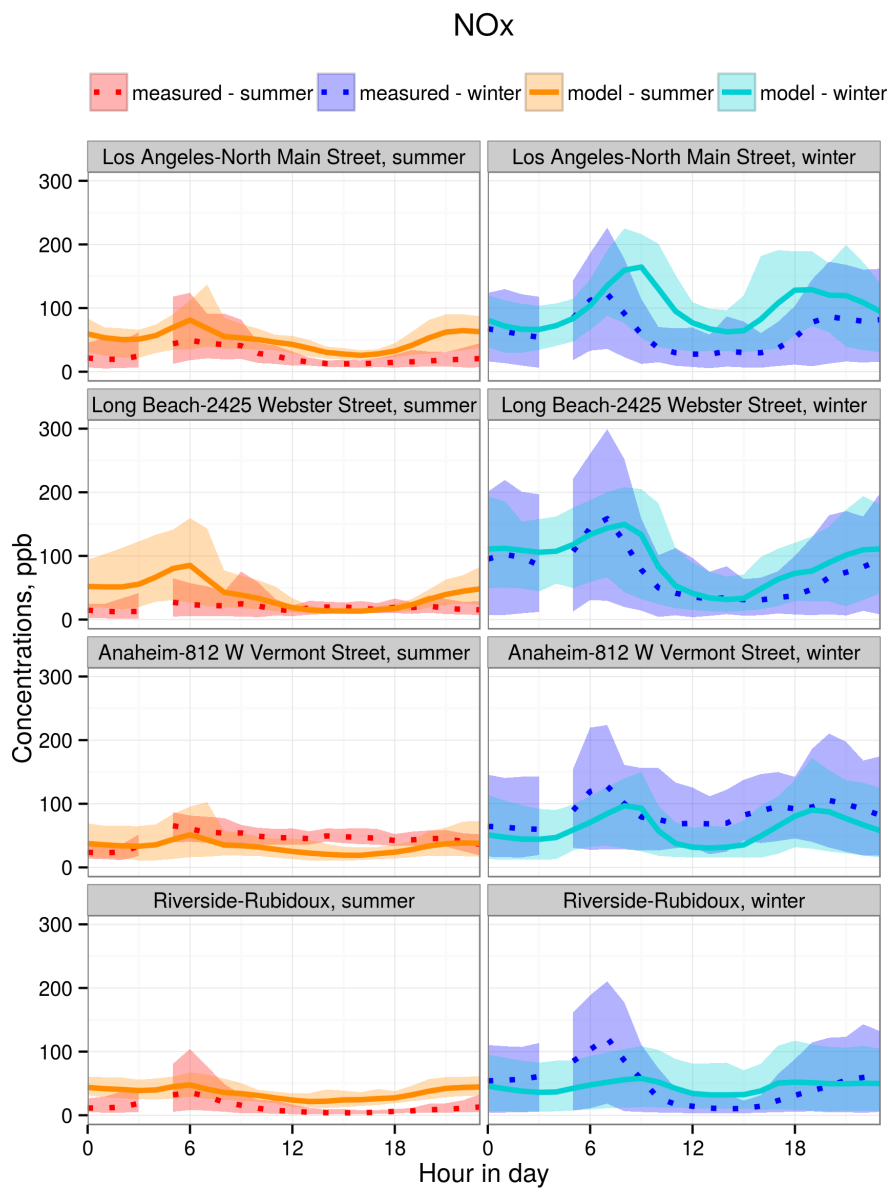


Figure 4.8: Diurnal variations in weekday NO_x concentrations in summer (red/orange) and winter (blue/cyan) at four selected sites. Sites are located from west to east. Dotted lines indicate 2015 measured concentrations and solid lines indicate 2016 model predictions. Color bands indicate 95% confidence intervals. Hours with less than 75% measured data available were not plotted (3 and 4AM).

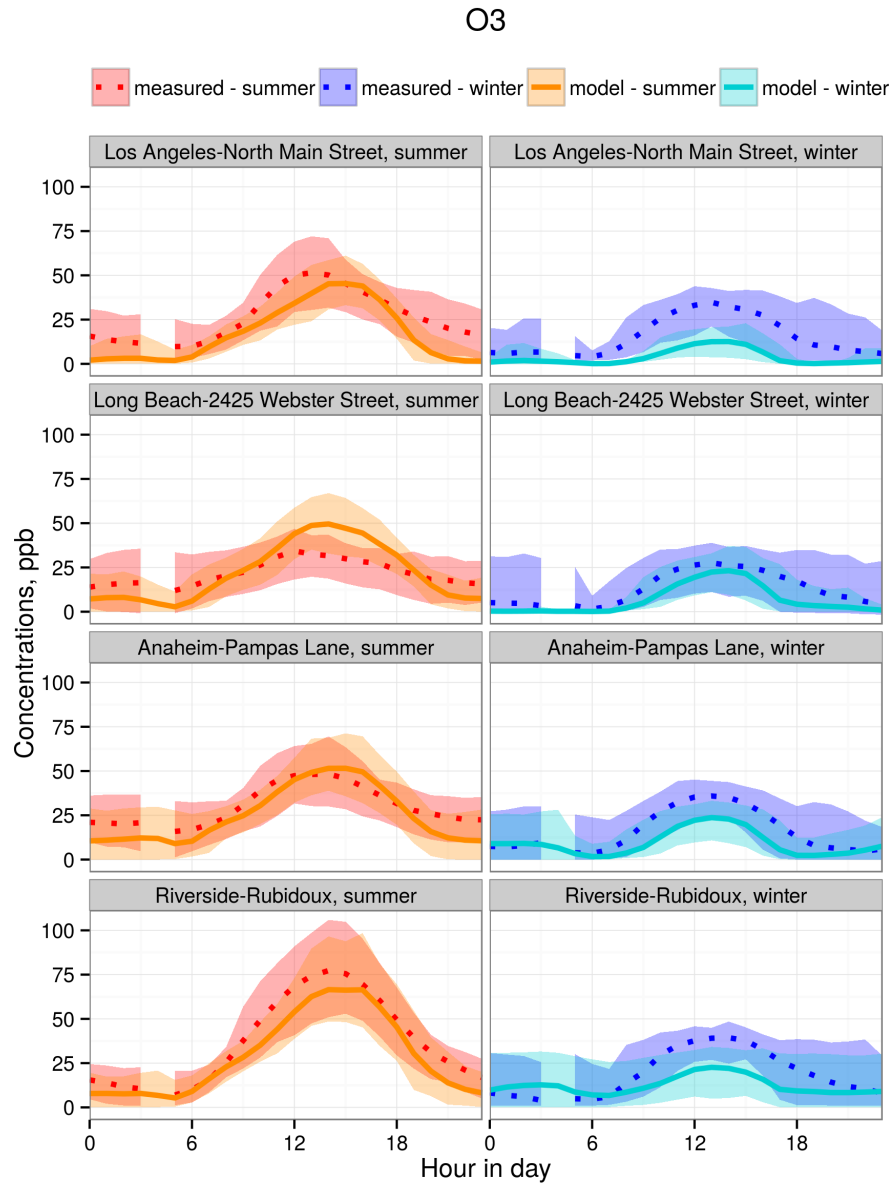


Figure 4.9: Diurnal variations in weekday O₃ concentrations. Plot specifications are the same as in Figure 4.8.

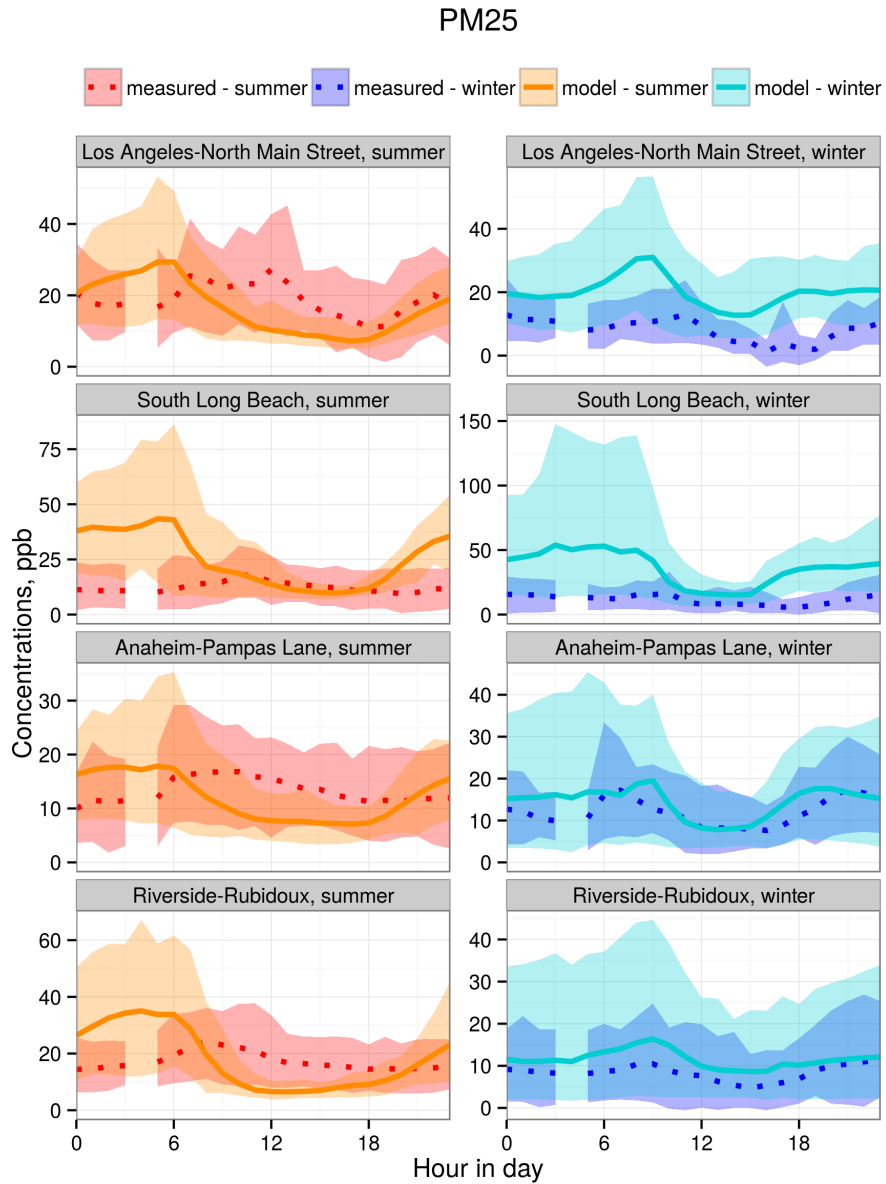
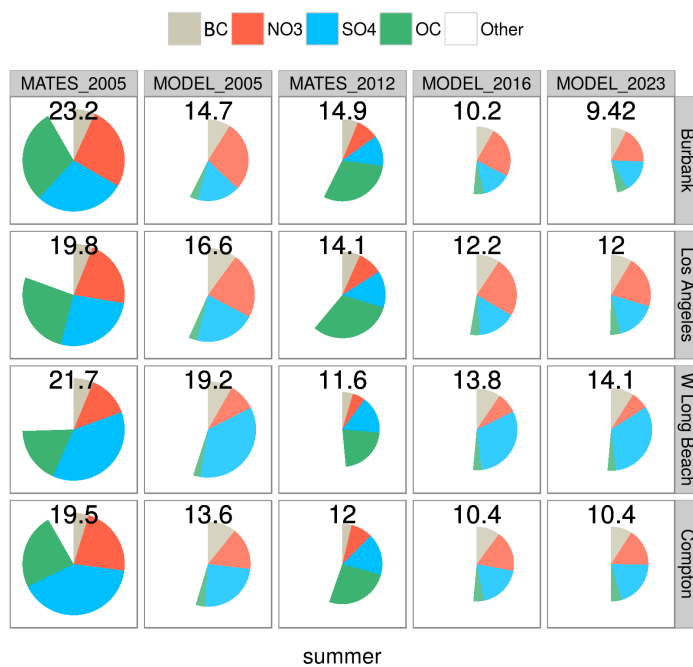
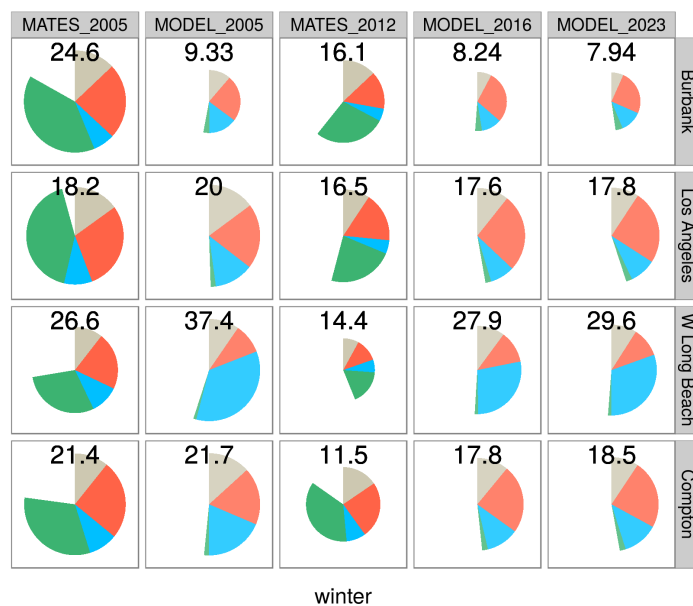


Figure 4.10: Diurnal variations in weekday PM_{2.5} concentrations. Plot specifications are the same as in Figure 4.8.

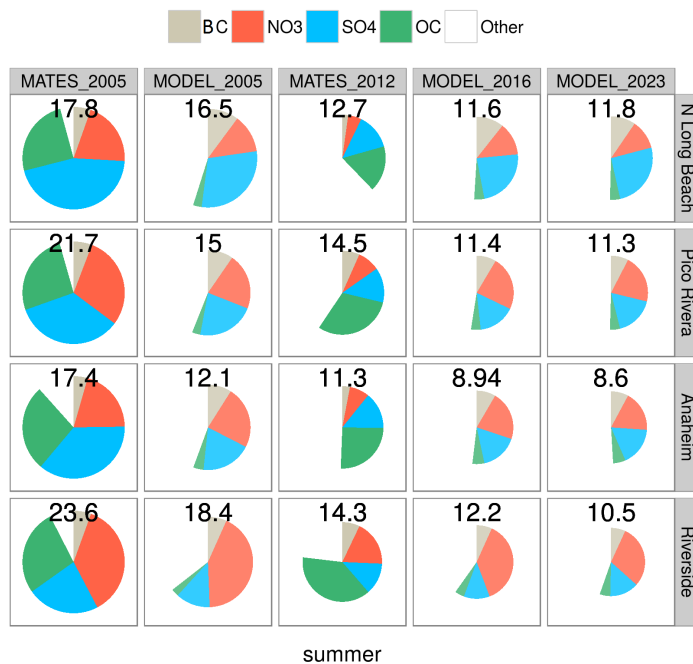


(a)

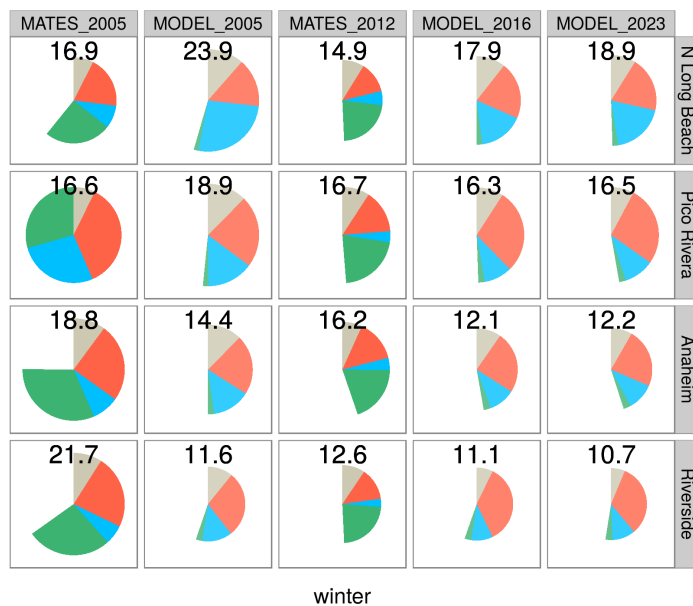


(b)

Figure 4.11: $\text{PM}_{2.5}$ speciation pie charts from the 2005, 2016 and 2023 model simulations and 2005 and 2012 MATES measurements in summer (top) and winter (bottom). Both weekdays and weekends are included. Average $\text{PM}_{2.5}$ mass concentration is written above each pie in $\mu\text{g}/\text{m}^3$. BC, NO_3^- , SO_4^{2-} , OC are represented in grey, red, blue, and green, respectively. All other components are lumped into 'Other', in white. The four sites are Burbank, Los Angeles, West Long Beach and Compton in the western half of the air basin.



(a)



(b)

Figure 4.12: PM_{2.5} speciation pie charts from the 2005, 2016 and 2023 model simulations and 2005 and 2012 MATES measurements. Plot specifications are the same as in Figure 4.11 except that the sites are North Long Beach, Pico Rivera, Anaheim and Riverside, in the Eastern (inland) half of the air basin.

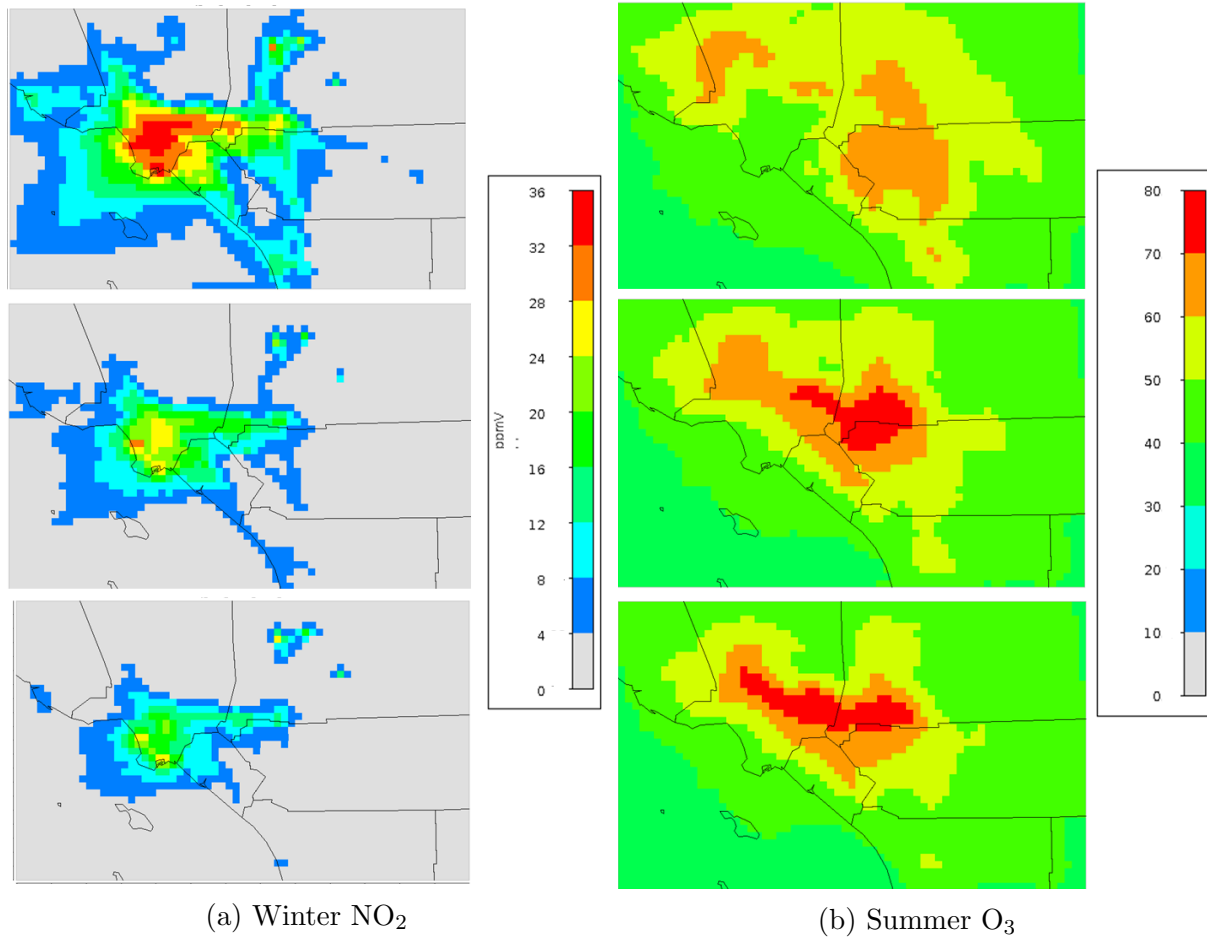


Figure 4.13: Maps of predicted concentrations in ppb for (a) Summer NO_2 and (b) Winter O_3 in 2005 (top), 2016 (middle), and 2023 (bottom). Daily average (24-hour) values are shown for NO_2 and only 10AM-6PM averages are used for O_3 . Color scales are kept the same across all three emission scenarios.

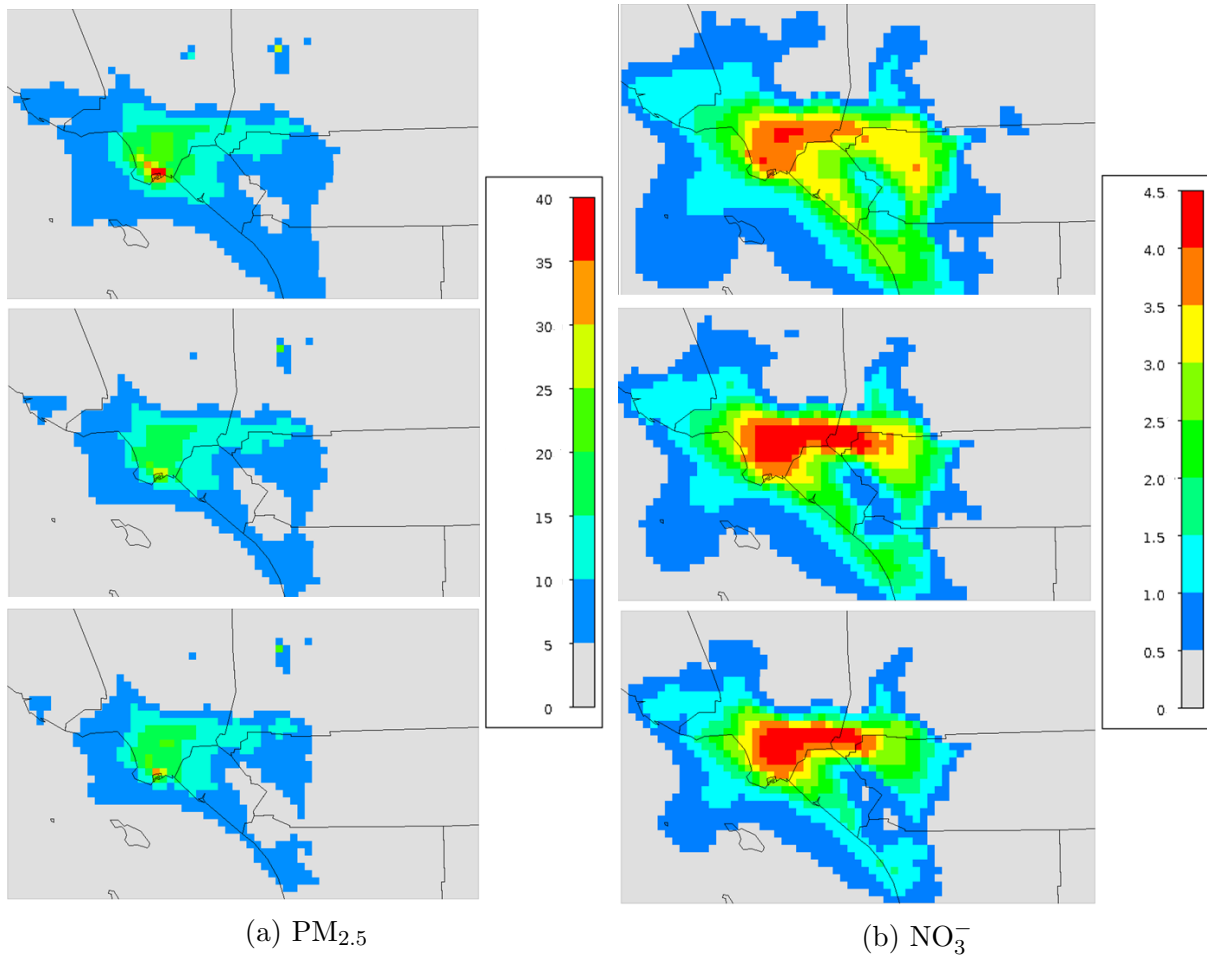


Figure 4.14: Maps of predicted winter concentrations in $\mu\text{g}/\text{m}^3$ for (a) $\text{PM}_{2.5}$ and (b) NO_3^- . All hourly values are used for both pollutants. Other plot specifications are the same as in Figure 4.13.

Chapter 5

Changes in Fine Particulate Matter Measurement Methods and Ambient Concentrations in California

5.1 Introduction

Airborne fine particulate matter with diameter less than $2.5 \mu\text{m}$ ($\text{PM}_{2.5}$) is a key air pollutant that affects human cardiovascular function negatively [123]. $\text{PM}_{2.5}$ also leads to visibility degradation [28] and perturbs both directly and indirectly the energy balance for planet Earth [70]. Ambient air quality standards for $\text{PM}_{2.5}$ were established in the United States in 1997 for both annual and daily average concentrations.

In the late 1990s, the US Environmental Protection Agency (EPA) mandated a nationwide $\text{PM}_{2.5}$ monitoring network. Monitoring sites within this network were required to use approved reference or equivalent sampling methods [63, 118, 121]. Prior to this, California had been measuring ambient fine and coarse particle concentrations using dichotomous (dichot) air samplers [27]. Both the dichot and reference methods approved by EPA are based on gravimetric sampling [62]. Ambient air is drawn through a size-selective inlet to exclude large particles, and $\text{PM}_{2.5}$ is collected on a pre-weighed filter, over a period of 24 hours. Filters are transported back to a central laboratory, conditioned at controlled relative humidity, and then reweighed. $\text{PM}_{2.5}$ concentration is computed as the increase in filter mass divided by the volume of air sampled. The sampling frequency using filter methods has typically been once every three or six days.

The beta attenuation monitor (BAM) is a continuous method for measuring airborne particle mass, described by [79] and [83]. The approach is based on the principle that beta

This chapter is a reproduction of the publication: Tao, L., & Harley, R. A. (2014). Changes in fine particulate matter measurement methods and ambient concentrations in California. *Atmospheric Environment*, 98, 676684. <http://doi.org/10.1016/j.atmosenv.2014.09.044>

radiation is mainly absorbed by atomic nuclei, and absorption cross sections scale with increasing atomic mass. Therefore, beta attenuation by particles collected on a filter scales linearly with particle mass. Current commercially available instruments can provide hourly measurements of ambient $\text{PM}_{2.5}$ concentrations in real-time. Side-by-side studies comparing BAM and filter-based methods have been reported [47, 46, 127]. In 2008, EPA designated the continuous beta attenuation monitor (BAM) as a non-gravimetric equivalent method for measuring $\text{PM}_{2.5}$, meaning the data are judged as suitable by EPA for use in state implementation plans [63]. As of 2013, BAM had been deployed at 103 sites in California [7]. Other states are also incorporating real-time $\text{PM}_{2.5}$ measurement methods into their monitoring networks. For example, 21 BAM samplers were operating in Pennsylvania as of 2013 [120]. Other measurement methods that also provide continuous or semi-continuous $\text{PM}_{2.5}$ mass readings, not discussed further in this study, include the Hi-Volume Dichotomous Sampler [130], Tapered Element Oscillating Microbalance [17], and Continuous Aerosol Mass Monitor [10].

Use of BAM improves the temporal resolution of measured $\text{PM}_{2.5}$ concentrations from daily averages to hourly data, which enables the study of short-term events relevant to assessing health effects of acute exposures to $\text{PM}_{2.5}$. Recent research has shown that exposure to high concentrations of $\text{PM}_{2.5}$ on time scales shorter than 24 hours is associated with myocardial infarction and ischemic events in sensitive groups, as well as changes in biomarkers such as C-reactive protein that responds to oxidative stress [124, 20, 30]. A monitoring network with high spatial coverage and temporal resolution may help to draw new connections between ambient $\text{PM}_{2.5}$ concentrations and health effects data, such as hospital visits for chest pain and asthma emergencies. The real-time nature of BAM can also help to improve air quality forecasting. Short-term air quality forecasts for time periods on the order of the next several days are currently based on multiple regression models and other empirical approaches. Current-day $\text{PM}_{2.5}$ observations have not been available to use in making forecasts due to time delays associated with transporting, conditioning, and weighing filters after sampling. With hourly measurements of ambient concentrations now available in real-time, air quality forecasts will be better able to constrain and update $\text{PM}_{2.5}$ predictions using current data [151].

This paper focuses on the evolution of the monitoring network and measured $\text{PM}_{2.5}$ concentrations in California over a period of about 25 years. Three California air basins, namely the San Francisco Bay area and the Los Angeles area along the coast, and the San Joaquin Valley inland, are the focus of this study. These air basins together encompass 75% of the total population in California, and include major metropolitan areas as well as industrial and agricultural centers [140]. In 2009, all three basins were designated as non-attainment for the $35 \mu\text{g}/\text{m}^3$ 24-hour $\text{PM}_{2.5}$ standard; the San Joaquin valley and the South Coast air basins have been tentatively designated as non-attainment areas for the $12 \mu\text{g}/\text{m}^3$ annual standard through 2012. Prior studies in California have shown downward trends in annual average $\text{PM}_{2.5}$ concentrations at several urban sites from 1988 to 2000 [115], as well as sig-

nificant reductions in fine particle sulfate at rural sites [99]. [45] showed that there was an overall improvement in $PM_{2.5}$ concentrations between 1982 and 1993 in the Los Angeles area. In addition to sulfate reductions, the mass of black carbon (BC) decreased significantly whereas organic carbon mass was not reduced as much. Large reductions in BC have also been reported in the San Francisco Bay area, by about a factor of three between 1967 and 2003, based on an analysis of coefficient of haze measurements [91]. A source apportionment study in San Jose in the Bay area found moderate reductions in $PM_{2.5}$ concentrations over ten years, and identified contributing factors such as control of winter season wood-burning and an enhanced street sweeping program in the area [144]. Key components of $PM_{2.5}$ also vary on shorter time scales. For instance, high nitrate contributions are observed in Fresno in the San Joaquin Valley, especially in wintertime [43, 44]. Nitrate also shows a weekly cycle in Fresno, with minima on Monday and maxima on Saturday [112]. In the Bay area, BC increases during winter months due to more wood-burning, and decreases on weekends due to reduced diesel truck traffic [91]. Due to the limited temporal coverage of past $PM_{2.5}$ measurements, few previous studies have focused on weekly cycles in $PM_{2.5}$ mass. BAM provides much more data compared to traditional filter sampling, and enables more thorough consideration of questions relating to weekly and diurnal variations in $PM_{2.5}$ mass concentrations.

This paper analyzes the available record of filter-based and BAM measurements of $PM_{2.5}$ concentrations in California, makes comparisons of data measured by different methods, evaluates long-term trends in $PM_{2.5}$, and explores seasonal, day of week and diurnal variations using new BAM data.

5.2 Approach

Measurement Methods

Dichotomous samplers use a virtual impactor to segregate particles in an air sample into two fractions: coarse (2.5 - 10 μm) and fine (<2.5 μm). 90% of the air stream flows through the fine particle filter at a rate of 15 L/min, and the remaining 10% flows through the coarse filter at 1.67 L/min. Sampling using the dichots was typically done for 24 consecutive hours every sixth day. At the end of each sampling period, Teflon filters were removed and delivered to a laboratory for weighing; the limit of detection is 2 $\mu\text{g}/\text{m}^3$ [5, 27].

A commonly used FRM sampler (Andersen, Fultonville, New York; model RAAS2.5-300) consists of a well impactor to exclude particles with diameters larger than 2.5 μm , and uses a pre-weighed Teflon filter to collect the remaining particles. The flow rate is set at 16.7 L/min \pm 5%, and the sampling period is 24 hours. Filters are recovered from the site within three days of sampling, maintained at a temperature of 4°C during transport to the laboratory, and equilibrated with ambient air at a fixed temperature (20-23°C) and relative humidity (30-40%) for 24 hours, before finally reweighing the filter.

A commercial version of BAM (Met One, Grants Pass, OR; model BAM-1020) includes a sharp cut cyclone inlet, a glass fiber filter tape to collect particles, a beta radiation source (60 μCi of Carbon-14, half life 5730 years), and a photomultiplier tube with plastic scintillator. At the start of every hour, beta rays are counted by the photo-detector to determine a blank reading for a strip of clean tape. The tape is then advanced to a nozzle where particles from the sample air stream deposit on the tape. At the end of the hour, the dust spot is moved back between the beta radiation source and the detector to measure the increase in beta attenuation due to particles collected during sampling [106]. The mass density is determined using the Beer-Lambert Law [83]. $\text{PM}_{2.5}$ concentrations are calculated based on particle mass loadings divided by air volume sampled. The relative humidity of the sampled air is controlled to be 35% at the inlet using a heater module. Manual replacement of the filter tape is required every two months.

California began to use dichot samplers in 1981, but consistent deployment of the instrument did not start until 1988 for a network of 31 sites. Dichot measurements ended in 2001, as FRM measurements had by then been deployed to replace the dichot network. Widespread BAM measurements across all three air basins did not start until 2008. Records of measured $\text{PM}_{2.5}$ concentrations made using all three of the above methods were retrieved from publicly available databases [8, 61, 6].

Data analysis

Data gaps are common when examining the record of measured $\text{PM}_{2.5}$ concentrations. Both the filter-based and BAM sampling methods experience occasional outages. For instance, there will be no measurement if a filter is mishandled or lost in transit between a monitoring site and the laboratory. BAM instruments may stop recording data if the filter tape jams or is not replaced in a timely manner. For the long-term and seasonal trend analyses in this study, years with more than one continuous month of missing data are not included. Regression analyses comparing filter-based and BAM data use maximum likelihood fitting. All analyses were carried out using the open source programming language R [128].

A similar set of analysis was done on measured nitric oxide (NO) and nitrogen dioxide (NO_2) ambient concentrations. The results are elaborated in Appendix A.

5.3 Results and Discussion

The $\text{PM}_{2.5}$ monitoring network in California has undergone significant expansion, and the inclusion of continuous measurements between 1988 and 2013, as shown in Table 5.1. The dichot network that was active through the 1990s was limited in both spatial coverage and sampling frequency. Historically, the San Francisco Bay area had only one dichot site located in San Jose. The establishment of new filter-based measurement sites starting in 1999

expanded the Bay area network dramatically. Both the Bay area and San Joaquin Valley air districts started deploying BAM shortly after 2000. Continuous measurements of PM_{2.5} in the South Coast air basin did not get underway at more than one site until 2008. Data availability for BAM sites increased from 91 to 96% of days in the San Francisco Bay area, and from 83 to 89% of days in the San Joaquin Valley between 2003 and 2013, perhaps reflecting increased operator experience and/or improvements in instrumentation as the online PM_{2.5} monitoring network has matured. In general, PM_{2.5} data availability is greater for BAM than filter measurements, for which percentages of days with data available often reflect deliberate once every third or sixth day sampling schedules, as well as missed samples. For instance, an average of 89% of days had BAM data in the San Joaquin Valley, as opposed to 38% of days with data from filter-based methods in 2013.

Table 5.1: Number of PM_{2.5} monitoring sites and fractions of days sampled in selected California air basins.^a

Air Basin	Method	1993		2003		2013	
		# of sites	% days available ^b	# of sites	% days available ^b	# of sites	% of days available ^b
San Francisco Bay area	Filter	1	17%	9	39 ± 15%	4	20 ± 11%
	BAM	0	0	1	91%	15	96 ± 3%
San Joaquin Valley	Filter	8	16 ± 0.6%	11	38 ± 23%	8	38 ± 27%
	BAM	0	0	4	83 ± 20%	19	89 ± 8%
South Coast	Filter	3	16 ± 0.4%	17	47 ± 29%	7	92 ± 3%
	BAM	0	0	0	0	15	87 ± 5%

^a Does not include data from the Interagency Monitoring of Protected Visual Environments (IMPROVE) network, which typically provides data for more remote/rural sites. Also excludes sites that began or ceased operation part way through the year.

^b Fraction of days with available PM_{2.5} data, mean ± standard deviation.

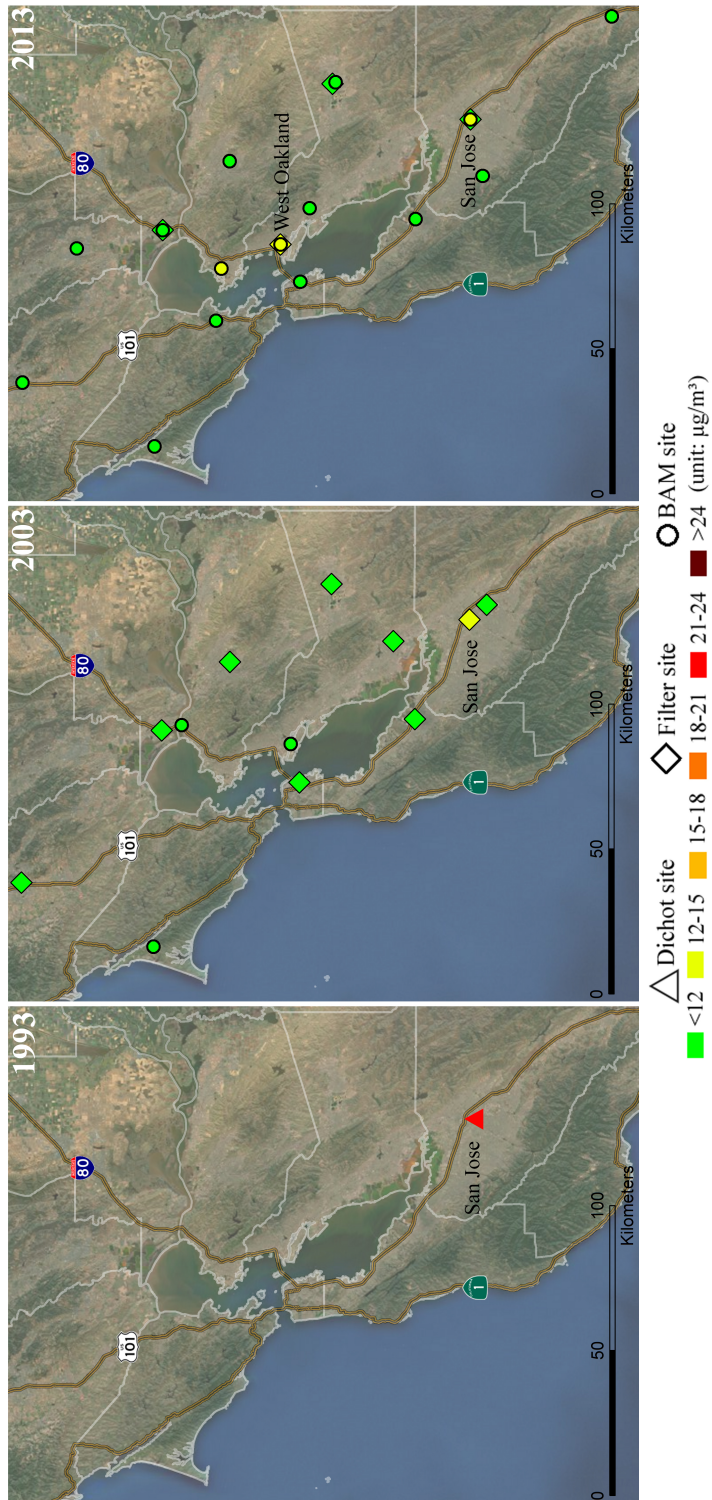


Figure 5.1: Fine particle measurement sites in the San Francisco Bay area, with colors indicating annual averages.

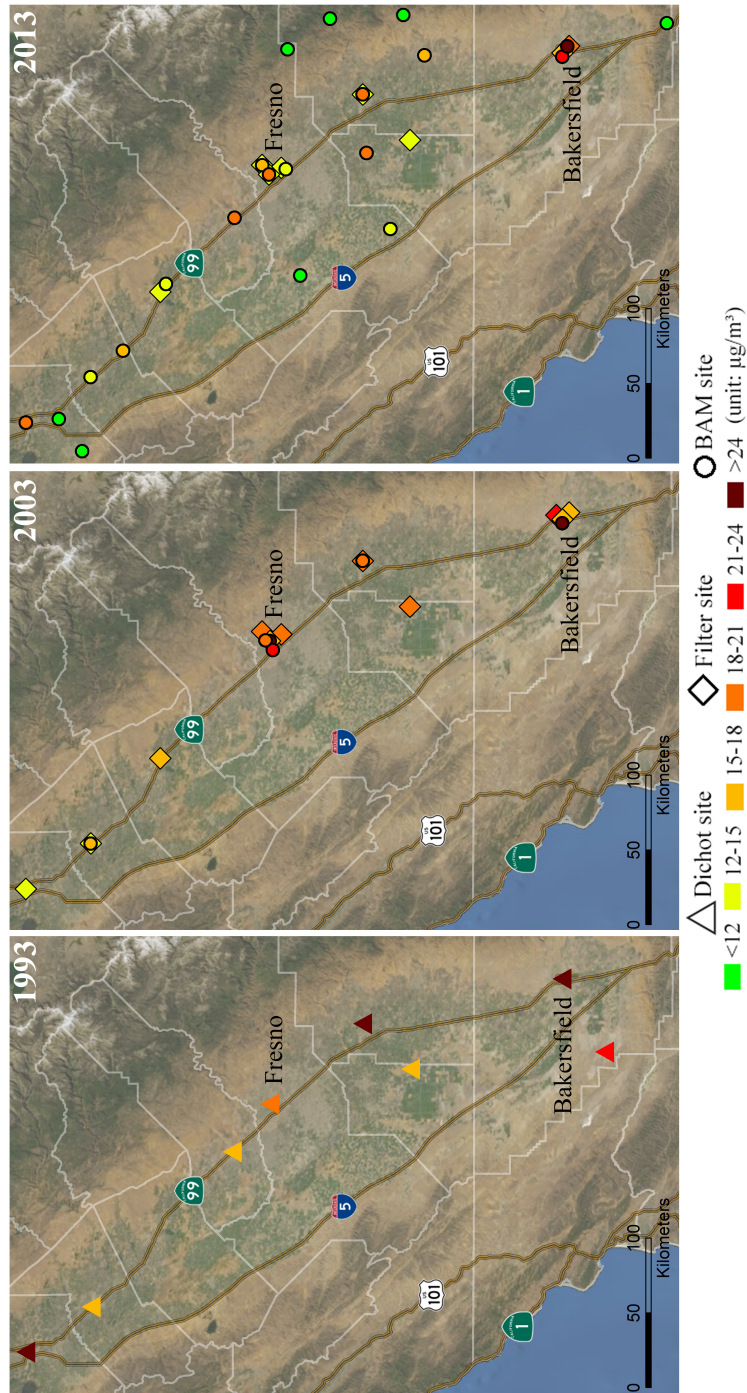


Figure 5.2: Fine particle measurement sites in the San Joaquin Valley

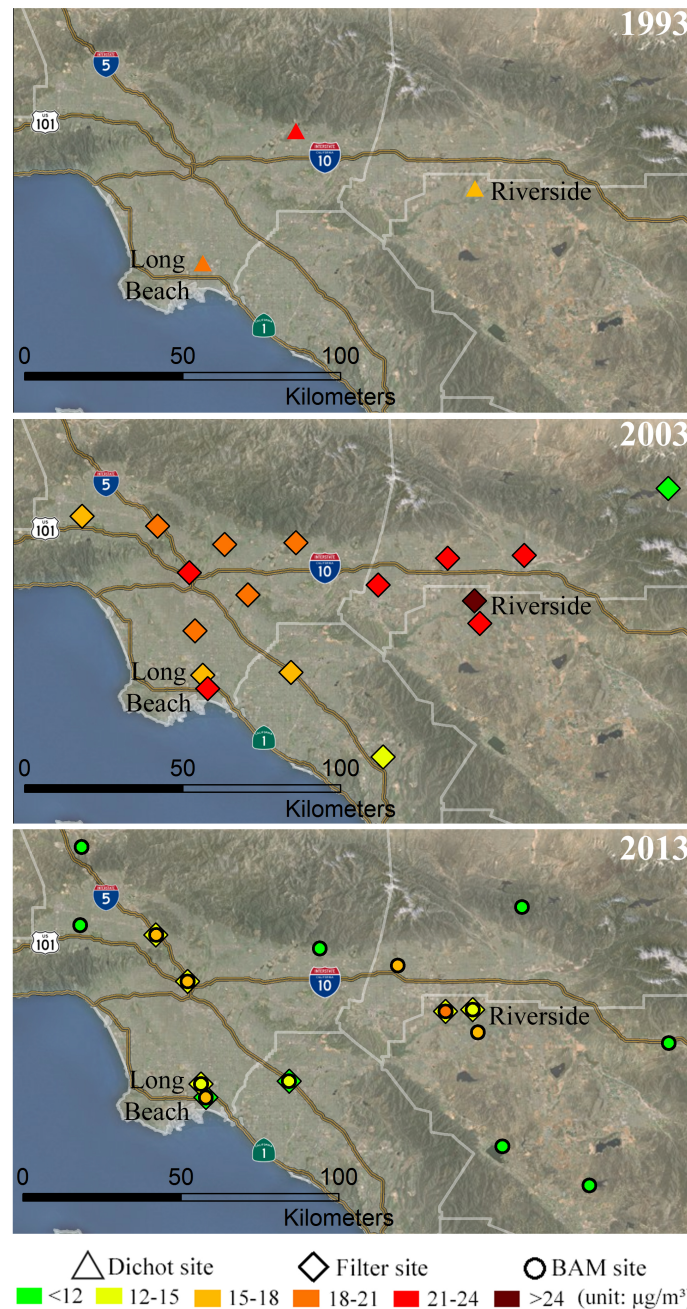


Figure 5.3: Fine particulate measurement sites in the South Coast Air Basin

Figures 5.1 - 5.3 show in detail the evolution of $\text{PM}_{2.5}$ measurement sites between 1993 and 2013. In 1993, the dichot network was most extensive in the San Joaquin Valley, followed by the South Coast air basin. Many more filter-based sites and some BAM sites had been established by 2003. As of 2013, in the Bay area, most of the $\text{PM}_{2.5}$ sites had switched from filter to BAM measurements, except for a collocated BAM/filter site in San Jose, and

three other filter sites in Vallejo, Livermore and West Oakland that measure both mass and speciation. The Bay area sites are relatively clean with $\text{PM}_{2.5}$ concentrations at or below the annual average standard of $12 \mu\text{g}/\text{m}^3$. Figure 5.2 shows clear region-wide reductions in $\text{PM}_{2.5}$ levels over time in the San Joaquin Valley, even though most urban sites along the highway 99 corridor are still above $12 \mu\text{g}/\text{m}^3$. Fresno has seen more improvement in $\text{PM}_{2.5}$ than Bakersfield. Reductions in $\text{PM}_{2.5}$ are most clearly apparent for Southern California, as shown in Figure 5.3.

Figures 5.1 - 5.3 suggest that for many of the collocated filter/BAM sites (*e.g.* San Jose, Bakersfield and Long Beach), the two measurement methods differ by $3\text{-}6 \mu\text{g}/\text{m}^3$, with BAM reading higher. Indeed, all three measurement methods used for $\text{PM}_{2.5}$ give different readings, with dichot being the lowest and BAM the highest. The dichot method under-reports $\text{PM}_{2.5}$ concentrations, at least in part because the virtual impactor leads to approximately 10% of fine particles being deposited on the coarse filter [**Dichot manual**]. Comparisons of BAM with filter-based methods, shown in Figure 5.4, indicate small differences for the San Francisco Bay area, and larger differences for the South Coast air basin, due to differences in absolute $\text{PM}_{2.5}$ mass concentrations and/or particulate matter composition. Past studies have also shown BAM reads higher compared to filter-based measurements for PM samples that include a high fraction of volatile ammonium nitrate [43]. Volatilization of nitrate from Teflon filters can occur when humidity and/or temperature fluctuates during the sampling period [76]. In California, where nitrate is a significant fraction of $\text{PM}_{2.5}$ especially during colder months, 24-hour filter-based readings are known to underestimate $\text{PM}_{2.5}$ mass. This has been reported previously for Fresno and Bakersfield in the San Joaquin Valley [42]. Another reason for divergent readings can be differences in size-selective sampling inlet designs, especially when $\text{PM}_{2.5}$ contains high amounts of dust which includes particle sizes close to the inlet cut-points. Differences in $\text{PM}_{2.5}$ readings due to this effect have been reported in the San Joaquin Valley in summer [43]. For selected collocated sites, Figure 5.4 shows that filter sampling gives lower $\text{PM}_{2.5}$ readings than BAM, when levels are below certain threshold concentrations (*e.g.* $13 \mu\text{g}/\text{m}^3$ at San Jose and $54 \mu\text{g}/\text{m}^3$ at Fresno). In Southern California, filter-based sampling gives lower readings at all levels at both Long Beach and Riverside. The differences between BAM and filter sampling methods can be large enough to affect attainment designations with respect to $\text{PM}_{2.5}$ air quality standards. This may be a contributing factor in explaining why the South Coast air basin has been slower than others in making the switch to BAM.

The record of $\text{PM}_{2.5}$ concentration data that has been collected in California enables the analysis of long-term trends for some monitoring sites that have been operating since the 1980s. Figure 5.5 shows trends in boxplot statistics for $\text{PM}_{2.5}$ at these sites. All sites show reductions, but to varying degrees. Fresno and Bakersfield in the San Joaquin Valley show gradual improvements in both annual average and peak 24-hour average values. Monitoring sites in San Jose, Long Beach and Riverside show clear reductions in $\text{PM}_{2.5}$, such that exceedances of the 24-hour average standard now pose a bigger challenge than meeting the

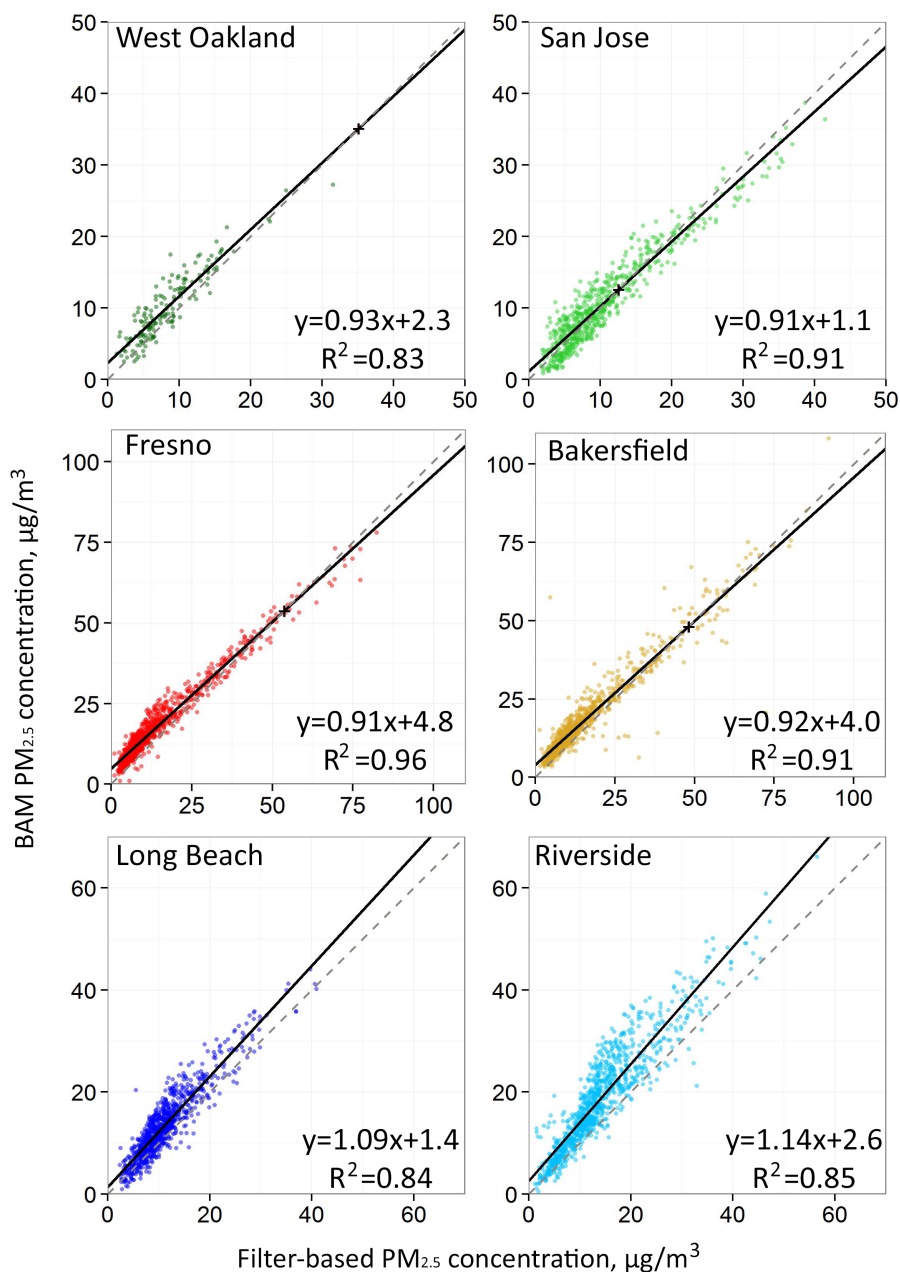


Figure 5.4: Correlation between BAM and filter-based PM_{2.5} concentrations using data from 2009-2011. The solid lines represent linear regressions, the dashed lines represent the 1:1 relation, and the crosses show where solid and dashed lines intersect (see text).

annual average standard at these sites. The large decrease in PM_{2.5} at Riverside, about 67% between 1999 and 2013, reflects both targeted air pollution control efforts and the migration of agriculture activities out of the basin as the surrounding area became increasingly urban-

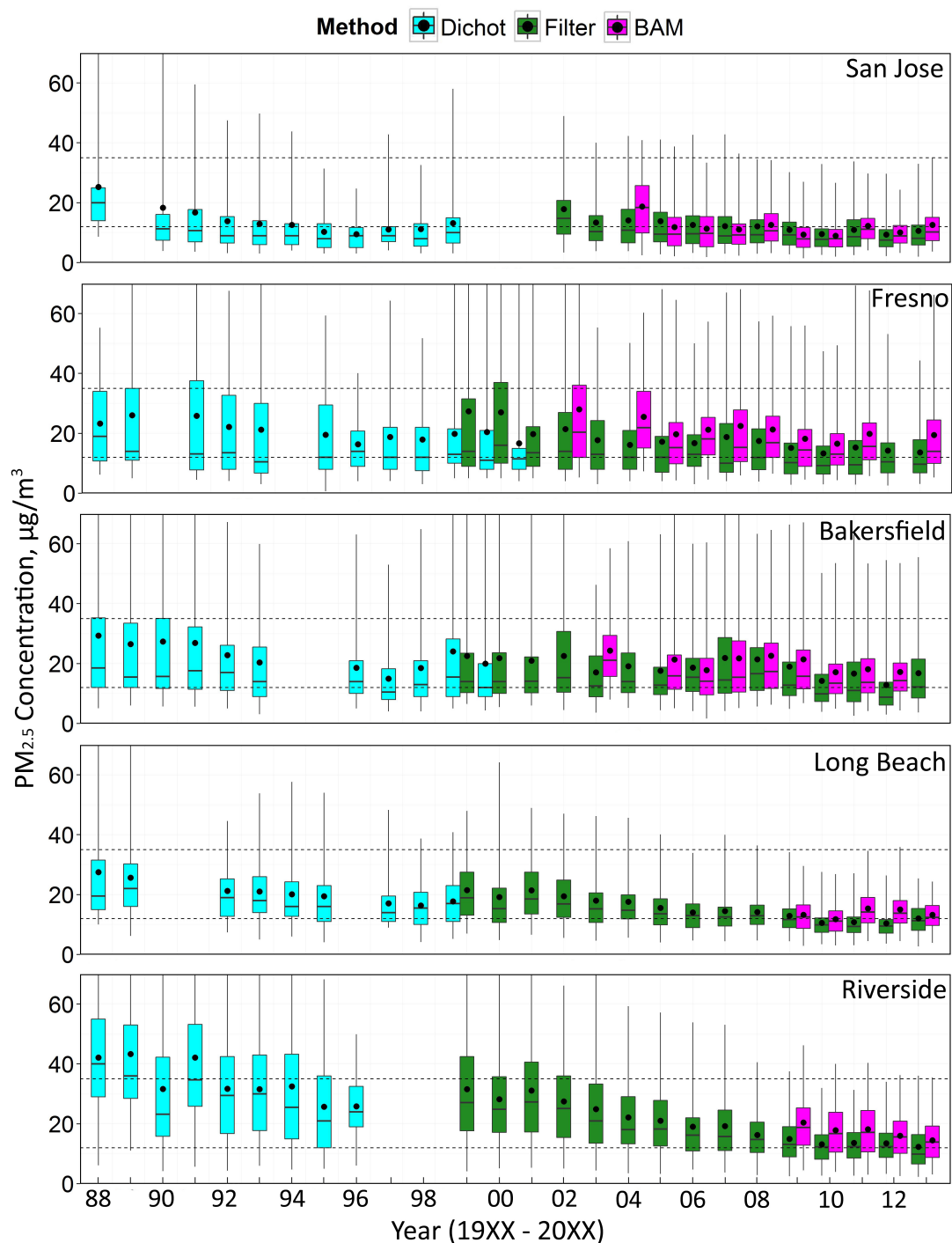


Figure 5.5: Boxplots of daily average PM_{2.5} concentrations.

ized [40]. For instance, prime farmland area in Riverside County dropped by 30% between 1984 and 2002. Since the PM_{2.5} measurement method has changed twice during the time

span of interest, and the current measurement methods tend to result in higher readings than methods in use earlier, actual $PM_{2.5}$ reductions may be larger than what is shown in Figure 5.5 for all sites.

There are two main ways through which reductions in $PM_{2.5}$ can happen: first is reducing frequencies of high $PM_{2.5}$ events, second is reductions for all concentrations. In California, San Jose, the cleanest site, sees reductions through the first mechanisms; all other selected sites show reductions across all concentrations 5.6. Riverside has seen an especially dramatic reduction in the upper percentiles of the distribution. For instance, the 98% percentile of daily average $PM_{2.5}$ decreased from 70 to 33 $\mu g/m^3$ since 2000. In addition, as expected, the distribution of BAM hourly average concentrations has a steeper slope than daily averages, meaning that fluctuations in $PM_{2.5}$ levels within a day are greater in magnitudes than what is observed from day to day on a 24-hour average basis. Similar plots for sites in the Bay area and the San Joaquin Valley yield straight lines, so at these sites, lognormal distributions are observed for daily average $PM_{2.5}$ concentrations.

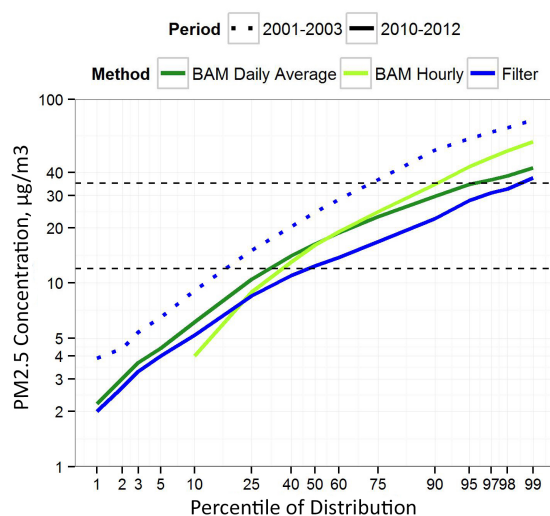


Figure 5.6: Distributions of hourly and daily-average $PM_{2.5}$ measured at Riverside.

The higher time resolution of BAM measurements allows characterization of diurnal profiles of $PM_{2.5}$ that was not possible previously using routine filter-based sampling data. Hourly $PM_{2.5}$ concentrations peak as high as 4-5 times the daily average value. In general, the diurnal profile of $PM_{2.5}$ at urban sites is bimodal with a first peak in the morning (8-10 AM), and a second peak in the late evening. The relative magnitudes of these two peaks vary by site, depending on local meteorological conditions and sources of $PM_{2.5}$.

Distinct seasonal patterns in $PM_{2.5}$ concentrations and diurnal profiles are apparent at the sites shown in Figure 5.7, as well as at additional sites included in Figures 5.9 through 5.16. With the exception of inland sites in Southern California, all sites in Figure 5.7 see higher $PM_{2.5}$ concentrations during winter months. On average, winter concentrations are $80 \pm 25\%$ higher than the summer concentrations in the San Francisco Bay area, and $123 \pm 28\%$ higher in the San Joaquin Valley. Only the San Francisco Bay area has sufficiently long records of BAM measurements at many sites for examining whether seasonal differences have changed over time. Figure S10 shows that in general, differences in $PM_{2.5}$ between summer and winter seasons have increased in 7 years, except at San Jose and West Oakland. In addition, variability in $PM_{2.5}$ during wintertime has decreased significantly for all six sites, possibly indicating more effective episodic control of winter season wood burning. Overnight peaks are especially prominent during the winter at Fresno and Bakersfield, consistent with prevailing stagnant meteorology and increased woodburning emissions at this time of year [43]. Point Reyes (see Figure S4), a rural site, does not show significant winter-summer differences, further confirming that elevated $PM_{2.5}$ concentrations observed in wintertime are mainly due to local emissions rather than changes in background levels. Inland sites in the Los Angeles area such as Riverside, Banning, and Lake Elsinore have low $PM_{2.5}$ concentrations during winter months when prevailing flow conditions are more likely to carry pollutants offshore at night rather than inland during the day. Coastal sites in Los Angeles and Orange counties see little winter/summer difference in daily averages ($-10 \pm 29\%$), especially at Long Beach, whereas inland sites see much greater reductions in $PM_{2.5}$ levels in the winter ($-46 \pm 12\%$). Daytime onshore flows are stronger in summer months, when heating of the land surface is greater. The highest concentrations of $PM_{2.5}$ in the South Coast air basin tend to occur mid-morning in summertime, as shown in Figure 5.7 for Riverside, before photochemical activity is at its maximum.

Compared to seasonal differences in $PM_{2.5}$, weekday/weekend differences are much smaller (see Figure 5.8 and Figures 5.13 through 5.16). West Oakland, a traffic-dominated site, sees the largest weekday/weekend difference (-25%); the reductions at 8 AM on weekends are approximately $4 \mu\text{g}/\text{m}^3$ relative to weekdays. Overall, weekday/weekend differences are most distinct in the San Francisco Bay area, with a basin-wide average of $-8.9 \pm 5.9\%$ reduction in $PM_{2.5}$ on weekends. Figure S11 also indicates that weekday/weekend effect have become discernible at all the Bay area sites except for San Francisco. Sites in the San Joaquin Valley and the South Coast basin have similar diurnal patterns: the morning peak on weekdays is slightly higher than the weekend, likely due to morning commute traffic, but the evening peak on weekends is either the same or higher as on weekdays [75, 41]. The San Joaquin Valley also sees a weekly cycle in $PM_{2.5}$, with an average reduction of $-8.0 \pm 3.0\%$ relative to mid-week values. The South Coast does not show significant weekday/weekend differences on average ($-1.2 \pm 4.2\%$). The afternoon traffic peak on weekdays is not obvious in hourly $PM_{2.5}$ records because the boundary layer height is high at this time. Some $PM_{2.5}$ components, such as BC and nitrate, have been reported in other studies to have larger weekly cycles that are expected given the dominance of on-road diesel trucks as a source of BC

and nitrogen oxides emissions [91, 109, 112]. However, another major component of $PM_{2.5}$, organic aerosol (OA), does show a strong weekly cycle [75, 12]. Therefore, when secondary contributions to OA and sulfate components are included, weekly cycles in $PM_{2.5}$ may be diminished.

More than two decades of $PM_{2.5}$ monitoring in California show that the state has made progress in reducing ambient $PM_{2.5}$ levels, with many sites seeing the 1988 levels cut in half by 2013. The monitoring efforts can serve as reference for other regions to demonstrate the importance of measurements to air basin management.

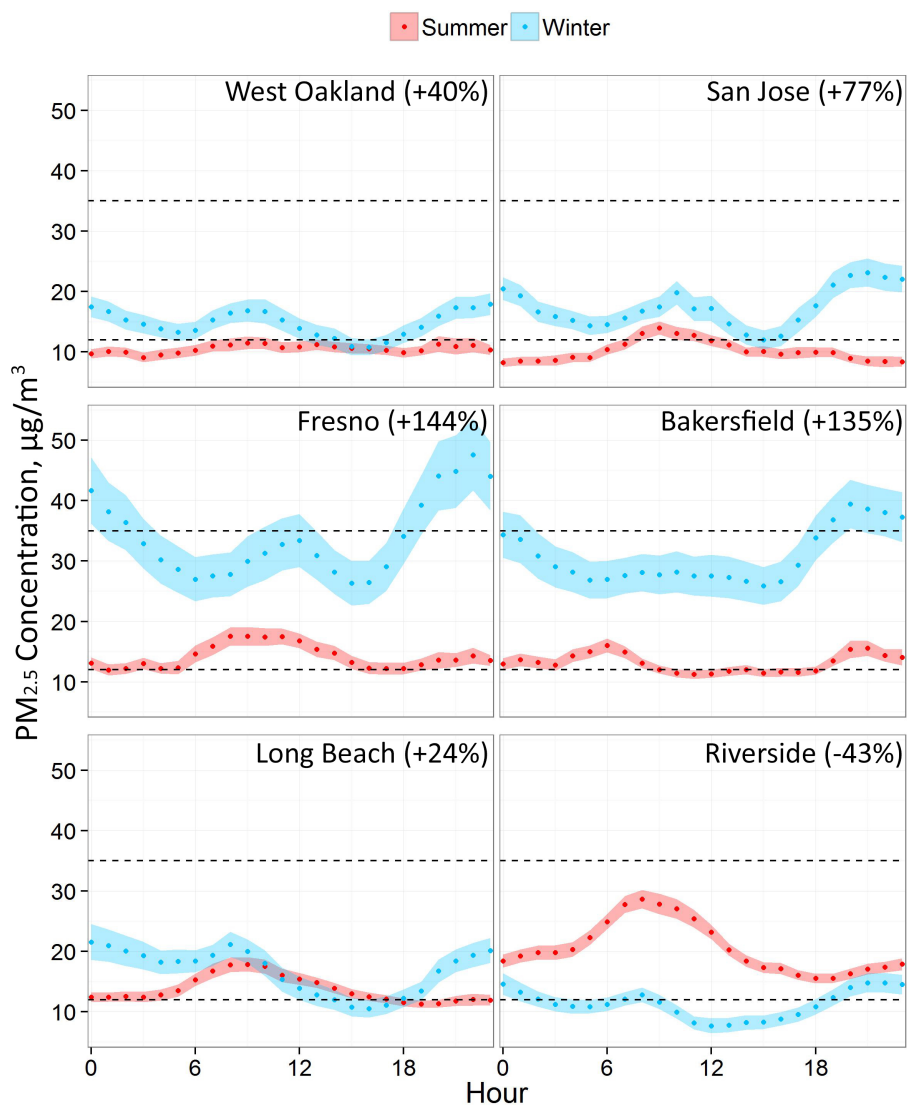


Figure 5.7: Diurnal variations in $PM_{2.5}$ by season at selected sites, averaged over three-year periods. Summer season (red) is from June through August; winter season (blue) is from December through February. Dots represent means and the color bands represent 95% confidence intervals for hourly average $PM_{2.5}$ concentrations. The exact years differ slightly from site to site depending on BAM data availability, but all profiles are for recent years between 2009 and 2013. Percentages following site names indicate the average changes in $PM_{2.5}$ in winter relative to summer values.

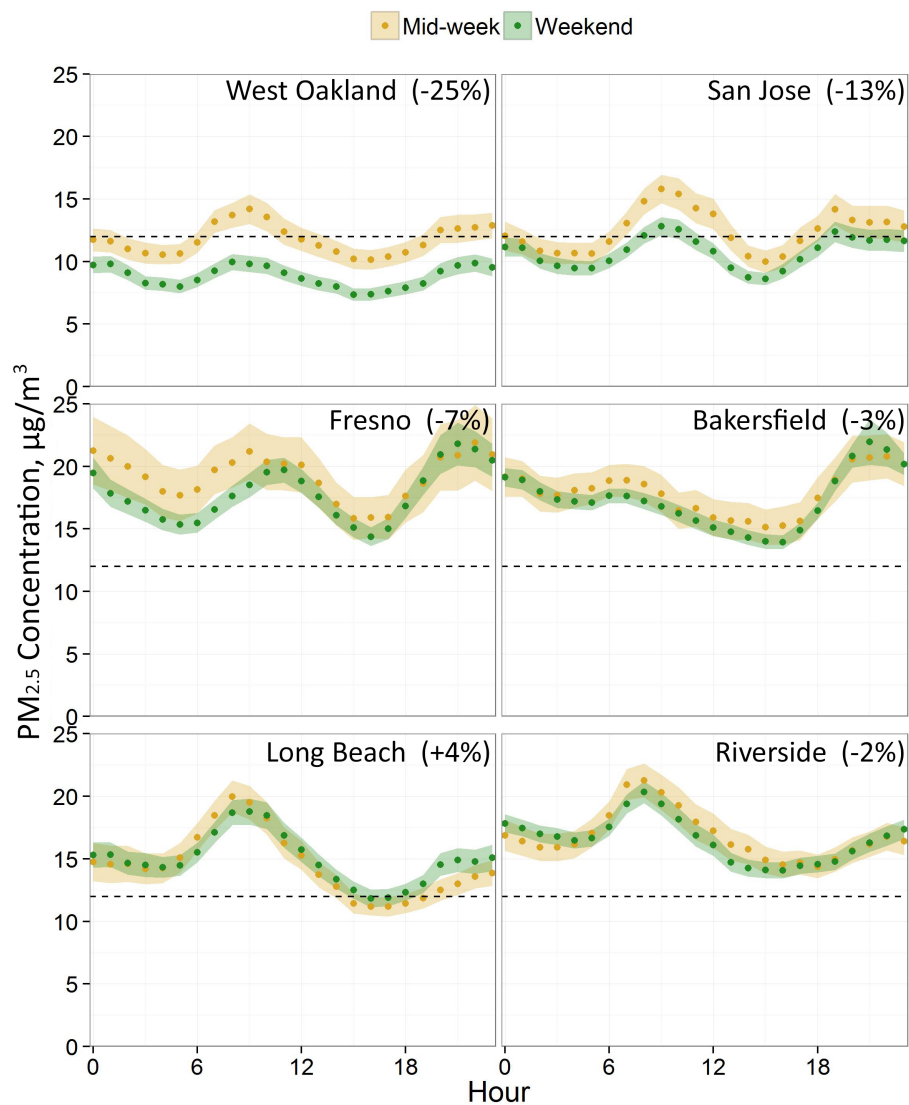


Figure 5.8: Diurnal variations in $PM_{2.5}$ for mid-week and weekend days at selected sites, averaged over three-year periods. Mid-week (yellow) is Tuesday-Thursday; weekend (green) is Saturday and Sunday. Percentages following site names indicate average changes on weekends relative to mid-week values.

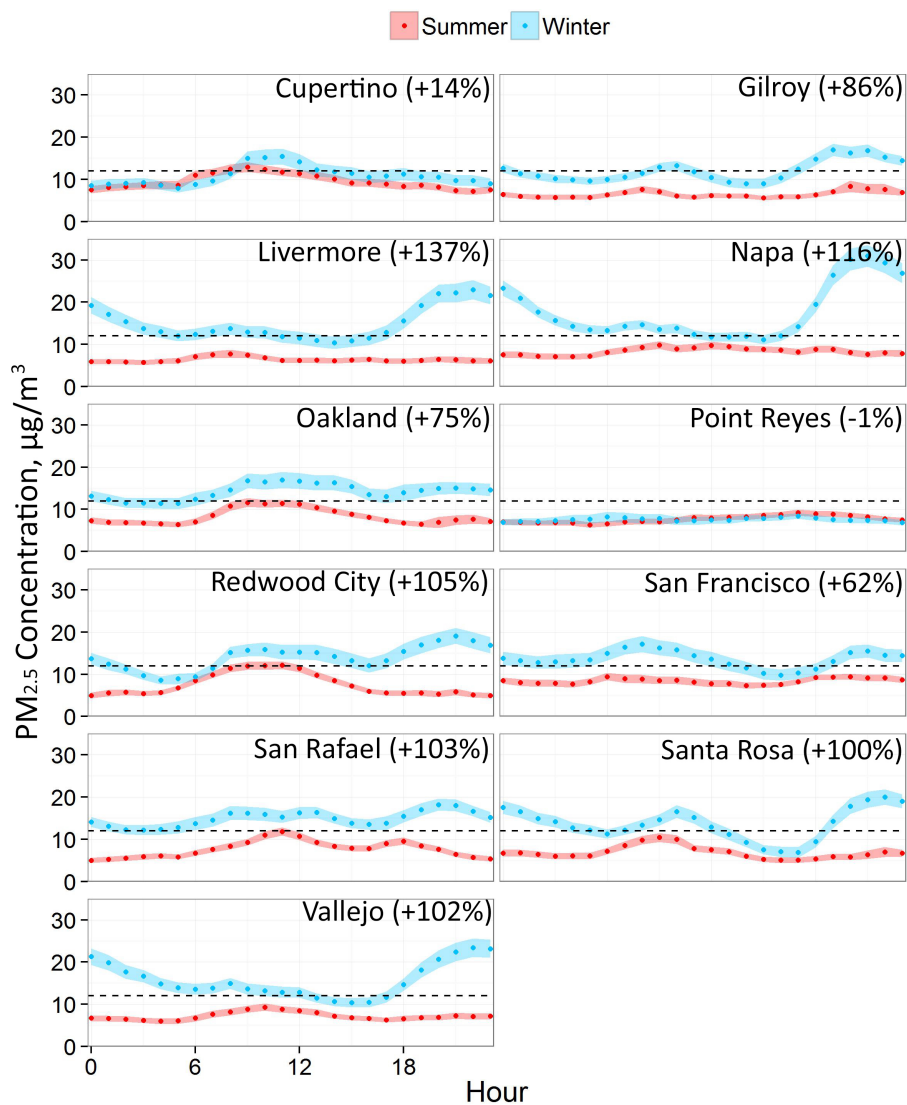


Figure 5.9: Diurnal variations by season in $PM_{2.5}$ in the San Francisco Bay area.

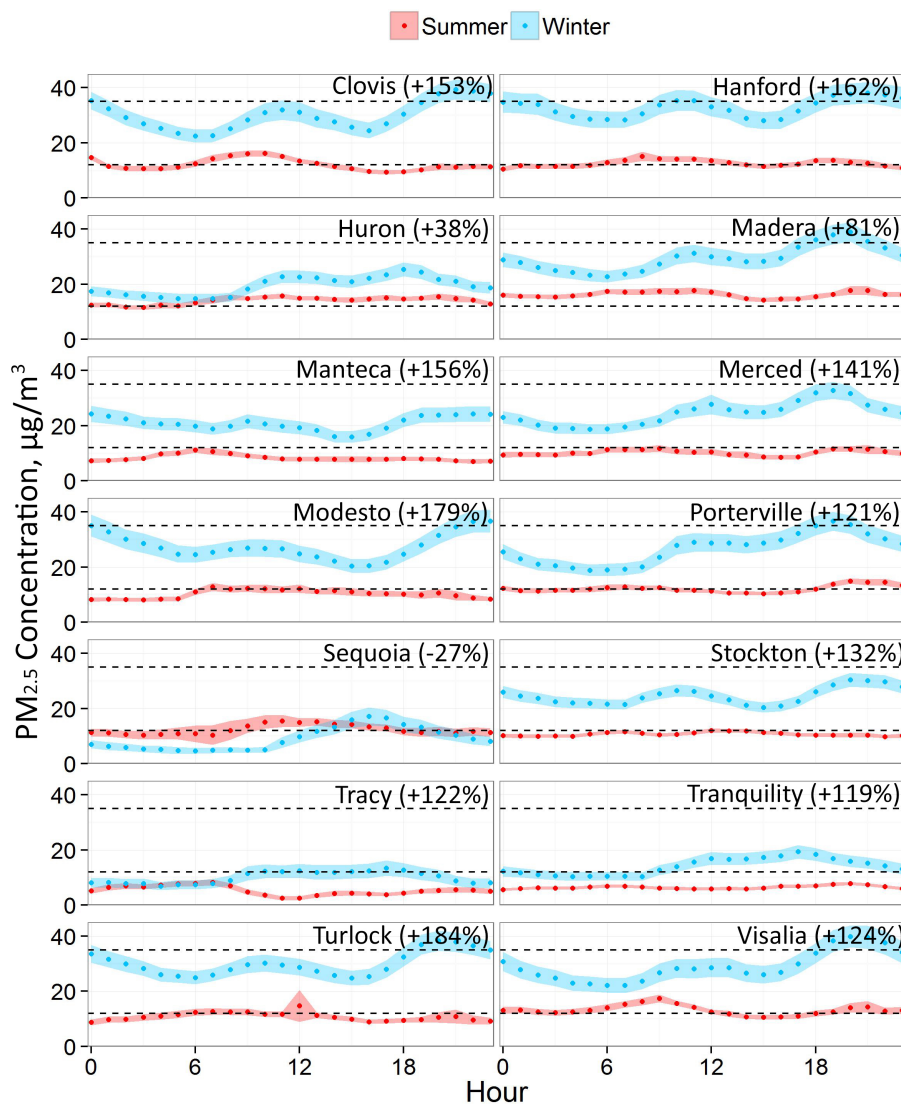


Figure 5.10: Diurnal variations by season in $PM_{2.5}$ in the San Joaquin Valley.

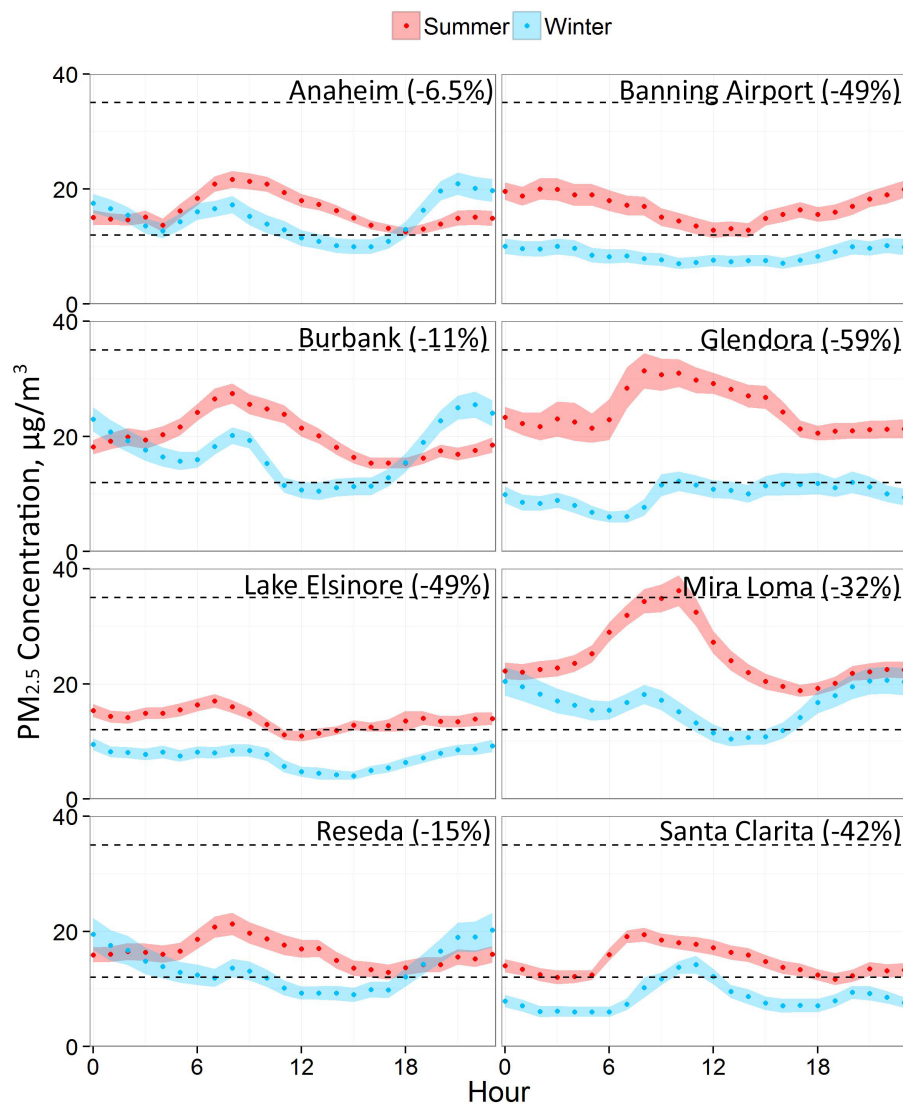


Figure 5.11: Diurnal variations by season in $PM_{2.5}$ in the South Coast Air Basin.

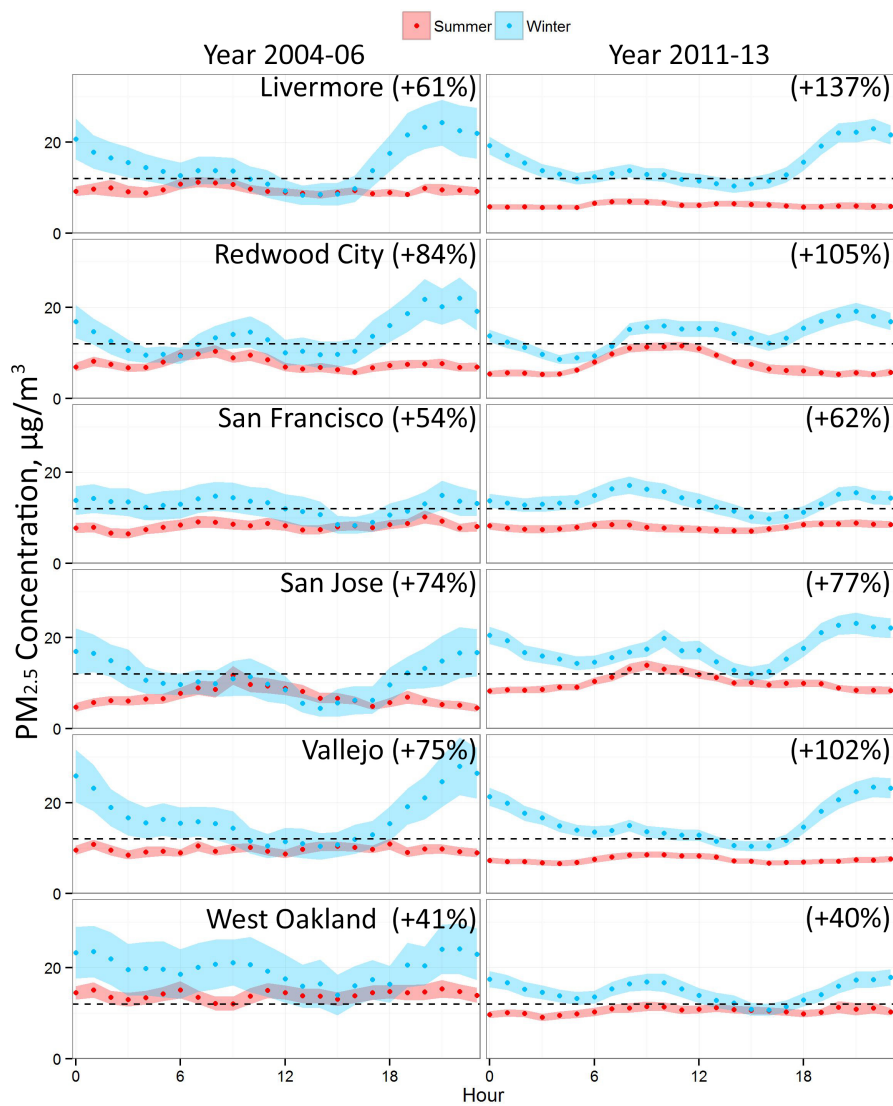


Figure 5.12: Diurnal variations by season in PM_{2.5} in the San Francisco Bay area in periods 2004-2006 and 2011-2013.

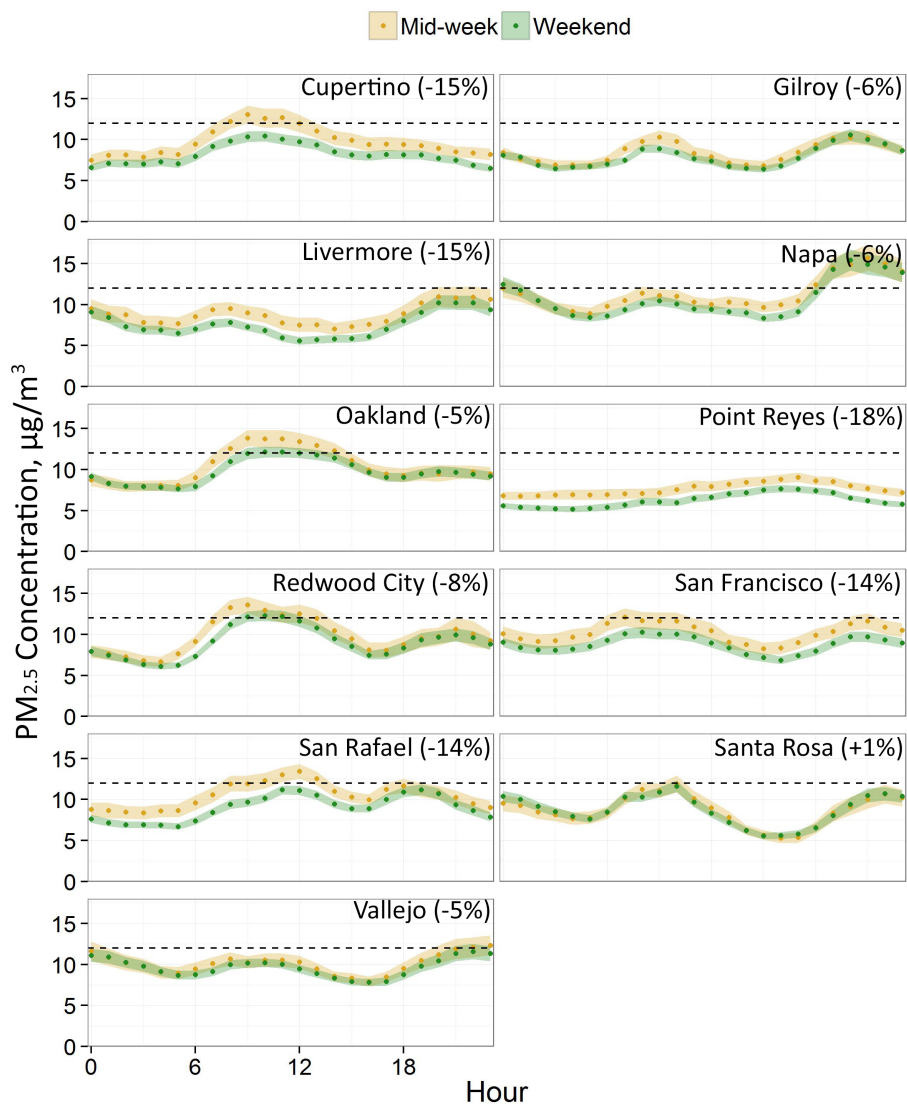


Figure 5.13: Diurnal variations in $PM_{2.5}$ for mid-week (Tues-Thurs) and weekend (Sat-Sun) days in the San Francisco Bay area.

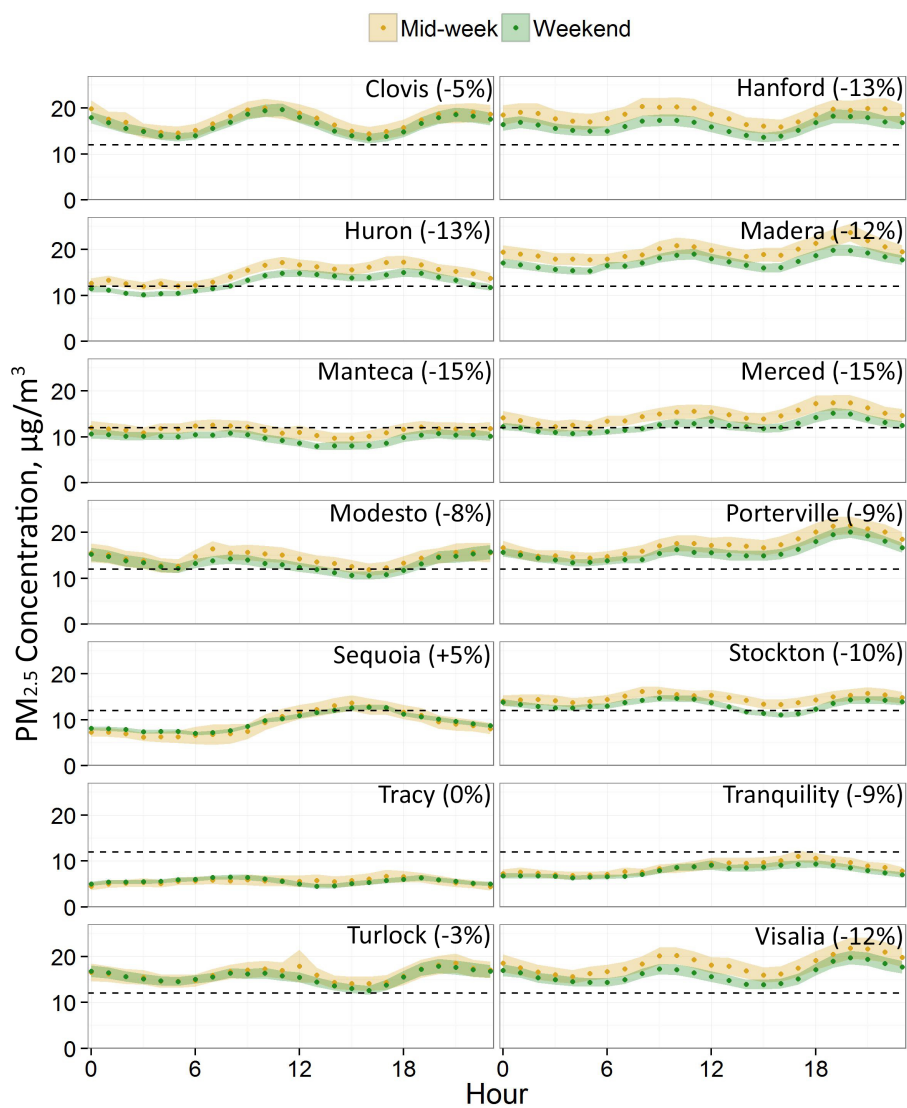


Figure 5.14: Diurnal variations in $PM_{2.5}$ for mid-week (Tues-Thurs) and weekend (Sat-Sun) days in the San Joaquin Valley.

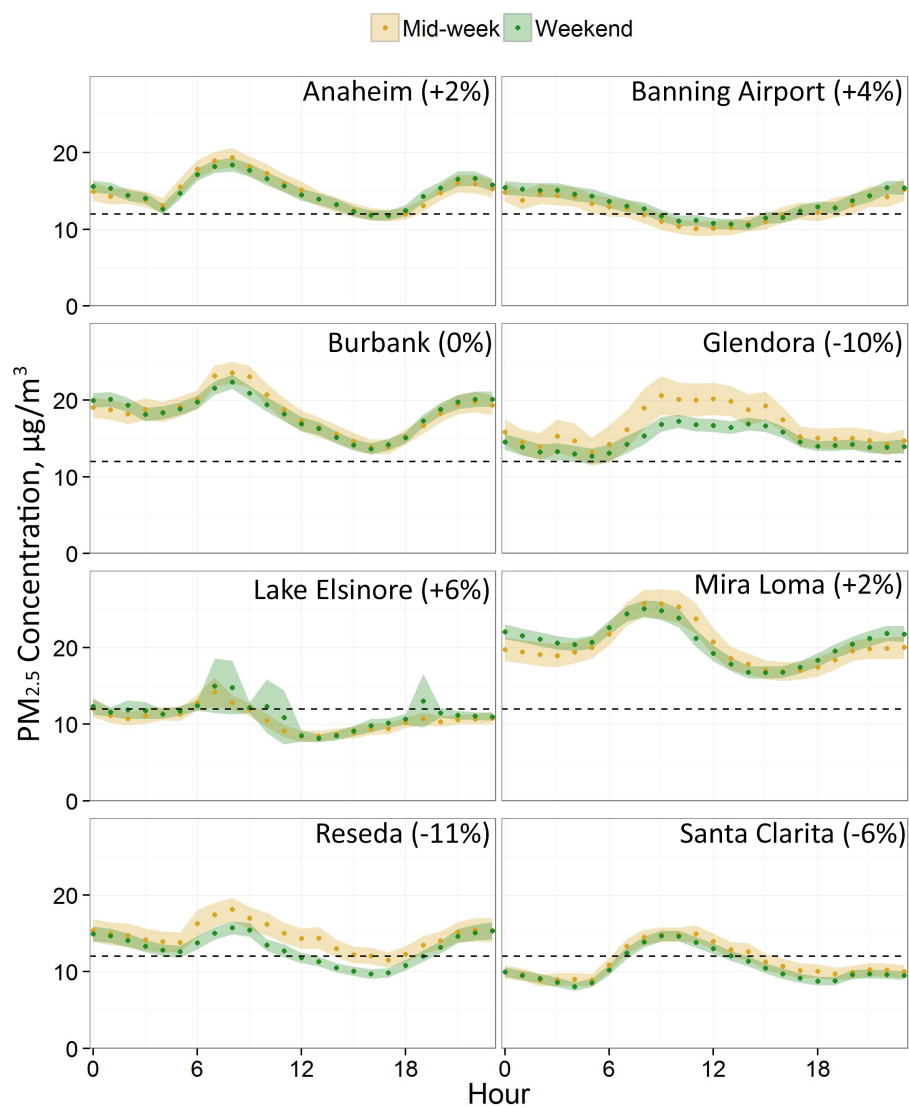


Figure 5.15: Diurnal variations in PM_{2.5} for mid-week (Tues-Thurs) and weekend (Sat-Sun) days in the South Coast Air Basin.

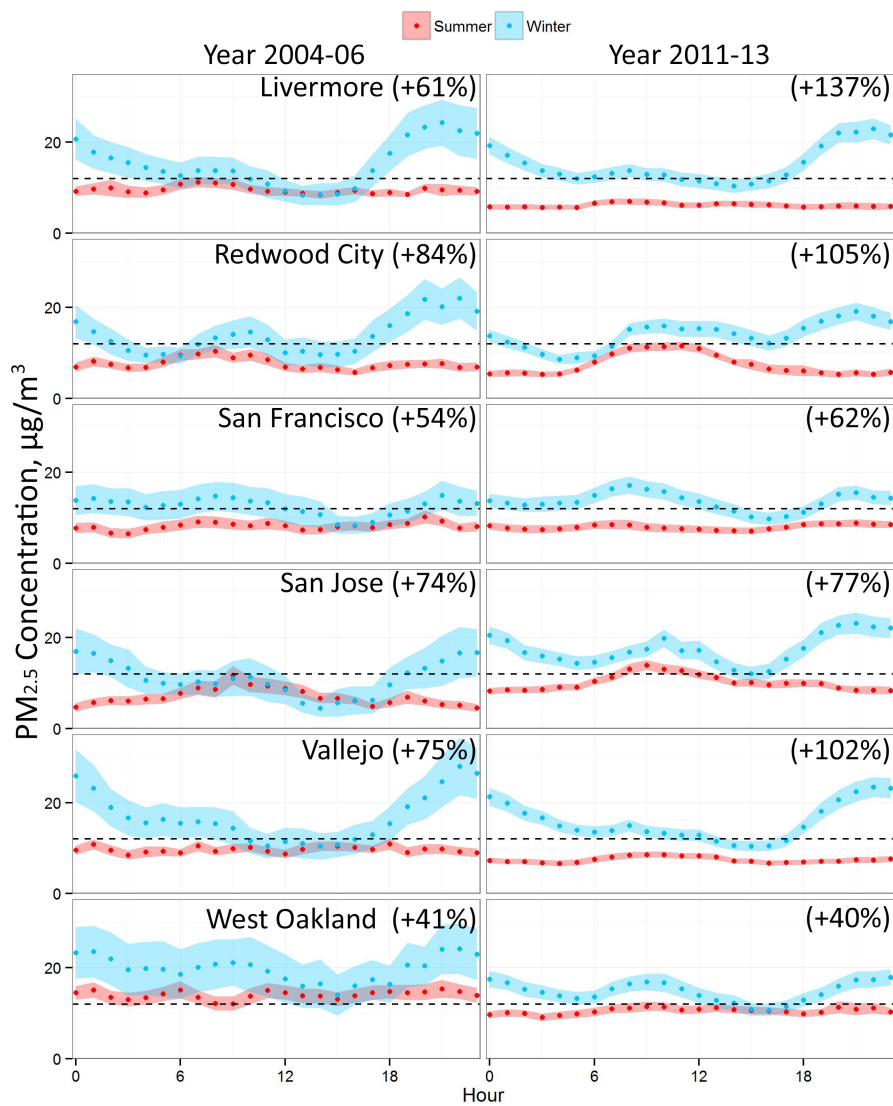


Figure 5.16: Diurnal variations by season in PM_{2.5} in the San Francisco Bay area in periods 2004-2006 and 2011-2013.

Chapter 6

Conclusions

6.1 Summary of Major Findings

The overall objective of this dissertation is to make the connection between changes in ambient air quality and a series of emission regulations. The research is distinct from the past literature because it evaluates several important regulations from the ambient air quality perspective. Specifically, it examines the impacts of controls on the shipping sector and on-road mobile vehicles, and has placed these two sources in a larger context where the ambient monitoring network has been evolving.

Chapter 2 studied the air quality changes in a coastal region before and after July 2009, when an emission control area was put into effect at ports and along the California coastline, requiring use of lower sulfur fuels in place of heavy fuel oil in the main engines of ships. To assess impacts of the fuel changes at the Port of Oakland, and in the surrounding San Francisco Bay area, we analyzed speciated fine particle concentration data from four urban sites and two more remote sites. Measured changes in concentrations of vanadium, a specific marker for heavy fuel oil combustion, are related to overall changes in aerosol emissions from ships. There was a substantial reduction in vanadium concentrations after the fuel change and a 28 - 72% decrease in SO₂ concentrations, with the SO₂ decrease varying depending on proximity to shipping lanes. The changes in ship fuel reduced ambient PM_{2.5} mass concentrations at urban sites in the Bay area about $-3.1 \pm 0.6\%$, or $-0.28 \pm 0.05 \mu\text{g}/\text{m}^3$. The largest contributing factor to lower PM mass concentrations was reductions in particulate sulfate. Absolute sulfate reductions were fairly consistent across sites throughout the region, whereas trace metal reductions were largest at a monitoring site in West Oakland near the port.

Chapter 3 developed estimates of diesel and gasoline engine emissions of CO, NO_x, and NMHC for six domains in California using a fuel-based approach, and compares the results with those from California's on-road mobile source emission model (EMFAC). Emission factors were estimated using linear or logarithmic fits to real-world measurements from highway

tunnels, near roadways, and at truck weigh stations. The comparison of total emissions between EMFAC and the fuel-based method shows good agreement. The contribution to NO_x from diesel engines is similar in magnitude, but slightly higher than the contribution from gasoline engines. On the other hand, on-road gasoline sources dominate CO and NMHC emissions. There are discrepancies in vehicle age distribution between EMFAC and the on-road measurements. At some sites, EMFAC tends to overestimate the population of newer engines and underestimate engines that are 10 years and older, for both diesel and gasoline vehicles. Therefore, using EMFAC may result in unrealistic predictions for individual engine model years and the emission factors associated with them. The comparison study showed that EMFAC is fairly good at predicting overall emissions and trends over time.

Chapter 4 investigated the effects on air quality of an accelerated diesel engine replacement program using the Community Multiscale Air Quality Model (CMAQ) applied to Southern California. The model was run using emission scenarios modified according to data from on-road measurements, EMFAC, population growth, and overall emission predictions for other sectors from the Air Resources Board. Compared to 2005, before the implementation of the program, BC emission is predicted to decrease by 37% in 2016, and 46% in 2023, NO_x emission decreases by 50% in 2016, and 66% in 2023. The simulations were evaluated against ground-level measurements and showed an overall negative bias. According to the model, average wintertime NO_x concentration decreases by 71% and NO_3^- by 13% in 2023 compared to 2005, but summertime peak O_3 increases by 32%, possibly due to the fact that the Los Angeles area is VOC-limited. Comparisons on an hourly basis and with $\text{PM}_{2.5}$ speciation data show that the aerosol chemistry in the model fails to capture the photochemistry of secondary organic aerosol formation in the summer.

Chapter 5 analyzed the temporal patterns of $\text{PM}_{2.5}$ concentrations from the monitoring network in California, which underwent major changes between 1988 and 2013 with the addition of continuous beta attenuation monitors (BAM). Regressions of BAM against filter measurements generally show BAM reads higher by 3 - 6 $\mu\text{g}/\text{m}^3$ for annual averages. Most monitoring sites show clear downward trends in $\text{PM}_{2.5}$ concentrations over time, especially in the Los Angeles area where concentrations have decreased by more than 50% since the 1990s. In most cases, $\text{PM}_{2.5}$ concentrations are elevated in winter compared to summer, with basin-wide winter season increases of $80 \pm 25\%$ for the San Francisco Bay area and $123 \pm 28\%$ for the San Joaquin Valley. The differences are more prominent at night due to wood-burning and stagnant atmospheric conditions. The reverse is true at inland sites in southern California, which show reductions of $46 \pm 12\%$ in winter. Weekend $\text{PM}_{2.5}$ concentrations are slightly lower than on weekdays. Average weekend reductions relative to mid-week values are $8.9 \pm 5.9\%$ for the San Francisco Bay area and $8.0 \pm 3.0\%$ for the San Joaquin Valley. Up to 25% reductions in $\text{PM}_{2.5}$ are observed on weekends at traffic-dominated sites such as West Oakland.

6.2 Policy implications

A key aspect of this dissertation is studying the effectiveness of air pollution control efforts. California has been at the forefront of environmental regulation and many lessons can be learned from the implementation of the policies studied in this dissertation.

California was the first state to replace the traditional filter-based measurement method for $PM_{2.5}$ with beta attenuation monitoring (BAM). BAM was chosen over other high time resolution devices, such as tapered element oscillating microbalance (TEOM) and the Dust-trak aerosol sampler for its consistency of performance. The data obtained from the BAM network has proved to be a reliable and rich data source to support studies of air pollution, especially to extract temporal patterns and to examine severe pollution episodes. The use of BAM in California may prompt the environmental departments in other states and countries to consider integrating the same technology into their monitoring networks.

Emission control regulations discussed in this dissertation, such as the ship fuel requirement, and the accelerated diesel engine replacement program, may also be of interest to other states and countries where emissions from the transportation sector contribute significantly to local air pollution.

Enforcement is necessary to ensure the effectiveness of emission control regulations. During the ship fuel study in Chapter 2, some spikes in Vanadium concentrations could still be observed even after the use of heavy fuel oil was banned. This leads to the question of how well the fuel requirement is enforced once vessels sail within 24 nautical miles of California's coastline. It could be helpful to install SO_2 monitors near the major shipping routes, such as at the Golden Gate to monitor ships going to the Port of Oakland, since the banned fuel has much higher sulfur content that can be used as a tracer, and SO_2 monitors are relatively inexpensive.

It proves difficult to lower O_3 levels by controlling NO_x emissions in California, as shown in Chapter 4, because some areas are VOC-limited. Air districts should carefully evaluate their full emission inventory before determining NO_x and VOC control strategies, since O_3 response to reductions in primary pollutants is uncertain and related to whether a region is NO_x -limited or VOC-limited.

6.3 Recommendations for Future Research

The results from Chapter 3 indicated that in EMFAC, engine age distributions as well as some vehicle age-specific emission factors need further examination. Specifically, further investigation is needed for the finding that the current EMFAC model overestimates the emission factors of newer diesel engines and underestimates those of older engines. In addition, EMFAC only outputs emission of the criteria pollutants and carbon dioxide, but in

Chapter 5, it was found that having accurate estimates of NH_3 emissions from the on-road sector is crucial for running air quality models. This is especially true for future scenarios where more gasoline engines will be on the road, and natural gas trucks, with potentially elevated NH_3 emissions, are becoming an attractive alternative to traditional heavy diesel trucks. Therefore, future versions of EMFAC should quantify NH_3 .

Another factor that will alter the emissions from the on-road sector in the upcoming years is the widespread use of new selective catalytic reduction (SCR) systems to control diesel NO_x emissions. It is possible for SCR not to achieve the expected removal rate of NO_x for two causes: first, the operating temperature of the device may be too low for effective removal, especially in stop-and-go traffic; second, SCR will not function at all if truck drivers are not diligent in refilling the urea reagent reservoir. The former cause could be quantified by more remote-sensing and/or tunnel measurements at a variety of urban locations. The latter issue can only be managed by ensuring compliance among all trucks. Therefore, it is important to evaluate and update the on-road emission inventory periodically to reflect these uncertainties.

The modeling study in Chapter 4 shows that aerosol chemistry, implemented in CMAQ using the module AE5, is not sufficient to capture secondary organic aerosol formation in the South Coast Air Basin. Chapter 4 focuses mainly on the changes in emission inventory and the resulting effects, but modifications to the current aerosol chemistry are clearly needed for successful model applications on regions similar to Southern California, where photochemistry plays a major role.

In the next decade, the monitoring network in California is likely to keep growing with more near-road sites, special campaigns, and measurements with higher time resolution. The emissions from many sources, including on-road vehicles, off-road engines, and point sources, are likely to decrease further. This means the air pollution in California may become concentrated in hot spots, instead of remaining as a region-wide problem. With increasing data availability from monitoring networks and portable measuring devices, and advances in both deterministic air quality modeling and machine learning, it is possible to develop methodology that narrows down pollution to the neighborhood scale, such as near the Port of Oakland. For future studies, efforts should be made to incorporate meteorological measurements, industrial activities, commute patterns, and demography into one single framework to better identify exposed communities.

Appendix A

Trends in ambient NO_x concentrations

NO_x concentrations have undergone dramatic decrease in the past three decades, as shown in five representative sites in California in Figure A.1, identical to sites where the $\text{PM}_{2.5}$ concentrations were measured in Figure 5.5. NO_2 as a primary pollutant has not been of concern since 1990s. Among the five sites, Long Beach has the highest concentrations because of the major traffic arteries going through the Port of Los Angeles/Long Beach as well as the port diesel equipment and ship emissions at shore. In general, the reductions in NO_x are thanks to the early installment of SCCR in gasoline engines, and the stringent standards on off-road diesel equipments and point sources such as power plants.

Air districts in California have installed near-roadway NO_x monitors starting in 2012. At the time of study, there were about two years of hourly measurements available at two near-road sites, Laney College in Oakland and Knox Avenue in San Jose, in the San Francisco Bay area. The seasonal variations in the concentrations are captured in Figure A.2. Weekend concentrations are noticeably lower than those of weekdays, due to reduced truck traffic. Concentrations also tend to be higher during winter seasons due to lower mixing height in the atmosphere. However, the roadway concentrations of NO_2 were not high enough to pass the 53 ppb standard for annual average.

Near-roadway concentrations were compared with four nearby ambient sites in Figure A.3. The distances between the near-roadway and the ambient sites are the nearest (2.9 km) between Oakland Laney College and West Oakland, and the furthest (35 km) between San Jose Knox Avenue and Redwood City. The time period, winter mid-week morning rush hours from 6-10AM, was chosen to obtain the highest concentrations. It is apparent that near-road NO_2 and NO_x concentrations are higher than the ambient sites, especially the medians and 75% percentiles. However, the whiskers do not extend as much for the near-roadway sites compared to the ambient, indicating there is less variation in road-way concentrations. Overall, the highest concentrations at roadway hot spots, at least for the San Francisco Bay

area, are still not high enough to exceed the NAAQS.

Nitrogen oxides are emitted primarily in the form of NO, and undergo oxidation to other species in the atmosphere. For instance, for diesel trucks not equipped with post-combustion emission control devices, 96.6% of NO_x is emitted as NO (of NO_2 mass equivalent) [126]. Therefore, there's dependence between measured NO_2 concentrations and NO_x , varying geographically and seasonally.

Figure A.4 shows the linear fitting for NO_2 versus NO_x concentrations for two years a decade apart. The blue fitting lines have a gentler slope than the red ones, because oxidation rates for NO are higher in the summer due to higher temperature and more sunlight availability. From 2000 to 2010, both fitting lines for summer and winter have significantly decreased in slope, indicating larger NO_2/NO_x ratios. In fact, as shown in Figure A.5, all five sites show increases in slopes of linear fitting lines to different degrees in two decades from 1994 to 2014, for instance, San Jose for 75% increase in slope, and 25% for Riverside.

Increasing NO_2/NO_x ratios have been observed in the three major air basins in California for the latest decade, namely, 40 out of 54 sites in Figure A.6, particularly in San Francisco Bay area. Similar findings have been observed in Germany [93]. Since absolute NO_x concentrations have decreased during this time period as well, NO emissions must have decreased at a rate faster than that of NO_x . For San Francisco Bay area, for instance, NO_x concentrations have reduced about $50 \pm 15\%$, and total NO_x emissions from the on-road mobile sector (assuming all in the form of NO) decreased about 50% according to Figure 3.6, it is plausible that combined with NO emitted from the off-road sector, percentage reduction in NO is larger than 50% from 2000 to 2014.

Pseudo-steady-state O_3 concentration is proportional to NO_2/NO . If emissions of all other pollutants remain the same, an increase in NO_2/NO_x ratio is equivalent to increase in NO_2/NO , and may result in higher O_3 concentrations, a major air pollution problem for the South Coast Air Basin.

Vice versa, primary NO_x in the form of NO near roadway also results in the O_3 titration effect. Unfortunately, NO_x near-road monitoring has only begun in the recent years and not enough long-term record is available to examine the changes directly related to on-road fleet. However, diurnal trends in NO_2/NO_x ratios are available in Oakland and San Jose, shown in Figures A.7a and A.7b. The time periods during which the near-road sites differ significantly from ambient sites (The 75% of near-road ratios are lower than 25% of ambient ratios) are 8AM-16PM for Oakland, and 10AM-23PM for San Jose. This suggests that lower NO_2/NO_x ratios are from increase in freeway traffic, and that San Jose is likely to have later and longer traffic periods than Oakland. Wilcoxon test results show that on average, NO_2/NO_x is 0.17 lower at near-roadway sites than ambient sites.

Analysis of long-term NO_x measurements and near-roadway concentrations shows that absolute NO_x concentrations have decreased significantly in the last decades, while NO_2/NO_x ratios have risen for majority of the measurement sites, and are statistically lower at near-road locations. However, the instrumentation of NO_x measurement could lead to errors and

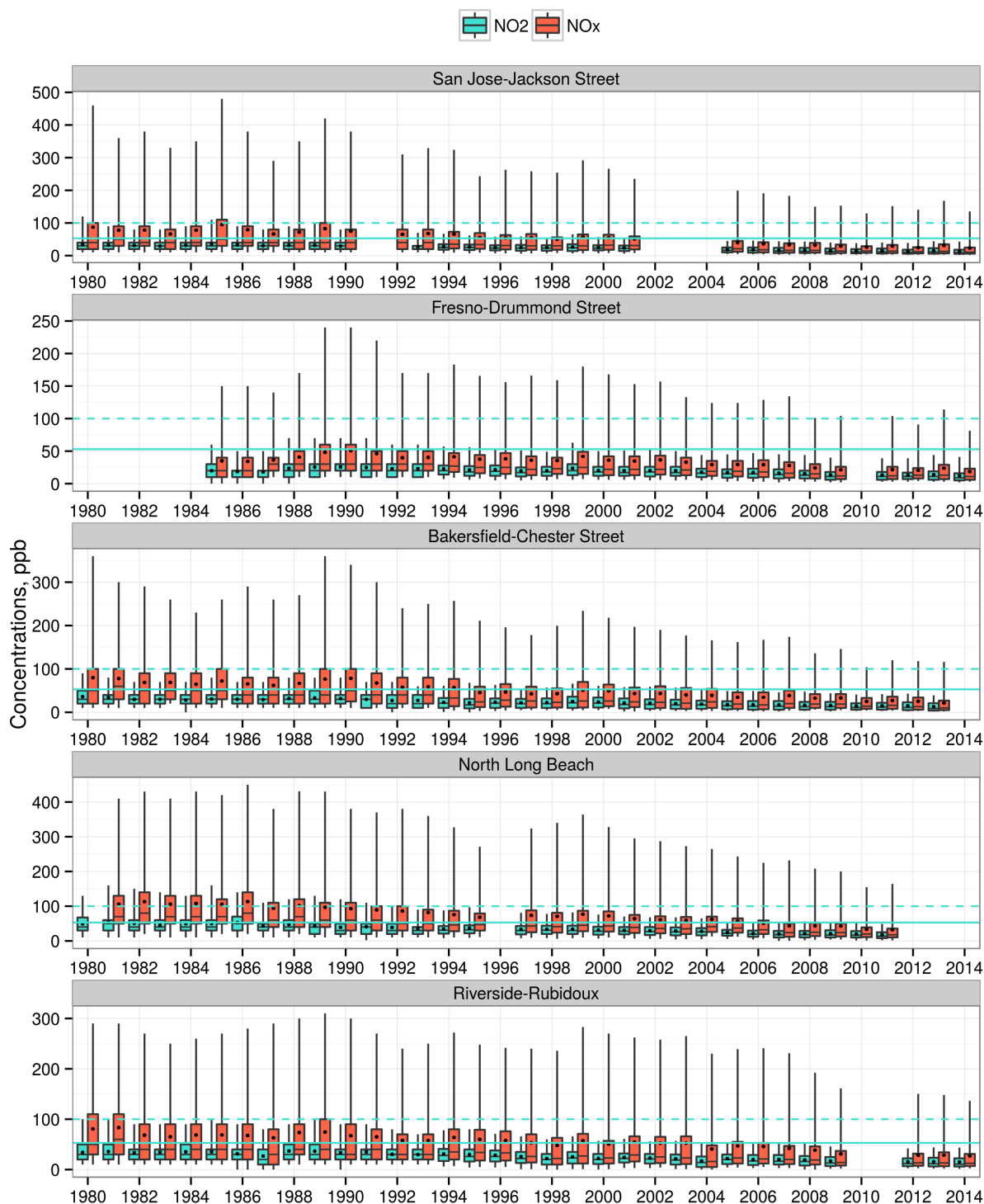


Figure A.1: NO_2 (blue) and NO_x (red) concentration boxplots from 1980 to 2014 for five sites: San Jose, Fresno, Bakersfield, Long Beach and Riverside. Blue horizontal lines indicate the current 100 ppb 98th percentile 1-hour daily maximum standard, and the 53 ppb annual mean standard, both for NO_2 .

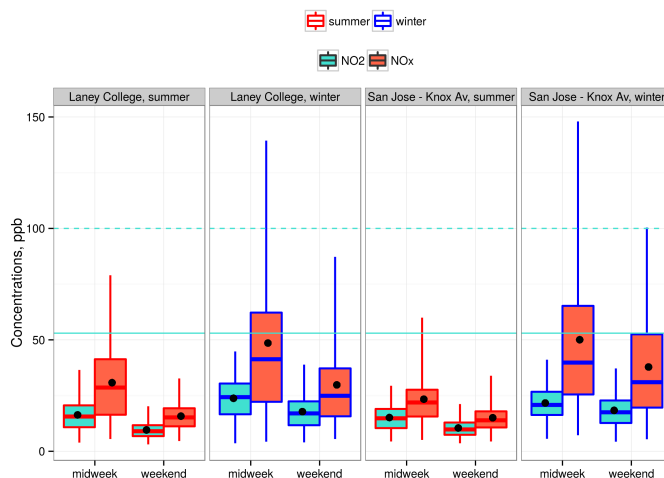


Figure A.2: NO_2 and NO_x concentration boxplot for two near-road sites in California, indicating weekday/weekend and seasonal variations. Weekdays are Tuesdays through Thursdays and weekends are Saturdays and Sundays. Red represents warmer months (April to September) and blue represents colder months (October to March). Horizontal lines are the same standards as in Figure A.1.

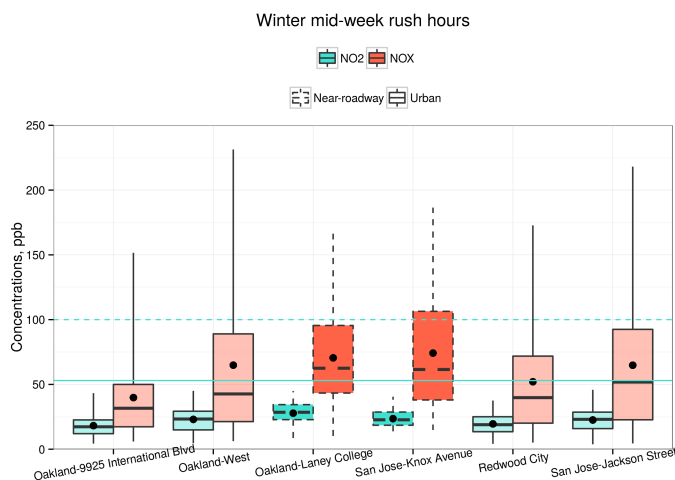


Figure A.3: NO_2 and NO_x concentration boxplot for two near-road sites and four ambient sites. Graphic features are similar to those in Figure A.2.

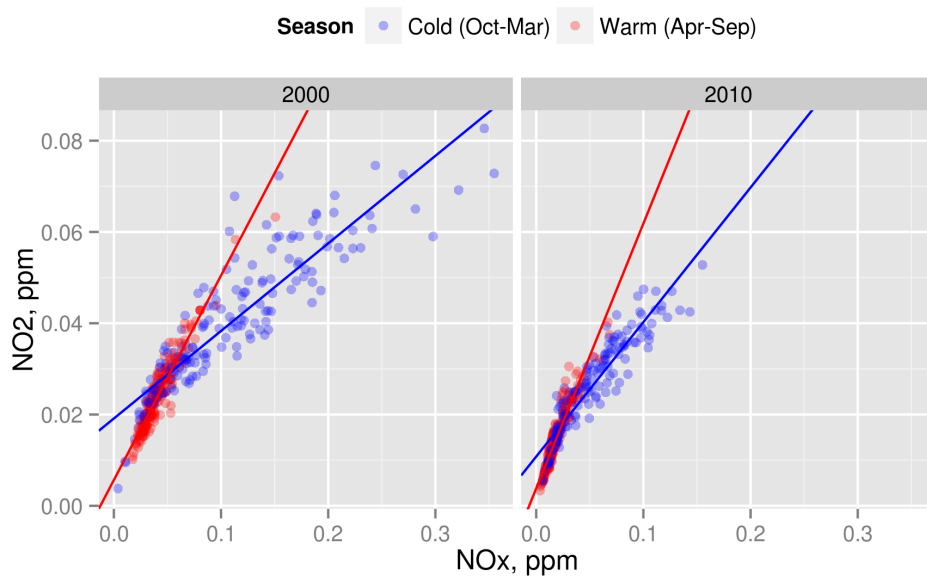


Figure A.4: Scatter plots for NO_2 and NO_x concentrations in 2000 and 2010 and the respective linear fits. Measurements were taken at the North Long Beach site. Color schemes are the same as those in Figure A.2

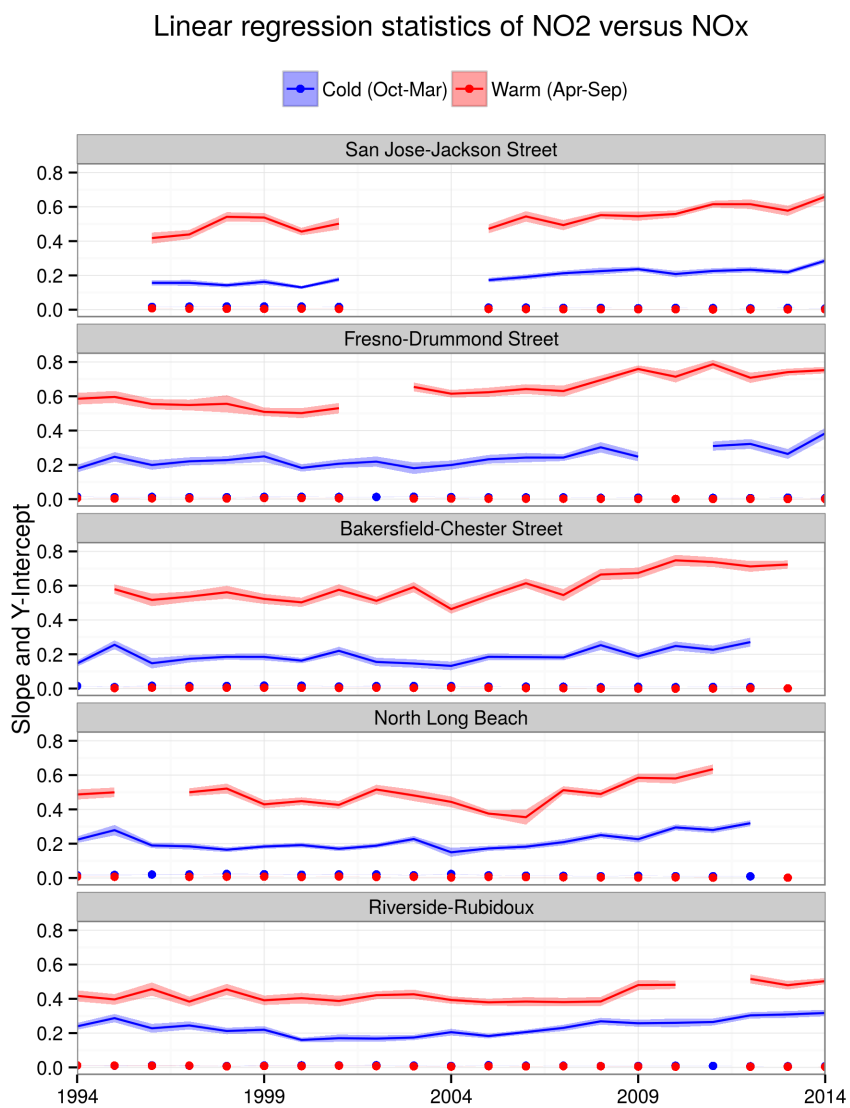


Figure A.5: Slopes (lines) and y-intercepts (dots) of linear regression done on NO_2 versus NO_x for five selected sites in California for two seasons. The bands around the line represent 95% uncertainty. Note that the missing data for some years is due to gaps in measurements.

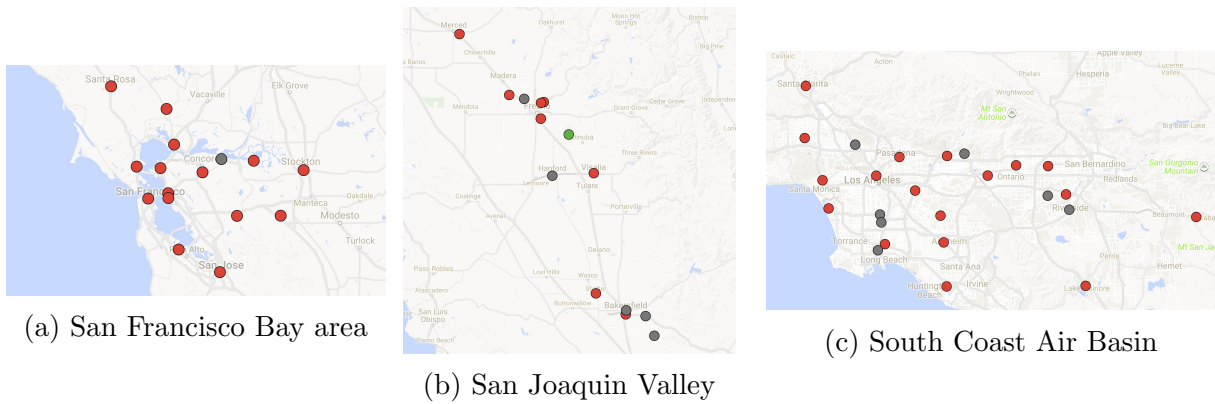
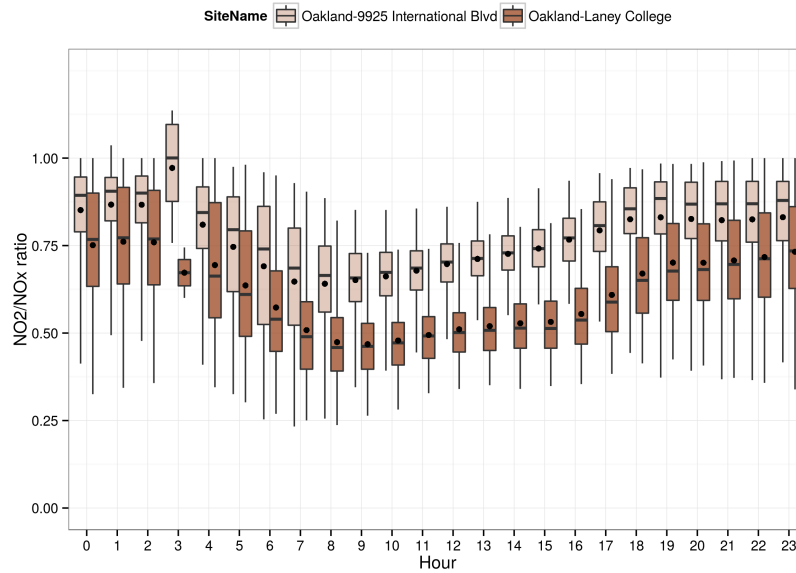
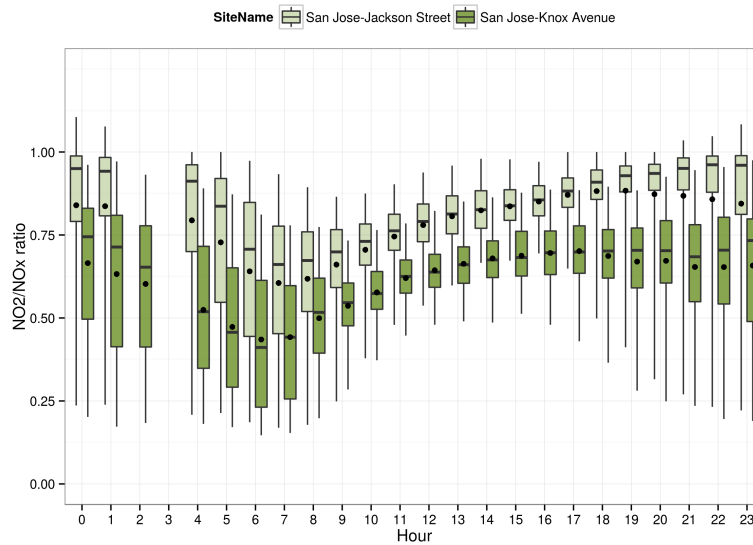


Figure A.6: Maps of selected NO_x monitoring sites in three major air basins in California. Sites were only shown if there were more than four consecutive years of data available during 2000-2014. Red indicates sites with clear trends in increasing ambient NO_2/NO_x ratios, gray indicates fluctuating ratios, and green indicates decreasing ratios.



(a) Oakland-9925 International Blvd (Ambient) and Oakland-Laney College (Near-roadway)



(b) San Jose-Jackson Street (Ambient) and San Jose-Knox Avenue (Near-roadway)

Figure A.7: Boxplots of NO_2/NO_x ratios by hour of the day.

uncertainties in the temporal trend analysis. Although NO_x technically only consists of NO and NO_2 , the chemiluminescence method used in the monitors also captures other reactive nitrogen species, such as HNO_3 , PAN and alkyl nitrites (R-NO_2). In polluted urban environment, the interference can be as high as 22% in Southern California [58]. Therefore, it is important to note that the results in this section emphasize more the comparative differences over time and among monitoring sites, rather than the absolute values and ratios.

References

- [1] Advisory to Owners or Operators of Ocean-Going Vessels or Ships Visiting California Ports. *California Air Resources Board, Sacramento, CA*. July, 2012.
- [2] Agrawal, H., Malloy, Q. G., Welch, W. A., Miller, J. W., and III, D. R. C. “In-use Gaseous and Particulate Matter Emissions from a Modern Ocean Going Container Vessel”. *Atmospheric Environment* 42.21 (2008), pp. 5504 –5510. ISSN: 1352-2310. DOI: 10.1016/j.atmosenv.2008.02.053.
- [3] Agrawal, H., Eden, R., Zhang, X., Fine, P. M., Katzenstein, A., Miller, J. W., Ospital, J., Teffera, S., and Cocker, D. R. “Primary Particulate Matter from Ocean-Going Engines in the Southern California Air Basin”. *Environmental Science & Technology* 43.14 (2009), pp. 5398–5402. DOI: 10.1021/es8035016.
- [4] *Air Quality Management Plan for the South Coast Air Basin, Appendix III, Base and Future Year Emission Inventories. South Coast Air Quality Management District: Diamond Bar. CA. June 2007.* <http://www.aqmd.gov/aqmp/07aqmp/07AQMP.html>.. Accessed: 2015-06-05.
- [5] ARB. *Air Monitoring Quality Assurance, Volume II, Standard Operating Procedures for Air Quality Monitoring, Appendix M, Dichotomous Sampler.* <http://www.arb.ca.gov/airwebmanual/aqsbdocs1/v2apxm.pdf>. California Air Resources Board, Sacramento, CA. 1997.
- [6] ARB. *Air Quality and Meteorological Information System.* Last accessed: February 1, 2014. www.arb.ca.gov/aqmis2/aqmis2.php. California Air Resources Board, Sacramento, CA. 2014.
- [7] ARB. *Annual Report on the Air Resources Boards Fine Particulate Matter Monitoring Program.* www.arb.ca.gov/research/apr/reports/pm25-monitoring-2014.pdf. California Air Resources Board, Sacramento, CA. 2014.
- [8] ARB. *California Air Quality Data - Selected Data Available for Download.* Last accessed: March 1, 2014. www.arb.ca.gov/aqd/aqcd/aqcd1d.htm. California Air Resources Board, Sacramento, CA. 2013.

- [9] Ault, A. P., Gaston, C. J., Wang, Y., Dominguez, G., Thiemens, M. H., and Prather, K. A. "Characterization of the Single Particle Mixing State of Individual Ship Plume Events Measured at the Port of Los Angeles". *Environmental Science & Technology* 44.6 (2010), 1954–1961. DOI: {10.1021/es902985h}.
- [10] Babich, P., Wang, P.-Y., Allen, G., Sioutas, C., and Koutrakis, P. "Development and Evaluation of a Continuous Ambient PM_{2.5} Mass Monitor". *Aerosol Science and Technology* 32.4 (2000), pp. 309–324. DOI: 10.1080/027868200303641. eprint: <http://www.tandfonline.com/doi/pdf/10.1080/027868200303641>.
- [11] Baek, J., Hu, Y., Odman, M. T., and Russell, A. G. "Modeling secondary organic aerosol in CMAQ using multigenerational oxidation of semi-volatile organic compounds". *Journal of Geophysical Research Atmospheres* 116.22 (2011). ISSN: 01480227. DOI: 10.1029/2011JD015911.
- [12] Bahreini, R. et al. "Gasoline Emissions Dominate over Diesel in Formation of Secondary Organic Aerosol Mass". *Geophysical Research Letter* 39.6 (2012), 10.1029/2011GL050718. ISSN: 1944-8007.
- [13] Bailey, D and Solomon, G. "Pollution Prevention at Ports: Clearing the Air". *Environmental Impact Assessment Review* 24.7-8 (2004), 749–774. DOI: {10.1016/j.eiar.2004.06.005}.
- [14] Balmes, J. R., Earnest, G., Katz, P. P., Yelin, E. H., Eisner, M. D., Chen, H., Trupin, L., Lurmann, F., and Blanc, P. D. "Exposure to traffic: lung function and health status in adults with asthma." *The Journal of allergy and clinical immunology* 123.3 (2009), pp. 626–31. ISSN: 1097-6825. DOI: 10.1016/j.jaci.2008.10.062.
- [15] Ban-Weiss, G. A., Mclaughlin, J. P., Harley, R. A., Kean, A. J., Grosjean, E., and Grosjean, D. "Carbonyl and nitrogen dioxide emissions from gasoline- and diesel-powered motor vehicles". *Environmental Science and Technology* 42.11 (2008), pp. 3944–3950. ISSN: 0013936X. DOI: 10.1021/es8002487.
- [16] Barnes, H. "Some Tables for the Ionic Composition of Sea Water". *Journal of Experimental Biology* 31.4 (1954), pp. 582–588.
- [17] Battelle Memorial Institute. *Environmental Technology Verification Report: Rupprecht & Patashnick, Co. Series 1400a TEOM Particle Monitor with Sample Equilibration System*. http://www.epa.gov/etv/pubs/01_vr_rupp_1400ateomses.pdf. Columbus, OH. 2001.
- [18] Bell, M. L., Dominici, F., and Samet, J. M. "A meta-analysis of time-series studies of ozone and mortality with comparison to the national morbidity, mortality, and air pollution study." *Epidemiology (Cambridge, Mass.)* 16.4 (2005), pp. 436–45. ISSN: 1044-3983. DOI: 10.1097/01.ede.0000165817.40152.85. eprint: NIHMS150003.
- [19] Bell, M. L., McDermott, A., Zeger, S. L., Samet, J. M., and Dominici, F. "Ozone and short-term mortality in 95 US urban communities, 1987-2000." *Jama* 292.19 (2004), pp. 2372–8. ISSN: 1538-3598. DOI: 10.1001/jama.292.19.2372.

- [20] Bhaskaran, K., Hajat, S., Armstrong, B., Haines, A., Herrett, E., Wilkinson, P., and Smeeth, L. “The Effects of Hourly Differences in Air Pollution on the Risk of Myocardial Infarction: Case Crossover Analysis of the MINAP Database”. *British Medical Journal* 343 (Sept. 2011), 10.1136/bmj.d5531.
- [21] Bishop, G. A., Schuchmann, B. G., and Stedman, D. H. “Heavy-duty truck emissions in the south coast air basin of California”. *Environmental Science and Technology* 47.16 (2013), pp. 9523–9529. ISSN: 0013936X. DOI: 10.1021/es401487b.
- [22] Bishop, G. A. and Stedman, D. H. “A decade of on-road emissions measurements”. *Environmental Science and Technology* 42.5 (2008), pp. 1651–1656. ISSN: 0013936X. DOI: 10.1021/es702413b.
- [23] Bishop, G. A. and Stedman, D. H. “Reactive Nitrogen Species Emission Trends in Three Light-/Medium-Duty United States Fleets”. *Environmental Science and Technology* 49.18 (2015), pp. 11234–11240. ISSN: 15205851. DOI: 10.1021/acs.est.5b02392.
- [24] Bishop, G. A. and Stedman, D. H. “The recession of 2008 and its impact on light-duty vehicle emissions in three western United States cities”. *Environmental Science and Technology* 48.24 (2014), pp. 14822–14827. ISSN: 15205851. DOI: 10.1021/es5043518.
- [25] Bishop, G. A., Schuchmann, B. G., Stedman, D. H., and Lawson, D. R. “Emission changes resulting from the san Pedro bay, California ports truck retirement program”. *Environmental Science and Technology* 46.1 (2012), pp. 551–558. ISSN: 0013936X. DOI: 10.1021/es202392g.
- [26] Bishop, G. a., Hottor-Raguindin, R., Stedman, D. H., McClintock, P., Theobald, E., Johnson, J. D., Lee, D.-W., Zietsman, J., and Misra, C. “On-road Heavy-duty Vehicle Emissions Monitoring System”. *Environmental Science & Technology* 49.3 (2015), pp. 1639–1645. ISSN: 0013-936X. DOI: 10.1021/es505534e.
- [27] Blanchard, C. L., Tanenbaum, S., and Motallebi, N. “Spatial and Temporal Characterization of PM_{2.5} Mass Concentrations in California, 1980 – 2007”. *Journal of the Air & Waste Management Association* 61.3 (2011), pp. 339–351. DOI: 10.3155/1047-3289.61.3.339. eprint: <http://www.tandfonline.com/doi/pdf/10.3155/1047-3289.61.3.339>.
- [28] Brewer, P. F. and Adlhoch, J. P. “Trends in Speciated Fine Particulate Matter and Visibility across Monitoring Networks in the Southeastern United States”. *Journal of the Air & Waste Management Association* 55.11 (2005), pp. 1663–1674. DOI: 10.1080/10473289.2005.10464755. eprint: <http://www.tandfonline.com/doi/pdf/10.1080/10473289.2005.10464755>.
- [29] Brunekreef, B. and Holgate, S. T. “Air pollution and health”. *The Lancet* 360.9341 (2002), pp. 1233–1242. ISSN: 0140-6736. DOI: [http://dx.doi.org/10.1016/S0140-6736\(02\)11274-8](http://dx.doi.org/10.1016/S0140-6736(02)11274-8).

- [30] Burgan, O., Smargiassi, A., Perron, S., and Kosatsky, T. “Cardiovascular Effects of Sub-Daily Levels of Ambient Fine Particles: a Systematic Review”. *Environmental Health* 9.1 (2010), pp. 26–41. ISSN: 1476-069X. DOI: 10.1186/1476-069X-9-26.
- [31] Burgard, D. A., Bishop, G. A., and Stedman, D. H. “Remote sensing of ammonia and sulfur dioxide from on-road light duty vehicles”. *Environmental Science and Technology* 40.22 (2006), pp. 7018–7022. ISSN: 0013936X. DOI: 10.1021/es061161r.
- [32] Byun, D. and Schere, K. L. “Review of the Governing Equations, Computational Algorithms, and Other Components of the Models-3 Community Multiscale Air Quality (CMAQ) Modeling System”. *Journal of Chemical Information and Modeling* 53.9 (2013), pp. 1689–1699. ISSN: 1098-6596. DOI: 10.1017/CB09781107415324.004. arXiv: arXiv:1011.1669v3.
- [33] California Air Resources Board. *Emission Inventory Data*. 2009. URL: <http://www.arb.ca.gov/ei/emissiondata.htm>.
- [34] California Air Resources Board. *Key Events in the History of Air Quality in California*. 2016.
- [35] California Air Resources Board. *Shore Power for Ocean-going Vessels*. 2013. URL: <http://www.arb.ca.gov/ports/shorepower/shorepower.htm>.
- [36] California Air Resources Board. *Area Designations Maps State and National*. <http://www.arb.ca.gov/desig/adm/adm.htm>. Accessed: 2016-07-13.
- [37] California County-Level Economic Forecast 2013-2040. http://www.dot.ca.gov/hq/tpp/offices/eab/socio_economic_files/2013/Revised_Full_Report.pdf. Accessed: 2016-07-16.
- [38] California Energy Commission. *California Electrical Energy Generation*. 2013. URL: http://energyalmanac.ca.gov/electricity/electricity_generation.html.
- [39] Carter, W. P. L. “Development of the SAPRC-07 chemical mechanism”. *Atmospheric Environment* 44.40 (2010), pp. 5324–5335. ISSN: 13522310. DOI: 10.1016/j.atmosenv.2010.01.026.
- [40] Chen, X., Li, B.-L., and Allen, M. F. “Characterizing Urbanization, and Agricultural and Conservation Land-Use Change in Riverside County, California, USA”. *Annals of the New York Academy of Sciences* 1195 (2010), E164–E176. ISSN: 1749-6632. DOI: 10.1111/j.1749-6632.2009.05403.x.
- [41] Chinkin, L. R., Coe, D. L., Funk, T. H., Hafner, H. R., Roberts, P. T., Ryan, P. A., and Lawson, D. R. “Weekday versus Weekend Activity Patterns for Ozone Precursor Emissions in Californias South Coast Air Basin”. *Journal of the Air & Waste Management Association* 53.7 (2003), pp. 829–843. DOI: 10.1080/10473289.2003.10466223. eprint: <http://dx.doi.org/10.1080/10473289.2003.10466223>.

- [42] Chow, J. C., Watson, J. G., Lowenthal, D. H., and Magliano, K. L. “Loss of PM_{2.5} Nitrate from Filter Samples in Central California”. *Journal of the Air & Waste Management Association* 55.8 (2005), pp. 1158–1168. DOI: 10.1080/10473289.2005.10464704. eprint: <http://www.tandfonline.com/doi/pdf/10.1080/10473289.2005.10464704>.
- [43] Chow, J. C., Watson, J. G., Lowenthal, D. H., Antony Chen, L. W., Tropp, R. J., Park, K., and Magliano, K. A. “PM_{2.5} and PM₁₀ Mass Measurements in California’s San Joaquin Valley”. *Aerosol Science and Technology* 40.10 (2006), pp. 796–810. DOI: 10.1080/02786820600623711. eprint: <http://www.tandfonline.com/doi/pdf/10.1080/02786820600623711>.
- [44] Chow, J., Watson, J., Lowenthal, D., Park, K., Doraiswamy, P., Bowers, K., and Bode, R. “Continuous and filter-based measurements of PM_{2.5} nitrate and sulfate at the Fresno Supersite”. English. *Environmental Monitoring and Assessment* 144.1-3 (2008), pp. 179–189. ISSN: 0167-6369. DOI: 10.1007/s10661-007-9987-5.
- [45] Christoforou, C. S., Salmon, L. G., Hannigan, M. P., Solomon, P. A., and Cass, G. R. “Trends in Fine Particle Concentration and Chemical Composition in Southern California”. *Journal of the Air & Waste Management Association* 50.1 (2000), pp. 43–53. DOI: 10.1080/10473289.2000.10463985. eprint: <http://www.tandfonline.com/doi/pdf/10.1080/10473289.2000.10463985>.
- [46] Chueinta, W. and Hopke, P. K. “Beta Gauge for Aerosol Mass Measurement”. *Aerosol Science and Technology* 35.4 (2001), pp. 840–843. DOI: 10.1080/027868201753227398. eprint: <http://dx.doi.org/10.1080/027868201753227398>.
- [47] Chung, A., Chang, D. P., Kleeman, M. J., Perry, K. D., Cahill, T. A., Dutcher, D., McDougall, E. M., and Stroud, K. “Comparison of Real-Time Instruments Used To Monitor Airborne Particulate Matter”. *Journal of the Air & Waste Management Association* 51.1 (2001), pp. 109–120. DOI: 10.1080/10473289.2001.10464254. eprint: <http://www.tandfonline.com/doi/pdf/10.1080/10473289.2001.10464254>.
- [48] Cooperative Institute for Research in the Atmosphere (CIRA), Colorado State University. *Interagency Monitoring of Protected Visual Environments: VIEWS Data Wizard*. 2012. URL: <http://views.cira.colostate.edu/web/DataWizard/>.
- [49] Corbett, J. J. “Emissions from Ships in the Northwestern United States”. *Environmental Science & Technology* 36.6 (2002), pp. 1299–1306. DOI: 10.1021/es0155985.
- [50] Corbett, J. J., Winebrake, J. J., Green, E. H., Kasibhatla, P., Eyring, V., and Lauer, A. “Mortality from Ship Emissions: A Global Assessment”. *Environmental Science & Technology* 41.24 (2007), pp. 8512–8518. DOI: 10.1021/es071686z. eprint: <http://pubs.acs.org/doi/pdf/10.1021/es071686z>.

- [51] Crutzen, P. J. “The role of NO and NO₂ in the chemistry of the troposphere and stratosphere”. *Annual review of earth and planetary sciences* 7.1 (1979), pp. 443–472. ISSN: 0084-6597. DOI: 10.1146/annurev.ea.07.050179.002303. arXiv: arXiv:1011.1669v3.
- [52] Dallmann, T. R., Harley, R. A., and Kirchstetter, T. W. “Effects of Diesel Particle Filter Retrofits and Accelerated Fleet Turnover on Drayage Truck Emissions at the Port of Oakland”. *Environmental Science & Technology* 45.24 (2011), pp. 10773–10779. DOI: 10.1021/es202609q.
- [53] Dallmann, T. R., Demartini, S. J., Kirchstetter, T. W., Herndon, S. C., Onasch, T. B., Wood, E. C., and Harley, R. A. “On-road measurement of gas and particle phase pollutant emission factors for individual heavy-duty diesel trucks”. *Environmental Science and Technology* 46.15 (2012), pp. 8511–8518. ISSN: 0013936X. DOI: 10.1021/es301936c.
- [54] Dallmann, T. R., Kirchstetter, T. W., Demartini, S. J., and Harley, R. A. “Quantifying on-road emissions from gasoline-powered motor vehicles: Accounting for the presence of medium- and heavy-duty diesel trucks”. *Environmental Science and Technology* 47.23 (2013), pp. 13873–13881. ISSN: 0013936X. DOI: 10.1021/es402875u.
- [55] Dedon, P. C. and Tannenbaum, S. R. *Reactive nitrogen species in the chemical biology of inflammation*. 2004. DOI: 10.1016/j.abb.2003.12.017.
- [56] Dockery, D. W., Pope, C. A., Xu, X., Spengler, J. D., Ware, J. H., Fay, M. E., Ferris, B. G., and Speizer, F. E. “An Association between Air Pollution and Mortality in Six U.S. Cities”. *New England Journal of Medicine* 329.24 (1993). PMID: 8179653, pp. 1753–1759. DOI: 10.1056/NEJM199312093292401. eprint: <http://www.nejm.org/doi/pdf/10.1056/NEJM199312093292401>.
- [57] Dominguez, G., Jackson, T., Brothers, L., Barnett, B., Nguyen, B., and Thiemens, M. H. “Discovery and Measurement of an Isotopically Distinct Source of Sulfate in Earth’s Atmosphere”. *Proceedings of the National Academy of Sciences of the United States of America* 105.35 (2008), 12769–12773. DOI: {10.1073/pnas.0805255105}.
- [58] Dunlea, E. J. et al. “Evaluation of nitrogen dioxide chemiluminescence monitors in a polluted urban environment”. *Atmospheric Chemistry and Physics* 7.2 (2007), pp. 2691–2704. ISSN: 1680-7316, 1680-7316. DOI: 10.5194/acpd-7-569-2007.
- [59] *EMFAC2014 Web Database*. <http://www.arb.ca.gov/emfac/2014/>. Accessed: 2016-07-13.
- [60] Endresen, O, Bakke, J, Sorgard, E, Berglen, T., and Holmvang, P. “Improved Modelling of Ship SO₂ Emissions - a Fuel-based Approach”. *Atmospheric Environment* 39.20 (2005), 3621–3628. DOI: {10.1016/j.atmosenv.2005.02.041}.
- [61] EPA. *Air Quality System Data Mart*. Last accessed: March 1, 2014. www.epa.gov/ttn/airs/aqsdatamart/. United States Environmental Protection Agency, Research Triangle Park, NC. 2008.

- [62] EPA. *List of Designated Reference and Equivalent Methods*. <http://www.epa.gov/ttnamti1/files/ambient/criteria/reference-equivalent-methods-list.pdf>. United States Environmental Protection Agency, National Exposure Research Laboratory, Human Exposure & Atmospheric Sciences Division, Research Triangle Park, NC. 2013.
- [63] EPA. *Revised Requirements for Designation of Reference and Equivalent Methods for $PM_{2.5}$ and Ambient Air Quality Surveillance for Particulate Matter*, 40 CFR Parts 53 and 58. <http://www.gpo.gov/fdsys/granule/FR-1997-07-18/97-18579/content-detail.html>. United States Environmental Protection Agency, Research Triangle Park, NC. 2013.
- [64] Fairley, D. *Sources of Fine Particulates in the San Francisco Bay area*. Bay Area Air Quality Management District, San Francisco, CA. 2012.
- [65] Farrauto, R. J. and Heck, R. M. “Catalytic converters: state of the art and perspectives”. *Catalysis Today* 51.34 (1999), pp. 351–360. ISSN: 0920-5861. DOI: [http://dx.doi.org/10.1016/S0920-5861\(99\)00024-3](http://dx.doi.org/10.1016/S0920-5861(99)00024-3).
- [66] Final Regulation Order. Airborne Toxic Control Measure for Auxiliary Diesel Engines and Diesel-electric Engines Operated on Ocean-going vessels within California Waters and 24 Nautical Miles of the California Baseline. *California Air Resources Board, Sacramento, CA*. Jan, 2007.
- [67] Final Regulation Order. Fuel Sulfur and Other Operational Requirements for Ocean-Going Vessels Within California Waters and 24 Nautical Miles of the California Baseline. *California Air Resources Board, Sacramento, CA*. Jul, 2009.
- [68] Final Regulation Order. Regulation to Reduce Emissions of Diesel Particulate Matter, Oxides of Nitrogen and Other Criteria Pollutants from In-Use Heavy-Duty Diesel-Fueled Vehicles. *California Air Resources Board, Sacramento, CA*. Dec, 2015.
- [69] Fine P. M. *Multiple Air Toxics Exposure Study IV*. South Coast Air Quality Management District, Diamond Bar, CA. 2013. URL: <http://www.aqmd.gov/prdas/MatesIV/Meetings/MatesIV031413.pdf>.
- [70] Fiore, A. M. et al. “Global Air Quality and Climate”. *Chemical Society Reviews* 41 (19 2012), pp. 6663–6683.
- [71] Fischbeck, P. S. and Farrow, R. S., eds. *Improving Regulation: Cases in Environment, Health, and Safety*. 1st. Routledge, 2001. ISBN: 978-1891853111.
- [72] *Fuel Efficiency Automobile Test (FEAT) Data Center*. <http://www.feet.biochem.du.edu/>. Accessed: 2015-12-10.
- [73] Golden Gate Ship Traffic. *The Marine Exchange of the San Francisco Bay Region, San Francisco, CA*. 2011.

- [74] Guidance for Using Air Quality-Related Indicators in Reporting Progress in Attaining the State Ambient Air Quality Standards. *California Air Resources Board, Sacramento, CA*. July 8, 1993.
- [75] Hayes, P. L. et al. “Organic Aerosol Composition and Sources in Pasadena, California, During the 2010 CalNex Campaign”. *Journal of Geophysical Research* 118.16 (2013), 10.1002/jgrd.50530. ISSN: 2169-8996. DOI: 10.1002/jgrd.50530.
- [76] Hering, S. and Cass, G. “The Magnitude of Bias in the Measurement of PM₂₅ Arising from Volatilization of Particulate Nitrate from Teflon Filters”. *Journal of the Air & Waste Management Association* 49.6 (1999), pp. 725–733. DOI: 10.1080/10473289.1999.10463843. eprint: <http://dx.doi.org/10.1080/10473289.1999.10463843>.
- [77] Hettmansperger, T. P. and McKean, J. W. *Robust Nonparametric Statistical Methods*. Second Edition. Boca Raton, FL: CRC Press, 2010. ISBN: 978-1-4398-0909-9.
- [78] Hulskotte, J. H. J. and Gon, H. A.C. D. van der. “Fuel Consumption and Associated Emissions from Seagoing Ships at Berth Derived from an On-board Survey”. *Atmospheric Environment* 44.9 (2010), 1229–1236. DOI: {10.1016/j.atmosenv.2009.10.018}.
- [79] Husar, R. B. “Atmospheric Particulate Mass Monitoring with a β Radiation Detector”. *Atmospheric Environment* 8.2 (1974), pp. 183–188. ISSN: 0004-6981.
- [80] International Maritime Organization. *North American emission control area comes into effect on 1 August 2012*. 2012. URL: <http://www.imo.org/mediacentre/pressbriefings/pages/28-eca.aspx>.
- [81] Isakson, J, Persson, T., and Lindgren, E. “Identification and Assessment of Ship Emissions and Their Effects in the Harbour of Göteborg, Sweden”. *Atmospheric Environment* 35.21 (2001), 3659–3666. DOI: {10.1016/S1352-2310(00)00528-8}.
- [82] Jacobs, L., Buczynska, A., Walgraeve, C., Delcloo, A., Potgieter-Vermaak, S., Grieken, R. V., Demeestere, K., Dewulf, J., Langenhove, H. V., Backer, H. D., Nemery, B., and Nawrot, T. S. “Acute changes in pulse pressure in relation to constituents of particulate air pollution in elderly persons”. *Environmental Research* 117.0 (2012), pp. 60–67. ISSN: 0013-9351. DOI: <http://dx.doi.org/10.1016/j.envres.2012.05.003>.
- [83] Jaklevic, J. M., Gatti, R. C., Goulding, F. S., and Loo, B. W. “A Beta-Gage Method Applied to Aerosol Samples”. *Environmental Science & Technology* 15.6 (1981), pp. 680–686. DOI: 10.1021/es00088a006. eprint: <http://pubs.acs.org/doi/pdf/10.1021/es00088a006>.
- [84] Jerrett, M., Burnett, R. T., Pope, C. A., Ito, K., Thurston, G., Krewski, D., Shi, Y., Calle, E., and Thun, M. “Long-term ozone exposure and mortality.” *The New England journal of medicine* 360.11 (2009), pp. 1085–95. ISSN: 1533-4406. DOI: 10.1056/NEJMoa0803894.

- [85] Kasper, A., Aufdenblatten, S., Forss, A., Mohr, M., and Burtscher, H. “Particulate Emissions from a Low-Speed Marine Diesel Engine”. *Aerosol Science and Technology* 41.1 (2007), pp. 24–32. DOI: 10.1080/02786820601055392.
- [86] Kean, A. J., Harley, R. A., and Kendall, G. R. “Effects of vehicle speed and engine load on motor vehicle emissions”. *Environmental Science and Technology* 37.17 (2003), pp. 3739–3746. ISSN: 0013936X. DOI: 10.1021/es0263588.
- [87] Kean, A. J., Harley, R. A., Littlejohn, D., and Kendall, G. R. “On-road measurement of ammonia and other motor vehicle exhaust emissions”. *Environmental Science and Technology* 34.17 (2000), pp. 3535–3539. ISSN: 0013936X. DOI: 10.1021/es991451q.
- [88] Kelly, J. T., Baker, K. R., Nowak, J. B., Murphy, J. G., Markovic, M. Z., VandenBoer, T. C., Ellis, R. A., Neuman, J. A., Weber, R. J., Roberts, J. M., Veres, P. R., De Gouw, J. A., Beaver, M. R., Newman, S., and Misenis, C. “Fine-scale simulation of ammonium and nitrate over the South Coast Air Basin and San Joaquin Valley of California during CalNex-2010”. *Journal of Geophysical Research Atmospheres* 119.6 (2014), pp. 3600–3614. ISSN: 21698996. DOI: 10.1002/2013JD021290.
- [89] Khan, M. Y., Giordano, M., Gutierrez, J., Welch, W. A., Asa-Awuku, A., Miller, J. W., and Cocker, D. R. “Benefits of Two Mitigation Strategies for Container Vessels: Cleaner Engines and Cleaner Fuels”. *Environmental Science & Technology* 46.9 (2012), pp. 5049–5056. DOI: 10.1021/es2043646. eprint: <http://pubs.acs.org/doi/pdf/10.1021/es2043646>.
- [90] Kim, E. and Hopke, P. K. “Source Characterization of Ambient Fine Particles at Multiple Sites in the Seattle Area”. *Atmospheric Environment* 42.24 (2008), pp. 6047–6056. ISSN: 1352-2310. DOI: 10.1016/j.atmosenv.2008.03.032.
- [91] Kirchstetter, T. W., Aguiar, J., Tonse, S., Fairley, D., and Novakov, T. “Black Carbon Concentrations and Diesel Vehicle Emission Factors Derived from Coefficient of Haze Measurements in California: 1967–2003”. *Atmospheric Environment* 42.3 (2008), pp. 480–491. ISSN: 1352-2310.
- [92] Kirchstetter, T. W., Singer, B. C., Harley, R. A., Kendall, G. R., and Traverse, M. “Impact of California reformulated gasoline on motor vehicle emissions. 1. Mass emission rates”. *Environmental Science and Technology* 33.2 (1999), pp. 318–328. ISSN: 0013936X. DOI: 10.1021/es9803714.
- [93] Kurtenbach, R., Kleffmann, J., Niedojadlo, A., and Wiesen, P. “Primary NO₂ emissions and their impact on air quality in traffic environments in Germany”. *Environmental Sciences Europe* 24.1 (2012), p. 21. ISSN: 2190-4715. DOI: 10.1186/2190-4715-24-21.
- [94] Kuwayama, T., Schwartz, J. R., Harley, R. A., and Kleman, M. J. “Particulate Matter Emissions Reductions due to Adoption of Clean Diesel Technology at a Major Shipping Port”. *Aerosol Science and Technology* 47.1 (2013), 29–36. ISSN: 0278-6826. DOI: {10.1080/02786826.2012.720049}.

- [95] Lack, D.A. et al. “Impact of Fuel Quality Regulation and Speed Reductions on Shipping Emissions: Implications for Climate and Air Quality”. *Environmental Science & Technology* 45.20 (2011), pp. 9052–9060. DOI: 10.1021/es2013424.
- [96] Laden, F., Schwartz, J., Speizer, F. E., and Dockery, D. W. “Reduction in fine particulate air pollution and mortality: Extended follow-up of the Harvard Six Cities Study”. *American Journal of Respiratory and Critical Care Medicine* 173.6 (2006), pp. 667–672. DOI: 10.1164/rccm.200503-4430C.
- [97] Larsen, L. C. “An assessment of the impact of California’s Phase 2 Reformulated Gasoline on ozone air quality”. *Journal of the Air and Waste Management Association* 51.1 (2001), pp. 37–48. ISSN: 21622906.
- [98] Lohmann, U. and Feichter, J. “Global indirect aerosol effects: a review”. *Atmospheric Chemistry and Physics Discussions* 4.6 (2004), pp. 7561–7614. ISSN: 1680-7324. DOI: 10.5194/acpd-4-7561-2004.
- [99] Malm, W. C., Schichtel, B. A., Ames, R. B., and Gebhart, K. A. “A 10-year Spatial and Temporal Trend of Sulfate Across the United States”. *Journal of Geophysical Research* 107.D22 (2002), 10.1029/2002JD002107. ISSN: 2156-2202. DOI: 10.1029/2002JD002107.
- [100] Mann, J. K., Balmes, J. R., Bruckner, T. A., Mortimer, K. M., Margolis, H. G., Pratt, B., Katharine Hammond, S., Lurmann, F. W., and Tager, I. B. “Short-term effects of air pollution on wheeze in asthmatic children in Fresno, California”. *Environmental Health Perspectives* 118.10 (2010), pp. 1497–1502. DOI: 10.1289/ehp.0901292.
- [101] Marr, L. C. and Harley, R. A. “Modeling the effect of weekday-weekend differences in motor vehicle emissions on photochemical air pollution in central California.” *Environmental science & technology* 36.19 (2002), pp. 4099–4106. ISSN: 0013-936X. DOI: 10.1021/es020629x.
- [102] Mazzei, F., D’Alessandro, A., Lucarelli, F., Nava, S., Prati, P., Valli, G., and Vecchi, R. “Characterization of Particulate Matter Sources in an Urban Environment”. *Science of The Total Environment* 401.13 (2008), pp. 81–89. ISSN: 0048-9697. DOI: 10.1016/j.scitotenv.2008.03.008.
- [103] McDonald, B. and Harley, R. A. *EMFAC 2011 Model Evaluation*. Tech. rep. Department of Civil and Environmental Engineering. University of California, Berkeley., July 2013.
- [104] McDonald, B. C., McBride, Z. C., Martin, E. W., and Harley, R. A. “High-resolution mapping of motor vehicle carbon dioxide emissions”. *Journal of Geophysical Research: Atmospheres* 119.9 (2014). 2013JD021219, pp. 5283–5298. ISSN: 2169-8996. DOI: 10.1002/2013JD021219.
- [105] Mcdonald, B. C., Gentner, D. R., Goldstein, A. H., and Harley, R. a. “Long-Term Trends in Motor Vehicle Emissions in U.S. Urban Areas”. *Environmental science & technology* 47.17 (2013), pp. 10022–31. ISSN: 0013-936X. DOI: 10.1021/es401034z.

- [106] Met One Instrument. *BAM-1020 Continuous Particulate Monitor Data Sheet*. www.metone.com/documents/BAM-1020_Datasheet.pdf. Grants Pass, OR. 2013.
- [107] Millero, F. J. *Chemical oceanography*. English. Boca Raton: CRC/Taylor and Francis, 2006. ISBN: 0849322804 9780849322808.
- [108] Millstein, D. E. and Harley, R. A. “Impact of climate change on photochemical air pollution in Southern California”. *Atmos. Chem. Phys. Atmospheric Chemistry and Physics* 9 (2009), pp. 3745–3754. ISSN: 16807375. DOI: 10.5194/acp-9-3745-2009.
- [109] Millstein, D., Harley, R., and Hering, S. *Analysis of Particulate Nitrate and Black Carbon Time Series*. www.crcao.org/publications/atmosphereImpacts. Report to the Coordinating Research Council, Project Number A-57. University of California and Aerosol Dynamics Inc., Berkeley, CA. November 2006. (2006).
- [110] Millstein, D. E. and Harley, R. A. “Effects of retrofitting emission control systems on in-use heavy diesel vehicles”. *Environmental Science and Technology* 44.13 (2010), pp. 5042–5048. ISSN: 0013936X. DOI: 10.1021/es1006669.
- [111] Millstein, D. E. and Harley, R. A. “Revised estimates of construction activity and emissions: Effects on ozone and elemental carbon concentrations in southern California”. *Atmospheric Environment* 43.40 (2009), pp. 6328–6335. ISSN: 13522310. DOI: 10.1016/j.atmosenv.2009.09.028.
- [112] Millstein, D. E., Harley, R. A., and Hering, S. V. “Weekly Cycles in Fine Particulate Nitrate”. *Atmospheric Environment* 42.4 (2008), pp. 632–641. ISSN: 1352-2310.
- [113] Moldanová, J., Fridell, E., Popovicheva, O., Demirdjian, B., Tishkova, V., Faccinnetto, A., and Focsa, C. “Characterisation of Particulate Matter and Gaseous Emissions from a Large Ship Diesel Engine”. *Atmospheric Environment* 43.16 (2009), pp. 2632–2641. ISSN: 1352-2310. DOI: 10.1016/j.atmosenv.2009.02.008.
- [114] Mooibroek, D., Schaap, M., Weijers, E., and Hoogerbrugge, R. “Source Apportionment and Spatial Variability of PM_{2.5} Using Measurements at Five Sites in the Netherlands”. *Atmospheric Environment* 45.25 (2011), pp. 4180–4191. ISSN: 1352-2310. DOI: 10.1016/j.atmosenv.2011.05.017.
- [115] Motallebi, N., Taylor, C. A., and Croes, B. E. “Particulate Matter in California: Part 2 – Spatial, Temporal, and Compositional Patterns of PM_{2.5}, PM_{10–2.5}, and PM₁₀”. *Journal of the Air & Waste Management Association* 53.12 (2003), pp. 1517–1530. DOI: 10.1080/10473289.2003.10466323. eprint: <http://www.tandfonline.com/doi/pdf/10.1080/10473289.2003.10466323>.
- [116] Murphy, S. M., Agrawal, H., Sorooshian, A., Padró, L. T., Gates, H., Hersey, S., Welch, W. A., Jung, H., Miller, J. W., Cocker, D. R., Nenes, A., Jonsson, H. H., Flagan, R. C., and Seinfeld, J. H. “Comprehensive Simultaneous Shipboard and Airborne Characterization of Exhaust from a Modern Container Ship at Sea”. *Environmental Science & Technology* 43.13 (2009), pp. 4626–4640. DOI: 10.1021/es802413j.

- [117] Nafstad, P., Håheim, L. L., Wisløff, T., Gram, F., Oftedal, B., Holme, I., Hjermann, I., and Leren, P. “Urban air pollution and mortality in a cohort of Norwegian men.” *Environmental health perspectives* 112.5 (2004), pp. 610–615. ISSN: 0091-6765. DOI: 10.1289/ehp.6684.
- [118] Noble, C. A., Vanderpool, R. W., Peters, T. M., McElroy, F. F., Gemmill, D. B., and Wiener, R. W. “Federal Reference and Equivalent Methods for Measuring Fine Particulate Matter”. *Aerosol Science and Technology* 34.5 (2001), pp. 457–464. DOI: 10.1080/02786820121582. eprint: <http://www.tandfonline.com/doi/pdf/10.1080/02786820121582>.
- [119] Nowak, J. B., Neuman, J. A., Bahreini, R., Middlebrook, A. M., Holloway, J. S., McKeen, S. A., Parrish, D. D., Ryerson, T. B., and Trainer, M. “Ammonia sources in the California South Coast Air Basin and their impact on ammonium nitrate formation”. *Geophysical Research Letters* 39.7 (2012). ISSN: 00948276. DOI: 10.1029/2012GL051197.
- [120] PA DEP. *Proposed Ambient Air Monitoring Network Plan - 2013-2014*. www.dep.state.pa.us/dep/deputate/airwaste/aq/aqm/docs/FinalDraft_PA_Air_Monitoring_Network_Plan_2013.pdf. Pennsylvania Department of Environmental Protection, Harrisburg, PA. 2013.
- [121] Peters, T. M., Norris, G. A., Vanderpool, R. W., Gemmill, D. B., Wiener, R. W., Murdoch, R. W., McElroy, F. F., and Pitchford, M. “Field Performance of PM_{2.5} Federal Reference Method Samplers”. *Aerosol Science and Technology* 34.5 (2001), pp. 433–443. DOI: 10.1080/02786820116873. eprint: <http://www.tandfonline.com/doi/pdf/10.1080/02786820116873>.
- [122] Petzold, A., Weingartner, E., Hasselbach, J., Lauer, P., Kurok, C., and Fleischer, F. “Physical Properties, Chemical Composition, and Cloud Forming Potential of Particulate Emissions from a Marine Diesel Engine at Various Load Conditions”. *Environmental Science & Technology* 44.10 (2010), pp. 3800–3805. DOI: 10.1021/es903681z.
- [123] Pope, C. A. and Dockery, D. W. “Health Effects of Fine Particulate Air Pollution: Lines that Connect”. *Journal of the Air & Waste Management Association* 56.6 (2006), pp. 709–742. DOI: 10.1080/10473289.2006.10464485. eprint: <http://www.tandfonline.com/doi/pdf/10.1080/10473289.2006.10464485>.
- [124] Pope C. Arden, I., Hansen, M. L., Long, R. W., Nielsen, K. R., Eatough, N. L., Wilson, W. E., and Eatough, D. J. “Ambient Particulate Air Pollution, Heart Rate Variability, and Blood Markers of Inflammation in a Panel of Elderly Subjects”. English. *Environmental Health Perspectives* 112.3 (2004), pp. 339–345. ISSN: 00916765.
- [125] Port of Oakland. *Facts & Figures*. 2012.

- [126] Preble, C. V., Dallmann, T. R., Kreisberg, N. M., Hering, S. V., Harley, R. A., and Kirchstetter, T. W. “Effects of Particle Filters and Selective Catalytic Reduction on Heavy-Duty Diesel Drayage Truck Emissions at the Port of Oakland”. *Environmental Science & Technology* 49.14 (2015). PMID: 26083075, pp. 8864–8871. DOI: 10.1021/acs.est.5b01117. eprint: <http://dx.doi.org/10.1021/acs.est.5b01117>.
- [127] Quok, M. and McDougall, M. *Comparison of the ARB Continuous PM_{2.5} Monitoring Network to the PM_{2.5} Federal Reference Method Network*. www.metone.com/documents/bam_paper_jan13.pdf. California Air Resources Board. Monitoring and Laboratory Division, Sacramento, CA 95812. 2006.
- [128] R Core Team. *R: A Language and Environment for Statistical Computing*. ISBN 3-900051-07-0. R Foundation for Statistical Computing. Vienna, Austria, 2012.
- [129] Salvi, S., Blomberg, A., Rudell, B., Kelly, F., SandstrM, T., Holgate, S., and Frew, A. “Acute Inflammatory Responses in the Airways and Peripheral Blood After Short-Term Exposure to Diesel Exhaust in Healthy Human Volunteers”. *American Journal of Respiratory and Critical Care Medicine* 159.3 (Mar. 1999), pp. 702–709. ISSN: 1073-449X, 1535-4970. DOI: 10.1164/ajrccm.159.3.9709083.
- [130] Sardar, S. B., Geller, M. D., Sioutas, C., and Solomon, P. A. “Development and Evaluation of a High-Volume Dichotomous Sampler for Chemical Speciation of Coarse and Fine Particles”. *Journal of Aerosol Science* 37.11 (2006), pp. 1455–1466. ISSN: 0021-8502.
- [131] Sax, T. and Alexis, A. *A Critical Review of Ocean-Going Vessel Particulate Matter Emission Factors*. California Air Resources Board, Sacramento, CA. 2007.
- [132] Schembari, C., Cavalli, F., Cuccia, E., Hjorth, J., Calzolari, G., Prez, N., Pey, J., Prati, P., and Raes, F. “Impact of a European directive on ship emissions on air quality in Mediterranean harbours”. *Atmospheric Environment* 61.0 (2012), pp. 661–669. ISSN: 1352-2310. DOI: <http://dx.doi.org/10.1016/j.atmosenv.2012.06.047>.
- [133] Scott, K. I. and Benjamin, M. T. “Development of a biogenic volatile organic compounds emission inventory for the SCOS97-NARSTO domain”. *Atmospheric Environment*. Vol. 37. SUPPL. 2. 2003. DOI: 10.1016/S1352-2310(03)00381-9.
- [134] Sources of Bay Area Fine Particles: 2010 Update and Trends. *David Fairley, Bay Area Air Quality Management District, San Francisco, CA*. 2012.
- [135] *South Coast Air Quality Management District. Health Studies. Air Toxic Studies*. <http://www.aqmd.gov/home/library/air-quality-data-studies/health-studies>. Accessed: 2016-07-16.
- [136] Stationary Source Division, Emissions Assessment Branch. *2005 Oceangoing Ship Survey Summary of Results*. Tech. rep. California Air Resources Board, Sacramento, CA, 2005.

- [137] *Summary of the Proposed Regulation to Reduce Emissions from In-Use On-Road Diesel Trucks and Buses*. <http://www.arb.ca.gov/msprog/onrdiesel/documents/dieselonrdtruckoverview.pdf>. Accessed: 2016-07-13.
- [138] Tao, I., Harley, R. A., and Bastien, L. *A Fuel-Based Evaluation of EMFAC 2014 Motor Vehicle Emission Inventory Model Predictions*. Tech. rep. Department of Civil and Environmental Engineering. University of California, Berkeley., Apr. 2016.
- [139] *Taxable Distributions of Diesel Fuel and Alternative Fuels*. http://www.boe.ca.gov/annual/2013-14/table_14/table25a_2013-14.pdf. Accessed: 2015-06-30.
- [140] US Census Bureau. *State and County Quick Facts*. Last accessed: March 27, 2014. <http://quickfacts.census.gov/qfd/states/06000.html>. Washington, DC. 2013.
- [141] US EPA. *NAAQS Table*. <https://www.epa.gov/criteria-air-pollutants/naaqs-table>. Accessed: 2016-06-30.
- [142] Viana, M., Amato, F., Alastuey, A., Querol, X., Moreno, T., García Dos Santos, S., Herce, M. D., and Fernández-Patier, R. “Chemical Tracers of Particulate Emissions from Commercial Shipping”. *Environmental Science & Technology* 43.19 (2009), pp. 7472–7477. DOI: 10.1021/es901558t.
- [143] Vutukuru, S. and Dabdub, D. “Modeling the Effects of Ship Emissions on Coastal Air Quality: A Case Study of Southern California”. *Atmospheric Environment* 42.16 (2008), pp. 3751–3764. ISSN: 1352-2310. DOI: 10.1016/j.atmosenv.2007.12.073.
- [144] Wang, Y. and Hopke, P. K. “A Ten-Year Source Apportionment Study of Ambient Fine Particulate Matter in San Jose, California”. *Atmospheric Pollution Research* 4 (2013), pp. 398–404. DOI: 10.5094/APR.2013.045.
- [145] Warneke, C., De Gouw, J. A., Holloway, J. S., Peischl, J., Ryerson, T. B., Atlas, E., Blake, D., Trainer, M., and Parrish, D. D. “Multiyear trends in volatile organic compounds in Los Angeles, California: Five decades of decreasing emissions”. *Journal of Geophysical Research Atmospheres* 117.17 (2012). ISSN: 01480227. DOI: 10.1029/2012JD017899.
- [146] Wickham, H. *ggplot2: elegant graphics for data analysis*. Springer New York, 2009. ISBN: 978-0-387-98140-6.
- [147] Wickham, H. *scales: Scale functions for graphics*. R package version 0.2.1. 2012.
- [148] Williams, E. J., Lerner, B. M., Murphy, P. C., Herndon, S. C., and Zahniser, M. S. “Emissions of NO_x, SO₂, CO, and HCHO from commercial marine shipping during Texas Air Quality Study (TexAQS) 2006”. *Journal of Geophysical Research-Atmospheres* 114 (2009). ISSN: 0148-0227. DOI: {10.1029/2009JD012094}.
- [149] Winnes, H. and Fridell, E. “Particle Emissions from Ships: Dependence on Fuel Type”. *Journal of the Air & Waste Management Association* 59.12 (2009), pp. 1391–1398. DOI: 10.3155/1047-3289.59.12.1391.

- [150] World Health Organization. *The world health report 2002 - Reducing Risks, Promoting Healthy Life*. Tech. rep. World Health Organization, Geneva, Switzerland, 2002.
- [151] Zhang, Y., Bocquet, M., Mallet, V., Seigneur, C., and Baklanov, A. “Real-Time Air Quality Forecasting, Part I: History, Techniques, and Current Status”. *Atmospheric Environment* 60.0 (2012), pp. 632 –655. ISSN: 1352-2310.
- [152] Zheng, X. Y., Ding, H., Jiang, L. N., Chen, S. W., Zheng, J. P., Qiu, M., Zhou, Y. X., Chen, Q, and Guan, W. J. “Association between Air Pollutants and Asthma Emergency Room Visits and Hospital Admissions in Time Series Studies: A Systematic Review and Meta-Analysis”. *PLoS ONE* 10 (2015), e0138146. ISSN: ISSN 1932-6203 EISSN 19326203. DOI: 10.1371/journal.pone.0138146.